CZECH TECHNICAL UNIVERSITY IN PRAGUE

Faculty of Civil Engineering
Department of Architectural Engineering

EXPERIMENTAL ANALYSIS OF THE EFFECTIVENESS OF WATERPROOFING SCREEDS IN BUILDING STRUCTURES

DOCTORAL THESIS

Ing. Michal Nývlt

Doctoral study programme:	Civil Engineering
Branch of Study:	Building Engineering
Chief supervisor:	doc. Ing. Jiří Pazderka, Ph.D.
Supervisor-specialist:	doc. Ing. Pavel Reiterman, Ph.D.

Prague, 2024

DECLARATION

I declare that this thesis has been composed solely by myself and that it has not been submitted, in whole or in part, in any previous application for a degree. Except where states otherwise by reference or acknowledgment, the work presented is entirely my own.

The doctoral thesis was written in connection with research on the projects:

- NAKI II DG18P02OVV063: "Development of the progressive rehabilitation methodology for restoration and conservation of military fortress objects from the 1930s"
- SGS19/145/OHK1/3T/11: "Analysis of construction details in concrete and brick buildings in terms of water permeability and durability";
- SGS22/138/OHK1/3T/11: "Study of the interaction of crystallization waterproofing coating with selected building structures";
- SGS17/117/OHK1/2T/11: "Experimental Verification of the Reliability of Selected Systems for the Protection of Substructure Against Water".

In Prague, on 25.4.2024 .....

Signature

ACKNOWLEDGEMENTS

I would like to thank my supervisors doc. Ing. Jiří Pazderka, Ph.D. and doc. Ing. Pavel Reiterman, Ph.D. for their support, guidance, and feedback.

Last but not least, my thanks go to my family and especially to my wife and daughter for their patience and support.

https://doi.org/10.14311/dis.fsv.2024.008

ABSTRACT IN ENGLISH

The aim of the research was focused on the functionality of three types of waterproofing screeds from the perspective of their use in building structures. Bitumen, polymer, silicate (mineral) screeds were studied in terms of their cohesion with the substrate and their sealing ability. The waterproofing screeds were tested in combination with commonly used building materials – ceramics, concrete, sand-lime bricks, marlstone and sandstone. The cohesion was also studied after the freeze-thaw exposure to take into account the aspects of durability.
The subject of the research from the point of view of functionality was also the verification of tightness against the penetration of radon, which occurs to a large extent in the soil environment, especially in the territory of the Czech Republic.
To maintain the continuity of the research, the aging of waterproofing screeds was carried out using freeze-thaw cycles.

Comparing the overall tested screeds, despite the best adhesion of the polymer-based screed, this material exhibited the lowest durability after the freeze-thaw exposure. The bitumen and silicate (mineral) screed attained similar values of adhesion to the studied base materials. However, they differ in their ability to withstand freeze-thaw cycles over time. The modified water permeability test on model masonry specimens was performed. No leakage of water during the test was monitored for the specimens with all types of applied screeds over time, and, in addition, water had not penetrated through the bricks, nor through the joints. The waterproofing effect of the screed is not affected by the joints in masonry.
The results of research investigating the effect of freeze-thaw cycles on the sealing ability of waterproofing screeds against radon showed minimal differences between the tested materials. The measured values correspond to commonly used insulating materials. Waterproofing screeds are a suitable material for use in underground structures.

Keywords: waterproofing screeds; freeze-thaw cycles; adhesion; building structures, radon

ABSTRACT IN CZECH

Cílem disertační práce bylo ověření a vzájemné porovnání funkčnosti tří typů hydroizolačních stěrek z hlediska jejich použití ve stavebních konstrukcích. Byly zkoumány tři vybrané hydroizolační stěrky lišící materiálovým složením – bitumenové, polymerní a silikátové (minerální). Byly zkoumány z hlediska jejich soudržnosti s podkladem a jejich těsnících schopností proti pronikání vody. Hydroizolační stěrky byly testovány v kombinaci s běžně používanými stavebními materiály – keramikou, vyzrálým betonem, vápenopískem, opukou a pískovcem. Soudržnost stěrek s podkladem byla zkoumána také po působení zmrazovacích cyklů tak, aby se zohlednily aspekty trvanlivosti (mrazuvzdornosti).
Předmětem výzkumu z hlediska funkčnosti bylo také ověření těsnosti proti pronikání radonu, který se ve velké míře vyskytuje v půdním prostředí zejména na území České republiky. Pro zachování kontinuity výzkumu bylo provedeno stárnutí hydroizolačních stěrek pomocí stejného počtu zmrazovacích cyklů.

Při porovnání výsledků se ukázalo, že i přes vysokou počáteční přilnavost polymerní stěrky vykazoval tento materiál nejnižší trvanlivost po působení zmrazování. Bitumenová a silikátová stěrka dosáhly podobných hodnot přilnavosti ke zkoumaným podkladním materiálům. Výsledky ukázaly rozdílné schopnosti odolávat působení zmrazovacím cyklům v průběhu času. Na modelových vzorcích zdiva byla provedena modifikovaná zkouška vodonepropustnosti. U všech typů použitých hydroizolačních stěrek nebyl v průběhu zkoušky sledován průsak vody. Hydroizolační účinek stěrek nebyl ovlivněn spárami mezi zdícím materiálem.
Výsledky výzkumu zkoumajícího vliv zmrazování a rozmrazování na těsnící schopnost hydroizolačních stěrek proti radonu ukázal minimální rozdíly mezi testovanými materiály. Naměřené hodnoty odpovídají běžně používaným izolačním materiálům. Zkoušené hydroizolační stěrky jsou vhodným materiálem pro použití v podzemních stavbách.

Klíčová slova: hydroizolační stěrky; mrazuvzdornost; přídržnost; stavební konstrukce, radon, hydroziolace

TABLE OF CONTENT

1. INTRODUCTION

The issue of protecting the structures of buildings against water concerns not only new buildings, but also older buildings that require remedial intervention. Waterproofing systems in ground structures can be divided into two groups: waterproofing strips and screeds. While the functional principles of waterproofing strips are usually fairly well mapped, the functional principles of waterproofing screeds are in many cases not described in full detail. In construction details, the advantages of both systems are often used and a combination of the two occurs, e.g. the contact of a footing with a reinforced concrete column. Nowadays, the use of waterproofing membranes is becoming increasingly common, both for new buildings and for additional waterproofing measures in renovations. The different types of waterproofing screeds differ not only in their chemical composition but also in their physical and mechanical properties, especially in their interaction with the underlying building structure. Along with the widespread application of waterproofing screeds, some weak points of these systems are becoming apparent, such as: the solution of the connection to downstream structures, ensuring flexibility in critical areas by means of additional elements, failure to observe technological discipline during implementation, including subsequent treatment, high demands on substrate preparation, durability under various boundary conditions, etc. In particular, the interaction of certain types of waterproofing screeds with different substrates can be a risk factor for their use.

Selected physical parameters of waterproofing screeds under different boundary conditions and in interaction with different types of building structures will be investigated in laboratory conditions. Experimental analyses of different types of waterproofing screeds will be carried out. Thus, their durability (especially frost resistance and adhesion to the substrate) will be determined. In addition, waterproofing and radon resistance will be verified. The advantage of these laboratory tests is direct comparability with the reference model.

2. AIM OF DOCTORAL THESIS

The aim of the dissertation is to deepen the knowledge in the field of waterproofing screeds in ground structures, especially in reinforced concrete and masonry buildings. The main objective is to study the interaction between waterproofing screed and building structure in terms of material parameters, especially the adhesion of the layers to the surface. To this end, frost resistance, water permeability, radon permeability as well as related physical-mechanical properties, which also influence the resulting reliability of the waterproofing envelope, will be investigated through laboratory tests. All experiments were conducted on selected waterproofing screeds at different boundary conditions.
Laboratory experiments will be carried out following practical experience, firstly selected waterproofing screeds with different binders (asphalt, polymer, silicate) were selected. Subsequently, these screeds will be compared with each other.
Due to the wide use of screeds today, the work will not only focus on new buildings but also on renovations of older buildings (e.g. concrete from the 1930s). The focus on concrete from

the 1930s is part of the NAKI II research project DG18P02OVV063 with which the topic of the thesis is partly linked.

Within the dissertation experiments were carried out in laboratory conditions, where the durability and physical and technical properties of waterproofing screeds especially water permeability, radon permeability and mainly frost resistance were investigated on the made models. Different boundary conditions were simulated under laboratory conditions.

3. STATE OF THE ART

3.1. THE INFLUENCE OF WATER ON CIVIL ENGINEERING STRUCTURES

Most masonry materials especially brick, sandstone, lime and cement mortar have the ability to take up and give off water due to their porous structure. The amount of water (in whatever state) contained in the porous environment of a substance determines the moisture content of the material. The water content of the material depends on the temperature, the humidity of the surrounding air, the porosity of the substance, the amount of hydroscopic salts in the damp masonry, etc. All building materials do not occur in practice in a dry state, they always contain, under given atmospheric conditions a certain amount of moisture.

Several parameters affect the durability of structures of civil engineering buildings. One of the most common is the effect of degradation processes caused by the external environment. The external factors acting on the structure during its lifetime include mainly factors from the atmosphere, soil and water, as well as user loads. Depending on their effect on the structure, corrosion is divided into physical, chemical and biological corrosion, which, depending on the type of action, is also twofold - physical (mechanical damage by root growth) and chemical (products of higher animals and bacteria).

The durability of structures is determined by the ability of the surface layer of the material to resist aggressive agents. The most dangerous is chemical corrosion, caused either by liquid substances (chemical corrosion by liquid environment) or by gaseous aggressive environments (atmospheric corrosion). Aggressive substances cause deterioration of the surface layer of the structure. When the structure is exposed to deterioration processes for a longer period of time, the aggressive substances start to penetrate deeper into the cross-section. For example, in the case of concrete, "*The rate of corrosion is determined by the course of chemical reaction of the aggressive substances with the cementitious sealant components and the rate of exchange of the liquid medium at the concrete surface. The poorly soluble products form a layer on the concrete surface which prevents the ingress of other aggressive substances into the concrete. The rate of corrosion is determined by the diffusion of aggressive substances through the surface layer (governed by the laws of diffusion)*" [1]. All concrete corrosion processes are related to the reduction of the calcium hydroxide content of the cementitious sealant and have an effect on the corrosion of the steel reinforcement.

3.1.1. Water in building structures and its composition, humidity

Water does not occur in nature as chemically pure. It always contains dissolved gases and dissolved and undissolved inorganic and organic substances. Some substances are already taken up in the atmosphere, but the main enrichment in solutes occurs through infiltration by soil and rocks. Anthropogenic sources of inorganic and organic matter in natural waters are airborne contaminants and industrial and sewage effluents.

Amount of water (in any state) contained in the porous medium of a substance determines the moisture content of the material.
The water content of a material is dependent on temperature, on the humidity of the surrounding air, on the porosity on the porosity of the substance, on the amount of hydroscopic salts in the damp masonry, etc. All building materials do not occur in practice in a dry state, they always contain, under given atmospheric conditions a certain amount of moisture.

Under steady-state temperature and humidity conditions, when there is a balance between humidity of the material and the humidity of the surrounding air, equilibrium humidity occurs. Moisture in masonry construction affects the physical properties of the material and can cause widespread problems

Moisture content (1) is expressed as the mass or volume ratio of water to the solid phase of the dry substance [2].

(1) $$w = \frac{(m_w - m_d)}{m_d} * 100 \quad [\%]$$

w = mass humidity [%]
m_w = weight of wet material [g]
m_d= weight of dry material [g]

The classification table (Table 1) in the standard ČSN P 73 0610 [3] prescribes and classifies reasonable and elevated values of mass moisture content, which are guideline values. The moisture levels given are principally for masonry structures constructed with common mortar.

Table 1.

Moisture content of masonry "w" in [%] moisture	The degree of humidity
w < 3%	Very low humidity
3% < w < 5%	Low humidity
5% < w < 7,5%	Increased humidity
7,5% < w < 10%	High humidity
w > 10%	Very high humidity

In the literature, the limit values may vary, depending in particular on the material used (ceramic, brick, lime sand, concrete, etc.). For the purposes of this thesis, the values given in the Czech standard are considered

The basic moisture properties that affect material properties are porosity, water absorption and equilibrium moisture content [4 a 5].

3.1.1.1. Porosity

Porosity expresses the total percentage of free space that is not filled with solid particles. The following equation (2) is used to determine the porosity p:

(2) $$p = \frac{Vv}{Vs} \times 100 \qquad [\%]$$

p = porosity [%]
v_v = the volume of free space[m^3]
v_s = volume of solid particles [m^3]

Porous substances are classified according to pore size in terms of transport processes. The size of the pores influences their filling with water by absorption and capillary forces.
Pores are divided into three groups [6]:

- macroscopic pores with an effective radius greater than 2×10^{-7} m,
- capillary pores with an effective radius of 2×10^{-7} - $1,5\times10^{-9}$ m,
- microscopic pores with an effective radius of less than $1,5\times10^{-9}$ m

3.1.1.2. Water absorption

Absorbency is characterised by the amount of water that a dried porous substance can hold when immersed in water for a certain period of time and under the conditions specified in the standard. From the water absorption can be determine the total amount of open pores and the frost resistance of a given building substance [7].

The following (3) can be used to determine the water absorption of NV from the water content by weight equation [7]:

(3) $$NV = \frac{(w_w - w_d)}{w_d} \times 100 \qquad [\%]$$

NV = water absorption [%]
w_w = weight of the sample before drying [g]
w_d= weight of the sample after drying [g]

The water absorption of building materials is influenced by their hydrophobic and hydroscopic properties. A hydrophobic surface reduces the water absorption of the material used. The degree of hydrophobisation indicates how many times the water absorption of the material is

reduced compared to the initial state. The absorbency of treated masonry should decrease by at least 70 % compared to untreated masonry and the water vapour permeability should not decrease by more than 10 % [8].

3.1.1.3. Equilibrium moisture content

Equilibrium humidity is the moisture that a substance takes up from the surrounding air at steady state temperature and humidity conditions.

In the case of building structures, the most common absorbent is water vapour. The building materials in the structure absorb water vapour from the atmosphere until equilibrium is reached, or if the partial pressure of water vapour in the masonry is higher than the partial pressure of water vapour in the surrounding environment, water vapour is released until equilibrium is reached in the atmosphere. However, the equilibrium state depends on the temperature of the environment and the partial pressure of water vapour. These phenomena are called water vapour sorption and desorption [9].

If the humidity is in stable equilibrium between the humidity in the structure and the humidity in the ambient air, the humidity equilibrium state is reached. Equilibrium moisture content is characterized as zero moisture and temperature increment over time under given conditions. Equilibrium humidity is dependent on temperature, relative humidity and atmospheric pressure. If the atmospheric pressure is constant, the equilibrium moisture content of the air depends only on the temperature and relative humidity of the ambient air. The equilibrium moisture content increases with the content of water-soluble salts [10].

3.1.2. Moisture processes in building materials

As mentioned above, water is everywhere around us and in building structures. It becomes a problem when it starts to accumulate in one place. Its accumulation accelerates the ageing of materials, deteriorates thermal properties and causes biodegradation processes.
Water can be found in building materials in liquid, gaseous and solid forms. In order for water to spread, it needs a porous environment with open pores.

Selecting only one transport process for a particular permeant may represent a simplification of the real conditions. In a real design, we usually encounter a larger number of transport processes occurring either simultaneously or in different parts of the flow path, which we call mixed transport.

3.1.2.1. The diffusion

The flow of heat and moisture is generated when the different temperatures are balanced. The direction of the flow is determined by the desire to equalize the pressure differences, so it flows from a place with a higher partial pressure of water vapour to a place with a lower pressure (Figure 1). This phenomenon is called diffusion.

The size of the pores is important. Water vapour is only able to diffuse through pores larger than $2.78x10^{-10}$ m. Therefore, if the substance in question has smaller pores, water vapour diffusion is ruled out [9].

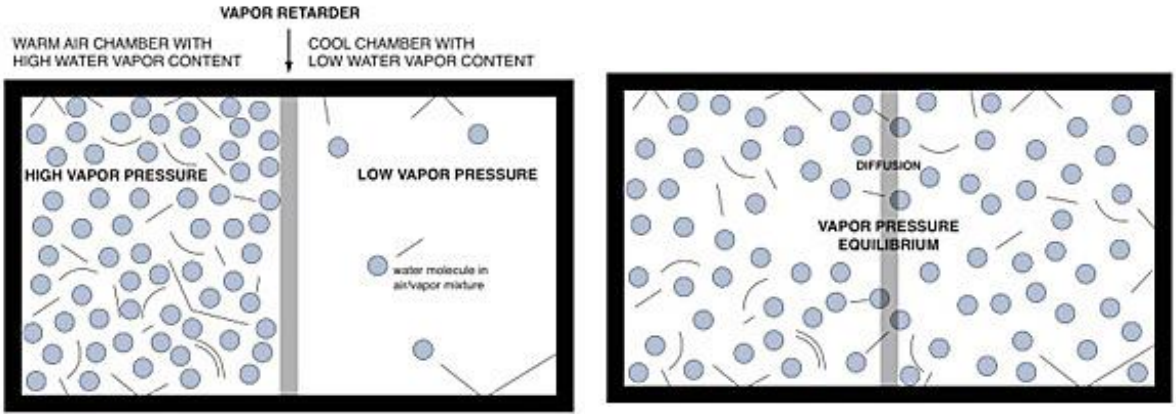

Figure 1: Water vapour diffusion
Source: [F1]

What we are most interested in with building materials is [9]:

- Diffusion coefficient
  Expresses the ability of a material to transmit water vapour by diffusion. For example, for concrete the diffusion coefficient is $\delta=0.013\times10^{-9}$ s and for ceramic brick $\delta=0.031\times10^{-9}$ s.
- Diffusion resistance factor
  Expresses how many times slower the transport of water vapour through a material is compared to the transport of water vapour in air. For example, for concrete the diffusion resistance factor is $\mu n=17-32$, for ceramic brickwork $\mu_n=9$
- Equivalent diffusion thickness
  Expresses how thick a layer of air would have to be to have the same diffusion resistance as the building material being measured.

Diffusion can be gaseous (carbon dioxide - causes carbonation of concrete) or ionic (chlorides - causes corrosion of steel reinforcement).

3.1.2.2. The capillary conduction

Capillary conduction can be observed for water-wetting materials, and most building materials (concrete, brick, brick, etc.) can be included in this category. When a water-absorbent material is partially immersed in water, the height of the water column is determined by the size of the pores. Although materials with large pores will absorb water quickly, it will not reach the same height as materials with small pores. In a simplified way, capillary conduction (buoyancy) can be described as capillary elevation, which is characterized by the difference in the height of the liquid level in the capillary versus the level of the surrounding area [2].

Capillary conduction can be defined by the following equation (4) [2]:

(4) $$h = \frac{2 \times \sigma \times cos\theta}{r \times \rho \times g}$$

σ = surface tension of the liquid [N/m]
θ = the wetting angle between the liquid and the capillary wall [°]
r = the capillary radius [m]
ρ = the bulk density [kg/m^3]
g = the gravitational acceleration [m/s^2]

If the walls of the capillaries are covered with substances that prevent wetting, the wetting angle will change accordingly.

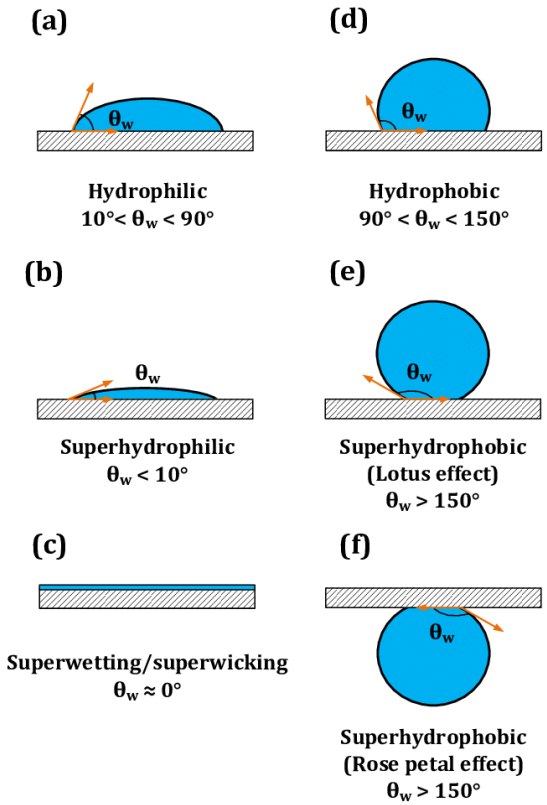

Figure 2: Illustration of Wettability
Source: [F2]

If the wetting angle θ ≥ 90°, capillary depression (hydrophobicity of the material) occurs (Figure 2).

3.1.2.3. The condensation

We distinguish capillary condensation inside porous materials. Surface condensation is more important in building structures. The relative humidity (ϕ [%]) is determined by the ratio of

the partial pressure of water vapour (p_v [Pa]) to the partial pressure of saturated water vapour ($p_{v,sat}$ [Pa]).
Completely dry air contains no water vapour ϕ = 0 %, saturated air ϕ = 100 %.

The percentage of water vapour saturation is temperature dependent. If $p_v = p_{v,sat}$ [Pa], the relative humidity has reached 100%, a further drop in temperature or increase in $p_{v,sat}$ [Pa] will cause condensation of excess water vapour (Figure 3). This will show up as water droplets on the building structures [2].

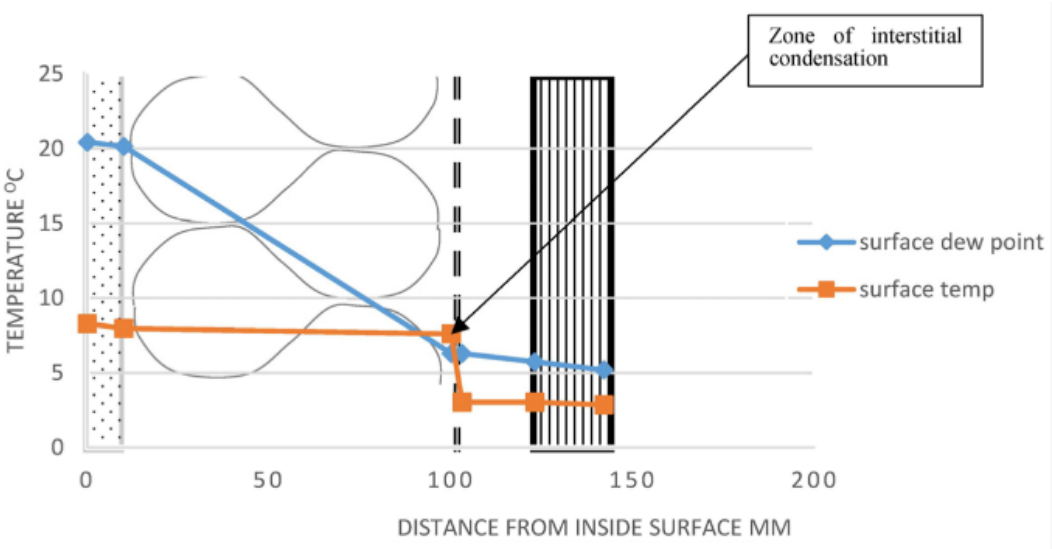

Figure 3: Interstitial condensation calculations
Source: [F3]

3.1.2.4. The sorption

All building materials absorb water vapour from the air, a phenomenon called sorption. There are 3 main types of sorption: adsorption, absorption and chemisorption [9].

- **Adsorption** is caused by van der Waals forces. There is a mutual attraction between solid molecules and water vapour molecules. The surface of the solid phase is typically characterised by the existence of undrained force fields towards free space. They arise as a result of the non-equilibrium mechanical state of the surface atoms in the solid phase crystals, where their attractive forces of an electrical nature towards the interior of the material are not compensated. As a consequence, the molecules of the surrounding gas are trapped on the surface of the solid phase, thus at the same time completely or at least partially compensating the aforementioned force fields.
- **During absorption**, the liquid or gaseous phase is absorbed by diffusion and conduction into the solid phase
- **In chemisorption**, the chemical bonding of water and the solid phase of the material is applied

The amount of water vapour absorbed by a material can be represented by a curve called **the sorption isotherm** (Figure 4). It is dependent on pressure and temperature. In the graphical representation, the relative humidity is on the x-axis, sometimes also the partial pressure of water vapour. On the y-axis is the moisture content or increment of moisture content. The curve is hysteretic meaning that it does not correspond to desorption. Thus, some moisture remains accumulated in the material.

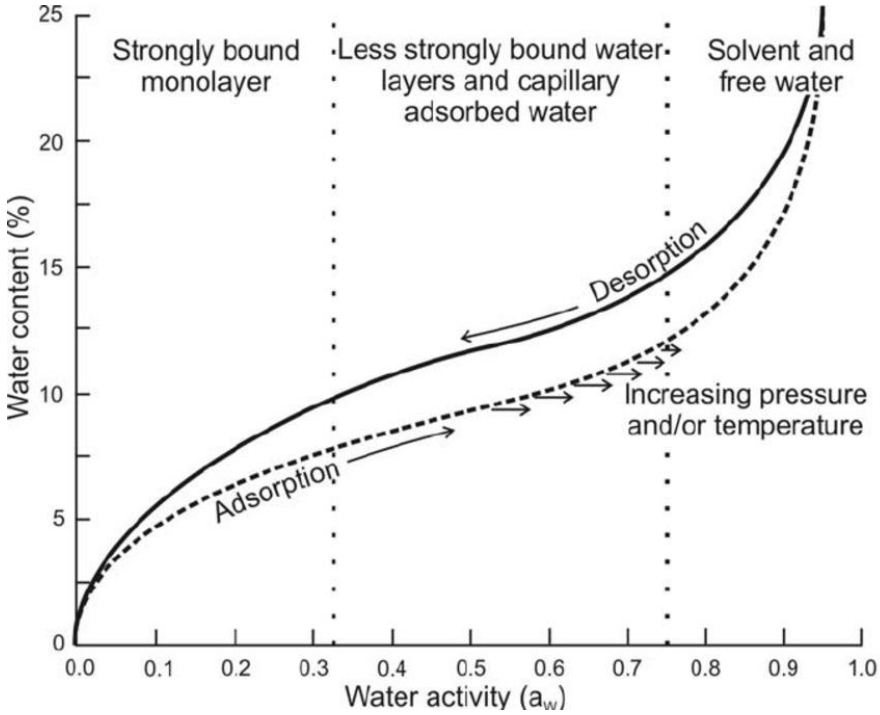

Figure 4: Adsorption isotherm with a hysteresis loop
Source: [F4]

The sorption isotherm is obtained by measuring, for example, dynamic methods. It is a gravimetric method that allows rapid measurement of mass changes. The mass of the sample is monitored by means of scales placed in a thermostatic chamber with controlled temperature and relative humidity.

3.1.3. Deterioration of selected building materials

3.1.3.1. Interaction of water and building material

The building materials are chemically degraded by a number of substances that affect its structure and properties. In liquid form they occur as solutions of acids, bases or salts and organic substances.
The rate of chemical corrosion corresponds to the migration of aggressive substances through the surface layer.

According to the type of reaction of building materials (concrete) with the liquid aggressive environment, three types of corrosion [11] are distinguished, as shown in the following diagram (Figure 5).

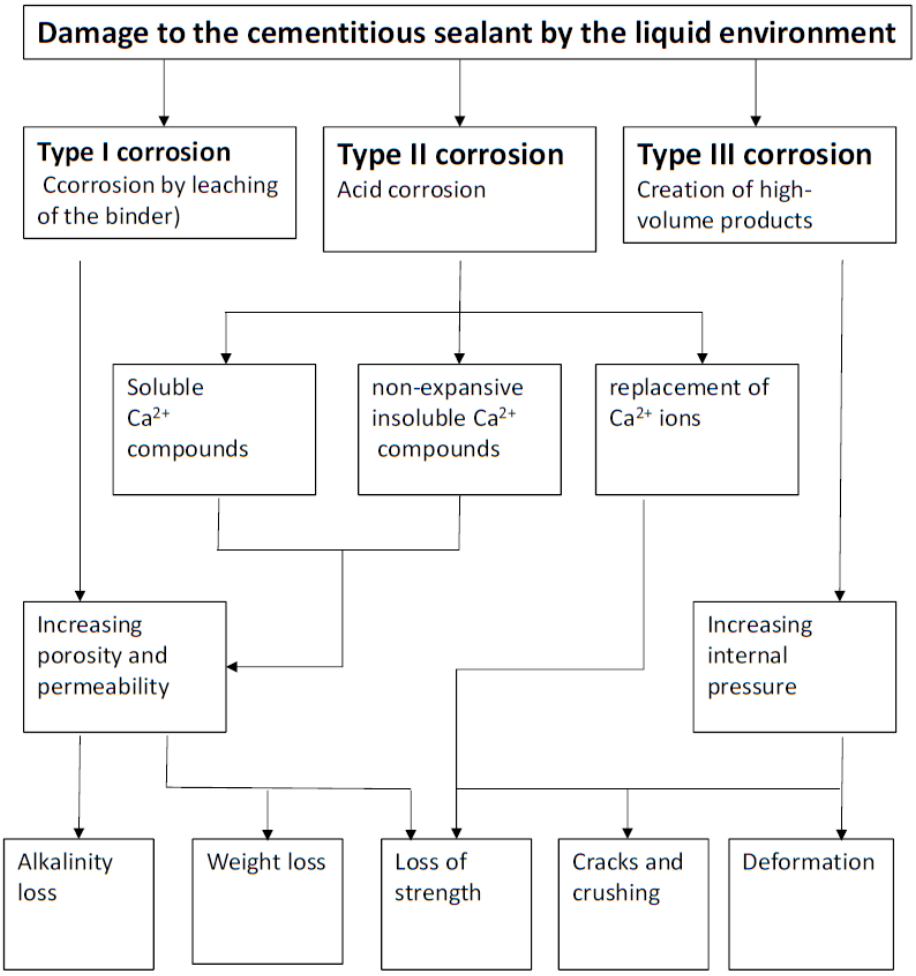

Figure 5: Diagram of concrete damage by liquid aggressive environment
Source: [F5]

Chemical corrosion means the erosion and change of material properties due to the action of aggressive substances in the liquid or gaseous state.

Type I corrosion (corrosion by leaching of the binder)

This type of corrosion can be easily illustrated **by the failure of concrete, plaster or mortar joints.**

Corrosion type I consists in the leaching of **calcium hydroxide** from the cementitious sealant (Figure 6, Figure 7). This is present both as a saturated solution and as portlandite crystals. Leaching reduces the concentration of hydroxide ions and lowers the pH of the pore solution. This reduction causes a decrease in the stability of the hydrated clinkers, as well as a decrease in the passivity of the steel reinforcement. With a significant decrease in pH, the clinker

minerals may also gradually decompose into SiO_2, Al_2O_3, Fe_2O_3 oxides. Clinker materials are highly basic compounds and are therefore only stable in alkaline environments. Structures that come into contact with so-called **hungry water**, i.e. water that contains very few calcium and magnesium ions, are at risk of this type of corrosion. These are mainly precipitation, river and pond waters [11].

The rate of leaching of calcium hydroxide (the solubility of $Ca(OH)_2$ is 160 mg/100 g of water at 20 °C) depends on the water permeability of the concrete and, in the case of water under pressure, on its hydrostatic pressure [11]. The released calcium hydroxide **carbonates** in contact with air, see equation (5). It is manifested on the surface of the concrete structure by craters or a firmly adhering layer of calcite.

(5) $Ca(OH)_2 + CO_2 \rightarrow CaCO_3 + H_2O$ *[11]*

The rate of this leaching is directly proportional to the amount of capillary pores in the cementitious sealant and the hydrostatic pressure of water on the structure. If the number of capillary pores is low and the diameter of these pores is small, leaching occurs only at the surface of the concrete, whereas at higher porosities with larger diameters, high filtration rates occur and large amounts of $Ca(OH)_2$ are dissolved and leached [11].

Figure 6: Corrosion I – leachates
Source: Author

Figure 7: Corrosion I – leachates
Source: Author

Type II corrosion (acid corrosion)

For the sake of context, corrosion type II is shown again **on the concrete structure.** The concrete structure was also used as an example because part of the dissertation is devoted to the development of a progressive rehabilitation procedure for the restoration and conservation of military fortress buildings from the 1930s. The dissertation is a continuation of the NAKI II research project DG18P02OVV063.

It is caused by exchange reactions between the cementitious putty components, especially $Ca(OH)_2$, and aggressive substances acting on the concrete. It includes reactions of aggressive CO2a, hydroxides, acids, magnesium and ammonium salts (excluding sulphates). This results

in either soluble or insoluble compounds that have no binding properties and are not expansive [11].

The acids react with calcium hydroxide, hydrated silicates and calcium aluminates from the cementitious putty to form the corresponding calcium salts. In general, the reaction of Ca(OH)2 with an acid can be written by the equation (6):

(6) $Ca(OH)_2 + 2H^+ \rightarrow Ca^{2+} + 2H_2O$ *[11]*

e.g. the reaction with hydrochloric acid is written by the equation (7):

(7) $Ca(OH)_2 + 2\ HCl \rightarrow CaCl_2 + 2H_2O$ *[11]*

At pH lower than 4, the reaction with hydrated clinker minerals already occurs to form a gel of $SiO_2 \cdot nH_2O$ and the aluminium and iron salts of the acid.
The soluble products are then washed away and attack other parts of the cementitious sealant; on the other hand, the resulting insoluble compounds form a protective layer on the surface and prevent further penetration of aggressive substances, sometimes leading to **a partial hardening of the concrete surface.**

Organic acids (most notably acetic acid, lactic acid, for example) react in a similar way. **These problems are encountered mainly in agricultural buildings and in buildings in the food and chemical industries** (Figure 8, Figure 9).

The presence of **mineral water** containing carbonic acid first leads to the formation of CaCO3 (concrete carbonation), which is poorly soluble and partially seals the pores in the cement stone. This carbonate is, however, further converted by carbonic acid into a soluble form to acid carbonate $Ca(HCO_3)_2$, which is highly soluble. There is an inverse relationship between carbonate hardness and water aggressiveness [11].

Concrete corrosion is caused by soft waters with a low carbonate (intermediate) hardness up to pH 6° (1° pH = 10 mg CaO/l). The higher the carbonate hardness of the water, the more CO32- can be present without corrosively compromising the concrete [11].

Water can also contain carbon dioxide, which comes in three forms: [1]

- *CO_2 (aq) a H_2CO_3 (circa 1%) at pH < 4,5*
- *HCO_3^- at pH 4,5 up to 8,3*
- *CO_3^{2-} at pH > 8,3*

There is an equilibrium between the different forms of CO_2 depending on the pH and the concentration of cations present. The aggressive carbon dioxide CO_2 is found in environments where this balance is disturbed by an excess of CO_2. It then reacts with calcium hydroxide from cement putty to form first $CaCO_3$ according to equation (8) [11] and then $CaCO_3$ starts to dissolve into bicarbonate according to Eq:

(8) $CaCO_3 + H_2O + CO_2 \rightarrow Ca^{2+} + 2HCO_3^-$ *[11]*

Calcium bicarbonate occurs only in solution, under suitable moisture and temperature conditions it is converted back to $CaCO_3$[11].

Furthermore, concrete is corroded by **seawater** (contains SO_4^{2-}, Cl, Mg^{2+} ions), **sewage water** (contains sulfur compounds H_2S, H_2SO_4, and ammonia compounds). The aggressive compounds NH_4+ are also present in urea. Industrial wastewater is also mostly harmful.

Figure 8: Type II corrosion (acid corrosion)
Source: [F6]

Figure 9: Type II corrosion (acid corrosion)
Source: [F7]

Type III corrosion

This includes building structure deterioration due to the formation of bulky compounds, for example **gypsum corrosion.** The reaction of calcium hydroxide with sulphates produces gypsum, which fills the pores. After recrystallisation into bulkier crystals, it increases its volume (up to 17 %) and presses against the pore walls (Figure 10, Figure 11). Microstructural changes occur in the cementitious putty which can lead to deterioration of physical properties, including mechanical properties. Permeability increases, water permeability decreases. A significant negative effect is a reduction in flexural tensile strength. The formation of ettringite is called Candlot salt.

The formation of primary ettringite by C_3A hydration can be described by the equation (9):

(9) $3\ CaO\ .\ Al_2O_3 + 3\ \mathbf{CaSO_4\ .\ 2\ H_2O} + 26\ H_2O \rightarrow \mathbf{3\ CaO\ .\ Al_2O_3\ .\ 3\ CaSO_4\ .\ 32\ H_2O}$ *[12]*

Formation of primary ettringite – Cement Chemistry (10):

(10) $C3A + 3CSH2 + 26H \rightarrow C6AS3H32$ *[11]*

Following are the primary compounds, their chemical formulas, and abbreviations used by cement chemists:

Tricalcium silicate	*3CaO . SiO2*	*= C3S*
Dicalcium silicate	*2CaO . SiO2*	*= C2S*
Tricalcium aluminate	*3CaO . Al2 O3*	*= C3A*
Tetracalcium aluminoferrite	*4CaO . Al2 O3 . Fe2 O3*	*= C4AF*

Gypsum reacts with hydrated and non-hydrated aluminates and causes so-called sulfoaluminate corrosion. The complex reaction produces a poorly soluble **secondary ettringite.**

The formation of secondary ettringite can be described by the eq. – Cement Chemistry (11):

(11) $C_3AH_6 + 3CSH_2 + 20H \rightarrow C_6AS_3H_{32}$ *[11]*

The risk of secondary ettringite can be reduced by using cements with a limited C3A content, so-called sulphate-resistant cements, and a lower water coefficient.

Sulphates can be internal or external. Internal sulphates (sulphates within the concrete) come from aggregates or improperly used water. External sulfate corrosion results from contact of concrete with water or vegetated soil with a high concentration of sulfates. Common forms of sulfate in the natural environment are calcium, magnesium, and sodium.

Figure 10: Corrosion III - sulphate corrosion
Source: [F8]

Figure 11: Corrosion III - sulphate corrosion
Source: Author

3.1.3.2. Effects of frost

The most stressed building structures exposed to the effects of frost in the presence of water are those in the plinth area, cornices, balconies, etc. According to the Erlin/Mather effect, the deterioration of a building structure is caused by stresses in the building material caused by the expansion of ice due to thermal expansion. According to this theory, deterioration is most intense when the temperature warms up (worst at temperatures just below 0 °C).

In general, two types of frost effect on building structures are distinguished:

- **Surface damage =** It occurs in the surface layer of the material (Figure 12, Figure 13). The degree of damage is expressed in terms of the mass of material detached (i.e., waste). In addition to aesthetic changes, this type of damage may result in reduced service life of the structure. The surface is distorted and cracks are formed. The damage increases proportionally with time and with the number of freeze cycles (cracks propagate).

- **Damage to the internal structure =** It is caused by freezing of water inside the material (depending on saturation). The physical-mechanical properties are degraded, which is significant both in terms of durability and in terms of load-bearing or serviceability limit states. Typically, there is a decrease in the dynamic modulus of elasticity E [Pa].

In both cases, **the pore structure** of the material is one of the decisive factors for the frost resistance of the material. The basic condition for freeze failure is the saturation of the material with water (water/ pore volume ratio). The water saturation of the material is due to the presence of capillary pores which draw water into themselves by capillary elevation.

Frost resistance by complying with the following requirements

- a reduction in the volume of the capillary pores, e.g. in concrete by reducing the water coefficient
- aeration of the material (possible for ceramics, concrete, etc.)
- use of dense, frost-resistant aggregates (e.g. for concrete)

Figure 12: Surface damage
Source: Author

Figure 13: Bridge ledge deterioration
Source: Author

3.1.3.3. Biological deterioration

Biological deterioration accompanies any of the above. The decay and roughening of the surface of the structures results in the retention of fine dust particles, humic substances and cracks, which provide a breeding ground for the invasion and growth of mosses and grasses (Figure 14, Figure 15). At this point there is a synergy with chemical corrosion, which greatly accelerates the deterioration processes. In the dusty and clay parts, weak sulfuric acid from acid rain is initially retained, which gradually reaches a concentration affecting the disintegration of the material structure. Moreover, the biological agent itself induces and maintains the moisture status and the formation of chemicals produced by the root system.

Figure 14: Biological deterioration
Source: Author

Figure 15: Biological deterioration
Source: Author

3.2. THE INFLUENCE OF RADON ON HUMANS AND CIVIL ENGINEERING STRUCTURES

3.2.1. Radon and its effect on humans

Radon is a ubiquitous natural radioactive gas. It is formed by the gradual transformation of uranium, which is present in varying amounts in all materials in the Earth's crust. Radon itself is converted into other radioactive elements (isotopes of polonium, lead and bismuth), which are trapped in the respiratory tract and irradiated when inhaled [13].

Table 2. Summary of risks of lung cancer from indoor radon based on international pooling studies that have combined individual data from a number of case-control studies and on studies of radon exposed miners

	Nbr. of studies included	Nbr. of lung cancers	Nbr. of controls	Exposure Window (years)[a]	Percentage increase in risk of lung cancer per 100 Bq/m³ increase in radon concentration	
					Based on measured radon	Based on long-term average radon[b]
Pooled analyses of studies of indoor radon in the home						
European (Darby et al. 2005, 2006)	13	7 148	14 208	5-35	8 (3, 16)	16 (5, 31)
North American (Krewski et al. 2005, 2006)	7	3 662	4 966	5-30	11 (0, 28)	-
Chinese (Lubin et al. 2004)	2	1 050	1 995	5-30	13 (1, 36)	-
Weighted average of above results of pooling studies					10	~20[c]

Figure 16: Summary of risks of lung cancer from indoor radon based on international pooling studies that have combined individual data from a number of case-control studies
Source: [13]

Scientific studies have provided clear evidence of a link between radon exposure in building interiors and lung cancer. This risk is already present at the relatively low levels of radon commonly found in residential buildings (Figure 16) [13, 14].

Radon is a radioactive gas that emanates from rocks and soil and concentrates in confined spaces such as underground cavities or building structures (especially at the contact between rooms and the subsoil = ground floor, cellars) [15, 16]. Infiltration of soil gases is considered the most important source of radon in residential buildings. Other sources, including building materials and water drawn from wells, are generally less important [13]. The use of conventional building materials contributes minimally to the overall exposure of the population [17].
Current estimates of the proportion of lung cancer caused by radon inhalation range from 3 to 14%, depending on the average contribution of radon to cancer [13].
Analyses show that the risk of lung cancer increases proportionally with increasing radon exposure (Figure 17). Most people are exposed to low and moderate concentrations of radon. This implies that most radon-related lung cancer cases are due to low concentrations.

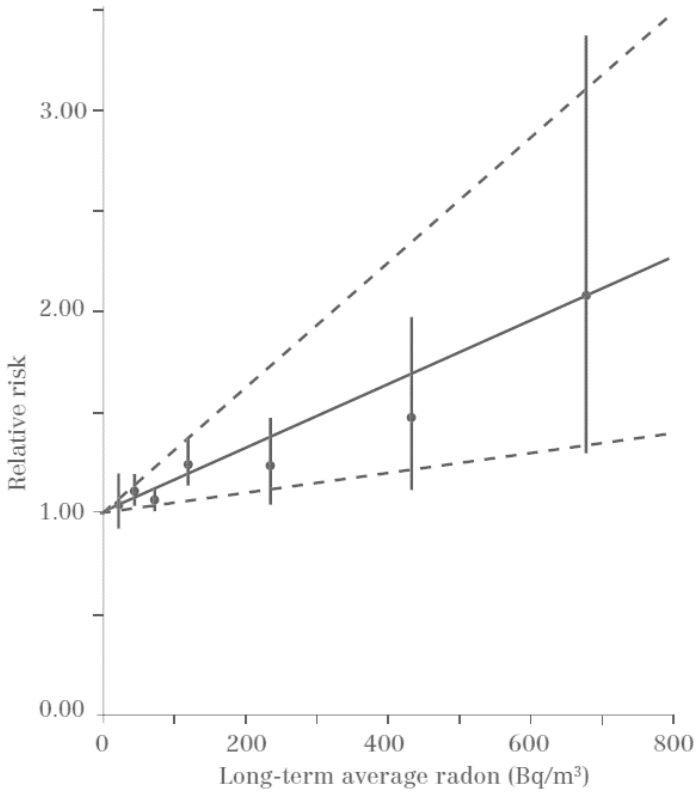

Figure 17: Relative risks and 95% confidence intervals are shown for categorical analyses and also best fitting straight line. Risks are relative to that at 0 Bq/m^3.
Source: [13]

Radon measurement is relatively simple and is essential for the assessment. radon concentration in houses. It needs to be based on standardised protocols in order to ensure accurate and consistent measurements. Concentrations vary considerably with time (by season, day and even hour). Because of these variations, estimating the average annual concentration of radon in indoor air requires reliable measurements of average radon concentrations. The recommended measurement period is at least three months and preferably longer. Short-term measurements provide only a rough indication of the actual radon concentration [13].

3.2.2. Radon in the building and its reduction

Consideration of radon exposure is important both in new building construction (prevention) and in existing buildings (mitigation or remediation). The primary measure is to seal the building structure in contact with the soil. Waterproof membranes placed continuously in the area that are in contact with the soil are among the cheapest and easiest solutions for reducing radon in a building.
Another way to address radon intrusion into a building is to reduce the pressure differential between the interior occupied space and the exterior soil. Reducing pressure differences is particularly important in countries where there is a high temperature difference between indoor and outdoor environments, especially in winter (Central and Northern Europe, North America, etc.). The installation of underfloor heating in contact with the ground also causes an increase in pressure (and thus an increase in radon concentration).
In most cases, a combination of several types of measures is best to reduce radon concentrations in a building.

Decree No. 307/2002 Coll., on radiation protection, as amended by Decree No. 499/2005 Coll. and Decree No. 389/2012 Coll., establishes so-called guideline values for radon content in existing and new buildings.

- in the living space of existing buildings, the average value of the so-called radon volume activity should not exceed 400 Bq/m^3 [19]. If it is exceeded, it is recommended to implement at least one of the anti-radon measures mentioned above. If a value even higher than 4000 Bq/m^3 is measured, the long-term stay of persons in such a room should be excluded [19].
- In the living space of a new house, the average volumetric radon activity should be less than 200 Bq/m^3 [19], so precautions must be taken in new construction.

In the Czech Republic, the average value of equivalent radon activity in buildings is around 120 Bq/m^3. with the highest concentration of radon in dwellings in the world [20]

About 2-3 % of residential houses have values higher than 400 Bq/m^3, these are mainly family houses (mostly ground floor parts of the building) [20]

In the outdoor atmosphere, the radon concentration is approximately 10 Bq/m^3, whereas the radon concentration in soil air at a depth of 1 m underground in the Czech Republic is between 20 000 and 2 000 000 Bq/m^3 [20].

The above implies the need to design the right solution to protect human health. The correct design procedure for designing measures is defined in the Czech Republic by the standard ČSN 73 0601 [21].

The primary measure is, as mentioned above, the implementation of an anti-radon membrane. To properly design such a measure, it is crucial to know the permeability of the insulation and building materials used [17]. The ability of the insulation material to provide sufficient protection against radon is determined by its thickness and the radon diffusion coefficient. The quantity that combines these two parameters is defined as the radon resistance [17, 18].

Radon resistance is defined as the ratio between the material thickness and the diffusion coefficient of radon in the material as expressed in equation (12) [18, 21].

(12) $$R_{Rn} = \frac{\sinh d/l}{\lambda \times \mathrm{l}}$$ [s/m]

R_{Rn} = radon resistance [s/m]
d = the thickness of the material [m],
l = the radon diffusion length in the material calculated as $l=(D/\lambda)^{1/2}$ [m],
D = the radon diffusion coefficient of the waterproofing material [m^2/s]
g = the gravitational acceleration [m/s^2]
λ = the radon decay constant [s^{-1}],

Radon values resistance values are given by the insulation manufacturers for each product in the relevant datasheet.

Radon insulation is designed so that its radon R_{Rn} [s/m] is greater than or equal to the minimum radon resistance $R_{Rn,min}$ [s/m]. $R_{Rn,min}$ shall be calculated depending on the parameters of the house and the design concentration value of radon in the soil air according to the relationship (13) [21]:

(13) $$R_{Rn,min} = \frac{3600 \times \alpha_1 \times C_s}{\mathrm{E}_{mez}}$$ [s/m]

C_s = the design radon concentration in soil air [Bq/m^3]
α_1 = dimensionless safety factor according to ČSN 73 0601 [21]
E_{mez} = maximum permissible rate of surface emission of radon into the building [Bq/(m^{2}h)].

To calculate the maximum rate of surface emission of radon into the interior of E_{mez} [MPa], the following relation applies (14):

(14) $$R_{mez} = \frac{C_{dif} \times V_k \times n_{nh}}{(A_p + A_s)}$$ [Bq/(m²h)]

V_k = volume of the calculation room in the contact floor [m³],
n_{nh} = design value of ventilation intensity [h⁻¹],
A_p = plan area of the calculation room in contact with the substrate [m²],
A_s = area of the basement walls of the calculation room in contact with the subsoil [m²]
C_{dif} = 10 % of the design value of the radon concentration in the building C_{nh} [Bq/m³].

It should be stressed that the effectiveness of insulation materials in reducing radon transport from the soil depends not only on their radon resistance, but also on other important properties (mechanical resistance, ability to form airtight joints, and detailing - penetrations). Another factor is compatibility with other building materials, sufficient durability, etc [18, 22, 21]. **A suitable solution may be, for example, waterproofing screeds, which can be used to create a continuous layer without leaks and joints.**

When designing measures, it is important to verify the extent to which the waterproofing materials meet the radon resistance requirements prescribed by the applicable design methodologies or building standards [18].

Several data analyses and research studies have been carried out to test commonly used building insulation materials. It is worth mentioning, for example, the extensive research of 650 materials on the Czech market, which was carried out in [18]. According to [18], most of the waterproofing materials used today provide sufficient protection against soil moisture, groundwater and radon. There is no need to develop new
waterproofing materials specifically designed against radon, as more than 95% of current waterproofing products meet the minimum requirements of the legislation [18].

As mentioned above, waterproof materials provide basic protection for buildings against moisture, groundwater and radon from the soil. These are most commonly polymer and asphalt strips or waterproofing membranes. The loss of their impermeable properties due to premature deterioration may cause a complete loss of protection of the building from radon ingress from the subsoil [22]. Degrading agents such as soil bacteria, radon, high temperature and high humidity and possibly combinations of these factors have already been investigated [22] and the results of the experiments published.

Experimental work was carried out to verify the ability of waterproofing membranes as an insulator against radon. And also, the effect of water and freezing cycles as a degrading agent.

3.3. WATERPROOFING SCREEDS

Waterproofing screeds are a common way of protecting structures against the ingress of water to enhance their durability. The commonly used screed has a number of proper applications in building structures (basements, balconies, wet rooms) [23-25] as well as in civil engineering (water reservoirs, bridges [26-27]), tunnels [28]).

According to national standards, waterproofing screeds are defined as waterproofing compounds resistant to water, which are applied to an insulated structure by painting, trowelling or cold or hot spraying under specific conditions. After the on-site application, they form seamless screed waterproofing.

Significance of Waterproofing screeds:

- Moisture prevention: One of the primary objectives of building waterproofing is to prevent water ingress, a key factor in preserving structural integrity. Fibrous materials, such as bituminous or polymeric screeds, create an effective barrier against moisture that could otherwise lead to structural damage.
- Protection deterioration: Waterproofing membranes prevent the deterioration of building materials caused by moisture. Without adequate insulation, wood could rot, metals corrode, and concrete deteriorate, negatively impacting the overall stability of the structure.
- Extension of building lifespan: Investing in quality waterproofing yields significant long-term benefits. Keeping a structure dry and secure helps minimize maintenance costs and enhances the overall resilience of building elements.

Waterproofing screeds can be divided into three groups according to the material composition. The first group are waterproofing screeds based on bitumen (bitumen varnishes, emulsions, dispersions). The second group of waterproofing screeds is based on synthetic polymers (polyurethane, epoxy, polyester, dispersion, special synthetic), and the third group is based on silicate screeds (a mixture of finely ground cement in a mixture with sand or limestone and modifiers). Alternatively, the advantages of individual groups can be used, and the above-mentioned materials can be combined [29].

Table 2 lists the types, compositions, and the main mechanisms of waterproofing screeds [29]. All the three main groups mentioned above and combinations thereof are included. These types of waterproofing screeds are covered in various international standards and guides such as ACI 515.1R [30], ACI 515.2R [31], EN 1504-2 [32] or as WTA [33], DIN 18195-1:2000 [34] and ČSN 73 0610 [3].

Table 2. Summary table [29]

Main group	Basic description	Compounds	Method of operation
Bitumen screeds	Liquid-applied membranes that are adhered to the surface (with possible fibrous reinforcement).	Bituminous materials and coal tar emulsion with possible modification with polymers (e.g., styrene-butadienestyrene copolymer).	Formation of external flexible barrier (dampproofing).
Polymer screeds		Polymeric compounds (e.g., acrylic, epoxy, polyurethane etc.).	Formation of external barriers with good adhesion to concrete and minimum blistering and cracking.
Silicate (cementitious) screeds	Cementitious dry powder blends including active ingredients, cement, fine sand, and other additives that require only the addition of water upon application.	Silicate and fluorosilicate compounds.	Formation of external rigid barrier with diffusible pore blocking reactive materials that form hydrophilic crystals that expands by swelling within the cementitious layer and concrete pores.
Polymer modified silicate screeds	Two-component system of blends of cement, fine sand, and fibers that require the addition of polymeric emulsion at the job site.	Fibers and polymers (e.g., acrylic polymer).	Formation of external flexible impermeable cementitious barrier with pore blocking effects.
	One-component dry powder blends of cement, fine sand with polymeric additives (and fibers) that require the addition of water upon application.	Redispersible polymer powders [e.g., poly (styrene-acrylic ester)].	

Today, waterproofing screeds are most often used in the case of solving complex construction details in combination with other screed sheet waterproofing [35-37]. They can also be used as waterproofing with protective utility layers (balconies, terraces, roof coverings). Common applications can also be found in the use of waterproofing screeds in the remediation of moisture faults [26], [37-40].

The use of waterproofing screeds may depend on the specific needs and conditions of the building. In areas such as (foundations, roofs, balconies, water tanks as well as interior applications such as bathrooms) these materials are often a key element for maintaining the waterproofness of the structure.

3.3.1. Types of waterproofing screeds

3.3.1.1. Bituminous screeds

Bituminous screeds have evolved from the commonly and traditionally used bitumen waterproofing. Bituminous screeds as well as asphalt strips are used to insulate all surfaces of the substructure (vertical and horizontal). Like asphalt strips, they can be used as protection against ground moisture and pressurized water. The protection is, therefore, comparable.
The bituminous insulating screeds (waterproofing putty according to national standards), known in Germany under the abbreviation of KMB (Kunststoffmodifizierte Bitumendickbeschichtung) [33], have an asphalt emulsion binder.

Figure 18: Application of bitumen waterproofing screeds with a reinforcing belt
Source: Author

Figure 19: Application of the bitumen waterproofing screed on a detail with a complex shape
Source: Author

Their sealing viscosity is enhanced by thickening with light flexible fillers (polystyrene granulate, rubber, etc.). The grain of the filler determines the thickness of the layer, and this is now specified by standards and guidelines. For the use of KMB in new constructions, the reference of DIN 18195 (08-2000) [34] applies, which requires a dry layer thickness of at least 3 mm for lower loads - ground moisture, unretained seeping water, non-pressurized water in damp areas, and a dry layer thickness of 4 mm for higher loads - pressurized water and retained leaking water.

The main advantage of bituminous screeds is their long service life. Unlike asphalt strips, they do not break and do not lose flexibility (do not become brittle) [41]. Significant effect also can be observed of heat and ultraviolet aging on the structure, and the properties of SBS-modified bitumen for watertightness [42]. The application of a waterproofing screed creates a screed without joints (Figure 18), which are a very common cause of failures of the waterproofing system with asphalt strips (no joints, cuts and waste are created). The screed is, therefore, suitable as insulation for rugged surfaces and easy connection of vertical and horizontal surfaces (Figure 19). The sealing details can also be easily solved. With the correct design and

adherence to the technological process, they adhere fully to the substrate, which can be uneven. The bituminous screed can also be used to seal joints [34].
Bituminous screeds are applied to the prepared substrate (concrete, plaster, brickwork, silicate blocks, etc.) [34]. Most often, the substrate is impregnated with a bitumen emulsion, and the mixed screed (it can be mixed mechanically or manually) is always applied in two layers [34].

According to the commonly used manufacturer's technical sheets, the first layer is applied up to a maximum of 50% of the total thickness. If protection against pressurized water is required, a reinforcing mesh is incorporated into the fresh first layer. The second layer can be applied only after the first layer has hardened.
The disadvantage of this type of screed, in general, is the complexity of the implementation (it is necessary to follow the manufacturer's technical sheet temperature, humidity, dosage, mixing speed, etc.) [34, 41-43]. Due to their appearance, bitumen screeds are not suitable for use in visible constructions, because the surface is usually black-brown, uneven and may be greasy.

3.3.1.2. Silicate (mineral) screeds

Thanks to the cement binder, these screeds are easy to process for a wide range of construction practices. Only a bucket for mixing the mixture and masonry tools are enough for processing.
The mineral insulating screed (a silicate waterproofing compound according to the technical standard) is listed in German-speaking countries under the abbreviation of MDS (Mineralische DichtungSchlämme) [33]. The composition is formed by micro-milled cements (often also sulphate-resistant) with mineral fillers and organic finishing additives. Its important advantage is high adhesion to mineral substrates [44-45].
The screed can withstand even the negative pressure of penetrating water. This pre-destines it especially for insulation on the inner face of masonry, on structures inaccessible from the outside. With such a mass, it is possible to create a kind of inner tube that retains water in the structure [46]. Compared to bitumen screeds, the matrix of silicate-based screeds is more porous and remains relatively diffusely open.

By adding a polymer to the silicate mixture, a modified silicate waterproofing com-pound is created. In addition to micronized cements and mineral fillers, it also contains a large admixture of a plastic or elastomer dispersion [33-34].
Unfortunately, the addition of polymers impairs adhesion to the substrate. Flexible MDS are, therefore, only used on the water pressure side, usually for the insulation of tanks, pools, and reservoirs. In cases where watertightness is necessary, the ability to bridge cracks wins. Another disadvantage of flexible MDS is the lower resistance to hot water [47].

Figure 20: Application of silicate (mineral) waterproofing screeds
Source: Author

Figure 21: Application of the silicate (mineral) waterproofing screed on the drain area
Source: Author

The disadvantage of purely mineral screeds is the inability to bridge cracks that additionally form in the substrate - the layer of hardened screed is brittle [33].
The inability of silicate screeds to bridge cracks can be solved by adding additives, most often polymers. The addition of this additive creates a third large group of the squeegees described below.

The specific type of waterproofing system is the application of a crystalline screed, primarily used for the protection of concrete structures against water ingress. The crystal-line screed can also be included in the group of the solved waterproofing materials. It has already been proven that the crystalline screed significantly increases the durability of the silicate-based structure [48-49], and is also a protective system for reinforced concrete, which prevents the corrosion of the reinforcement [50]. The specificity of the crystalline screed is its functionality only on calcium silicate materials. Therefore, crystalline screeds are not the subject of this study.

3.3.1.3. Polymer screeds

Polymeric materials are based on polymer compound(s) in an organic solvent carrier or emulsified in water and formulated with other additives to improve their properties. Materials that reduce viscosity are mostly used as additives, fillers and/or reinforcing fibers [29].

At the time of application, polymeric materials are semi-solid to liquid (Figure 22, Figure 23). Like other screeds, polymer membranes have a wide range of physic-chemical and mechanical properties (e.g. adhesion, strength, elasticity). According to [51], 23 types of polymer insulators are identified which are used for application in, for example, the United States, Canada and European countries [29].

Figure 22: Application of the polymer waterproofing screeds
Source: Author

Figure 23: Application of the polymer waterproofing screed on the detail under the door
Source: Author

Three basic types are most often used: Polyurethane liquid membranes, Epoxy coatings, Acrylic membranes.

Polyurethane liquid membranes

Polyurethane compounds, although costly, are highly versatile materials extensively employed for waterproofing flat roofs and surfaces exposed to varying weather conditions. These compounds encompass aliphatic and aromatic isocyanate polyurethanes, with the latter exhibiting superior resistance against water, chemicals, and abrasion. However, aromatic polyurethanes have lower flexibility and UV radiation resistance [52].
Polyurethane membranes come in single-component and two-component systems. Single-component systems cure through a reaction with moisture, while two-component systems, mixed on-site, cure through a chemical reaction among their ingredients [53]. It's crucial to limit the film thickness for moisture-cured single-component polyurethanes to prevent the accumulation of carbon dioxide bubbles generated during curing, which could compromise bond strength and durability [52].

Polyurethane compounds involve the reaction of harmful isocyanates necessitating careful consideration of human health during installation [29].

Spray-applied polyurethane systems, offer versatility, allowing horizontal, vertical, and overhead applications with consistent thickness [29]. These systems act as vaporproofing membranes. Generalizing the characteristics of polyurethane membranes proves challenging due to variations in chemical descriptions among different types [52].

Overall, polyurethanes excel in applications on concrete surfaces exposed to traffic and deicing salts. They boast excellent mechanical properties, bonding capabilities, crack bridging, and resistance to chemical and biological attacks. However, they are not suitable for environments with high alkalinity [54].

Epoxy coatings

Epoxy systems are liquid membranes consisting of two components, created by a thermosetting polymer resulting from the reaction between resin and an appropriate hardener. In concrete applications, these systems typically rely on bis-A epoxy resins, characterized by being solvent-free with relatively low molecular weights (approximately 380 ($g \times mol^{-1}$)) [52]. The curing process of epoxy systems can pose challenges, primarily linked to potential issues arising from water and carbon dioxide interaction. Uncured epoxy may react with these elements, forming carbonic acid, leading to film defects and compromising adhesion, strength, and chemical resistance [54]. Despite these challenges, epoxy membranes generally exhibit high performance in terms of waterproofing, effectively reducing chloride ion penetration, enhancing electrical resistivity, and providing chemical resistance [29].

Epoxy systems are often recommended for applications where superior adhesion, minimal shrinkage, and resistance to chemicals are essential. However, they do exhibit lower levels of fracture energy, hydrophobicity, and thermal stability. Similar to polyurethanes, variations in the performance of different epoxy membranes are commonly reported in the literature [52].

Acrylic membranes

Acrylic liquid membranes are commonly available as single-component polymeric solutions or emulsions. These membranes undergo curing primarily through the physical drying of the solvent [54]. Acrylic emulsions stand out as the most prevalent waterproofing systems, chosen for their practicality, cost-effectiveness, and environmental considerations [53]. They find frequent application in internal wet areas and can be specially formulated to yield UV-resistant membranes suitable for external use [29].
An advanced acrylic system within this category is the methyl-methacrylate's flooring or decking system. This system relies on two components that are mixed on-site and rapidly cure to form a flexible and durable coating. Notably, this system is advantageous for installations requiring quick accessibility [29].

Acrylic membranes exhibit breathability and resistance to deterioration under conditions of alkali exposure, oxidation, and weathering. Despite these positive attributes, they do have limitations, including low adhesion strength. Acrylic membranes are not deemed suitable for prolonged immersion in water or placement beneath soil [54].

3.3.2. Applications of waterproofing barriers

The successful application of waterproofing materials depends on various factors, including the substrate's surface characteristics, application methods, and the extent of surface coverage [54]. Meeting specific requirements is crucial, involving considerations like suitable ambient conditions and thorough surface preparation. Ambient conditions, encompassing substrate and environmental moisture levels and temperatures, play a vital role, often with specified minimum temperature thresholds for applying waterproofing barriers [51]. Typically, the surface temperature requirement is set at values above 2°C or 4°C [51]. Ambient temperature directly influences substrate dryness and, in the case of polymeric barriers (PB),

affects the air entrapped within substrate pores, potentially impacting bonding. Proper surface preparation is imperative to ensure effective bonding [29].

A significant number of barrier failures result from inadequate surface conditions and insufficient preparation [29]. It is important to establish a sound surface devoid of any residues from debonding materials. Manufacturers usually outline a series of surface preparation steps. For polymeric barriers, the surface must be smooth, dry, structurally sound, devoid of protrusions, rough edges, cracks, and free from oil, laitance, curing compounds, or other contaminants [51]. ACI 515.1R [30] recommends various preconditioning methods, including typical cleaning techniques for removing oils and dirt, mechanical actions like sandblasting for deep cleaning, and chemical treatments such as acid etching to open pores for better penetration [29].

Surface cleaning involves brooms or compressed air to eliminate loose materials and contaminants, such as residuals from previous coatings [51]. Polymeric barriers should not be applied to saturated surfaces to avoid bonding issues, necessitating the exclusion of water for surface cleaning. Experimental data have shown no significant differences in bonding between air blasting and abrasive blasting [51].

Waterproofing screeds can be applied in several different ways depending on the specific needs of the building.
The most common methods are application by brush, roller, trowel, spraying, etc. The spraying method is especially effective for horizontal or overhanging surfaces.

The selection of a suitable application method depends on the specific conditions, types of material and design requirements. It is always important to follow the manufacturer's instructions and ensure that the correct conditions are maintained for optimum performance of the waterproofing trowel.

Overall, it can be said that the correct way of applying waterproofing screeds is of key importance for achieving optimal waterproof properties and extending the life of the waterproofing system.

3.3.3. The current state (trends) of the issue

As environmental awareness grows and demands for greener and more efficient materials increase, new trends in this field are emerging. Two key trends include the development of eco-friendly alternatives and innovations in application technology.

With the rise of environmental consciousness, the importance of seeking ecologically sustainable alternatives becomes paramount. In the field of waterproofing, this translates into a shift towards using materials with a lower environmental impact that are easily recyclable. Biodegradable polymers and materials derived from renewable sources are becoming

increasingly popular choices. These eco-friendly alternatives not only reduce the negative impacts of construction on the environment but often also offer excellent water resistance.

Advancements in technology bring forth innovative application methods in the field of waterproofing. Modern application techniques, such as spray technologies utilizing specialized machinery or precise nanotechnology, enable precise and efficient coverage of various surfaces. These innovations not only increase the speed and effectiveness of installation but also ensure a more uniform and reliable waterproofing layer.

3.3.4. Dissertation motivation

Due to the above-mentioned use of waterproofing screeds, they age during their life due to environmental influences such as: high and low temperature, sunlight (UV radiation) and rainfall, causing deterioration phenomena, such as frost-thawing [55]. Research [55] has confirmed significant changes in the physical and chemical properties of the selected tested building materials. The physical and chemical properties have changed. Due to frost and UV radiation, the compressive strength was reduced by at least 13%. The external environment also negatively affected the adhesion of individual plasters [55]. By reducing adhesion and compressive and tensile strength, the material's ability to bridge cracks is also significantly reduced.

The subject of the study is a laboratory analysis of the interaction of different types of waterproofing screeds with different types of building structures. The above is a description of the properties of the used waterproofing screeds with a specific focus on their cohesion of different substrate materials. More recently, the change in mechanical properties will depend on freeze-thaw cycles [56-57]. The currently used waterproofing screeds exhibit suitable tightness, however, the aspects reflecting their durability during their expo-sure to freeze-thaw cycles have not been widely studied yet. A failure of the waterproofing system could rapidly reduce the lifespan of the entire structure, and usually leads to other undesired processes in the internal environment of the building. **Damage of waterproofing system can cause the penetration of not only water and moisture but also harmful radon.**

Research methods of aging processes are based primarily on the analysis of changes in material properties based on observations in natural or artificial conditions. We get the most reliable results from long-term aging tests that have been performed for many years [55,58]. Nowadays the trend is to apply for durability on the basis of short-term tests. Trend is for accelerating ageing tests replacing long-term deterioration processes in natural conditions. These methods are based on appropriate procedures or of a simulation origin in climate chambers [55].

4. EXPERIMENTAL PROGRAM – ANALYSIS OF A VERY MATURE CONCRETE BASE FOR THE APPLICATION OF WATERPROOFING SCREEDS

The doctoral thesis is partly linked to the NAKI II research project DG18P02OVV063, which started in 2018. This NAKI project deals with the development of a progressive rehabilitation procedure for the restoration and conservation of military fortress buildings from the 1930s. The concrete used in the experiments comes from military fortress structures.

Just before WW2, in the 1930's, a lot of concrete fortifications was built in the Czechoslovakia (Czechia today). After 80 years, most of these military objects evince numerous failures due to water penetration into the concrete structures. The major part of these objects consists of light infantry bunkers (type 36 and type 37) but along the Nord border of Czechia, there were constructed 260 heavy bunkers following the example of the French Maginot line. They were large two floored buildings with strengthening ballistic protection made of heavily reinforced concrete. Two of these objects became the target for subsequent research which was focused on analysis of corrosion products from concrete structures.

The first part of the experiments deals with the analysis of corrosion products from a historic concrete structure built in the 1930s. Most of these buildings show a number of failures caused by water intrusion into the concrete structures. Two heavy bunkers have been the target of research focused on chemical and biological analysis of the structures.

Further experiments on the application and testing of waterproofing screeds was necessary to determine the suitability of using this concrete as a substrate. The results show whether the concrete used for the analysed fortifications successfully resisted the long-term effects of corrosion and is suitable for further experiments.
Selected objects for sampling:

- **Object 1 - separate infantry cabin T-S 19 Turov (Figure 24)**
  Resistance: II, Concreting: 12-15 May 1938,
  The following information was provided by the association managing the building.
  The walls of the reinforced concrete monolith are approximately 1000 mm thick, the roof 2000 mm and the front wall 2250 mm. During World War II the building was heavily damaged by the acquisition of valuable material for the German arms industry and the testing of new explosives and weapons. Nazi Germany used Czechoslovak material in its own fortifications and partly on the so-called Atlantic Wall. After World War II, the log cabin was used as a waste dump. Since 2009 the building has been cleared of waste and rubble and reconstruction has begun.
- **Object 2 - separate infantry cabin T-S 20 Pláň (Figure 25)**
  Resistance: II, Concreting: 25-30 April 1938
  The following information was provided by the association managing the building.
  In 1938, the building was largely completed and earthworks started. The electrical, plumbing and air conditioning systems were also largely completed. However, the bells were not installed. The two L1 guns installed and the log cabin largely armed. After the signing of the Munich Agreement, the infantry cabin, unlike the T-S 19 building, was on the territory of the Third Reich. The infantry cabin was the only

one of the buildings of the ŽSV V in the occupied territory, and it was located directly on the future Protectorate border, which ran on the road to the neighbouring building T-S 19. Fortunately, the log cabin was spared the more thorough tests of the Reichswehr, and so, apart from a few interventions, it has been preserved in good condition. However, it did not escape the ripping out of the firing ports for the L1 and M guns. Today, the building is managed by the T-S 20 Pláň Military History Society, which is trying to restore part of the log cabin to its original state, and an exhibition is being created in the remaining part.

Figure 24: Object 1 – T-S 19
Source: Author

Figure 25: Object 2 – T-S 20
Source: Author

4.1. Materials and method

A total of 5 samples of concrete from two heavy fortification buildings were tested. Most inorganic compounds are water-soluble due to their ionic structure. It is possible to detect the contents of these by using an aqueous solution. The salinity evaluation was started by weighing 2 g of the crushed sample into the Erlenmeyer flasks. After addition of 100 ml of distilled water, the flasks were transferred to an electric cooker, where they heated to boiling point and then subjected to ultrasound. This step resulted in the fragmentation of individual parts (Figure 26).

Figure 26: The samples are exposed to ultrasound
Source: Author

Figure 27: Inserting the samples into clean glass caps
Source: Author

The prepared solution was sedimented for 24 hours. The portion of the sample without haze and sediment was removed using a pipette. The prepared samples were then placed in clean glass caps and prepared for further examination (Figure 27).
The Merck - UV-VIS photometer Spectrogant Pharo 300 was used to evaluate all methods.

4.1.1. pH measuring

The first step of experiment was made an indicative measurement of pH using analytical test strips. The reason for this was to determine the range of measurements for further use. In case of too high concentrations it would not be possible to obtain the results from the photometer. For samples 2 and 5, it was necessary to dilute with 1:10 distilled water.
Using a pipette, 1 ml of pre-prepared sample and 3 drops of universal indicators were added to the tube. After shaking and terminating the reaction, the sample changed color. On the basis of the colorimetric reaction, the approximate pH was determined (Figure 28, Figure 29).

Figure 28: Samples with added pH indicator
Source: Author

Figure 29: Colorimetric evaluation of pH by color and scale
Source: Author

4.1.2. Measurement of chloride salts Cl-

Chloride ions react with mercury thiocyanate to form slightly dissociated mercuric chloride [59]. Loose thiocyanate is reacted with ferric ions in a red ferric thiocyanate which was determined photometrically [60].

5 ml of the treated sample was measured using a pipette. Additionally, 2.5 ml of Cl-1 reagent and 0.5 ml of Cl-2 reagent were added. After thorough shaking and settling of the sample (1 minute), the sample was evaluated. The evaluation was carried out in the Spectrogant Pharo 300 UV-VIS photometer.

4.1.3. Measurement of ammonia NH_4^+

Ammoniacal nitrogen (NH4-N) occurs partly in the form of ammonium ions and partly as ammonia [1]. Among these forms there is a pH-dependent equilibrium [59]. In strongly alkaline solutions, NH4-N is present almost exclusively as ammonia which reacts with hypochlorites to form monochloramine [1]. Monochloramine is further reacted with thymol to give blue indophenol, the concentration of which is then determined photometrically [60].

A reagent is added to the 5 ml treated sample. 0.6 ml of NH4-1 reagent and 0.06 ml of Nh4-2 reagent are used. After shaking, the tube was left for 5 minutes and then 4 drops of NH4-3 were added. The evaluation was carried out in the Spectrogant Pharo 300 UV-VIS photometer.

4.1.4. Measurement of sulphate salts SO_4^{-2}

Sodium ions react with barium iodate, iodine ions are released [1]. They oxidize to form a brown-red compound that is photometrically determined [60].

In this assay method, 2.5 ml of the conditioned sample was metered into the prepared tubes. Experimental pH measurements for samples 2 and 5 found to be pH higher than 10. For this reason, these samples were diluted 1:10 with distilled water. Subsequently, 2 drops of SO_4^{-1} reagent and 0.06 ml of SO_4^{-2} reagent were added to every tube with samples. After shaking, the tubes were heated to 40 ° C for about 5 minutes. Then, 2.5 ml of SO_4^{-3} reagent was added and a sample was filtered through the filter paper into an empty tube. Four drops of SO_4^{-4} were added to the filtered solution followed by further heating to 40 ° C. After 7 minutes, the sample could be evaluated in a Spectrogant Pharo 300 UV-VIS photometer.

4.1.5. Measurement of nitrate salts NO_3^-

In concentrated sulfuric acid, the nitrate ions react with the benzoic acid derivative to form the red colored nitro compound whose concentrations are determined photometrically [60].

Prior to the start of the test, a solution of 0.06 ml of NO_3^{-1} reagent and ml of NO_3^{-2} reagent was required to be prepared. After shaking the vials and completely dissolving the reagents, add 1.5 ml of the conditioned sample. Subsequently, the samples were sedimented. sedimentation samples could be evaluated in a Spectrogant Pharo 300 UV-VIS photometer.

4.1.6. Microbiology and mold

Within the experiment, it was also interesting to deal with biological damage to objects. Biological damage can be investigated in several ways, for the purpose of the work, it was most appropriate to examine the samples using a microscope.
Sterile instruments were picked up in trace amounts of samples and seeded into the broth with agar solution in prepared Petri dishes.

Agar preparation was carried out in 200 ml Erlenmeyer flasks. For 200 ml of solution it is necessary to add 3.8 g of agar and 5 g malt broth. All ingredients were mixed and heated with 200 ml of distilled water (Figure 30). The prepared agar solution was sterilized in an autoclave for exactly 20 minutes at 120 ° C and pressure 100 kPa (Figure 31). To the clean, sterile Petri dishes, about 3 mm thick solution was poured and quickly covered to prevent contamination from outside. It is then possible to transfer specimens to the solid solution. Samples were cultured in a thermostat at 22 ± 3 ° C for 2 weeks. The mold appeared in all 5 samples (Figure 32, Figure 33).

Figure 30: Heating the agar solution on an electric cooker
Source: Author

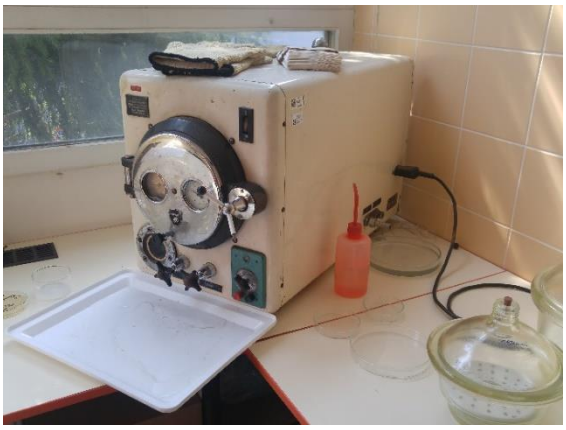

Figure 31: Using sterilization device
Source: Author

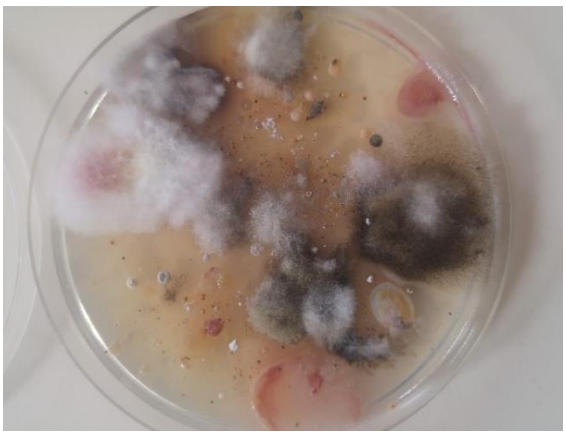

Figure 32: Mold on sample number 1
Source: Author

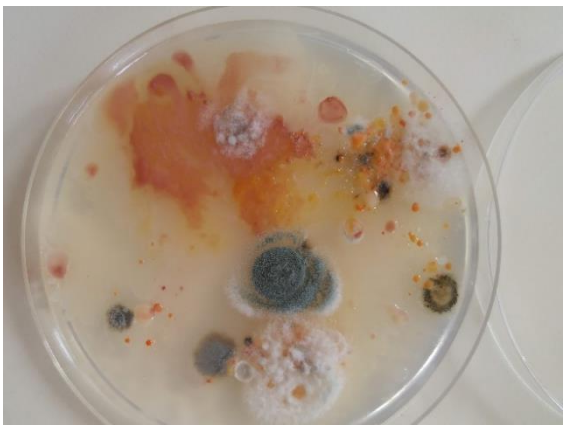

Figure 33: Mold on sample number 2
Source: Author

The mold sample was transferred to the glass slide. Then it was folded over the glass cover and viewed under a microscope with magnification of x40 and x100 (Figure 34). After consultation with the microbiologist, 6 species of mold were identified and identified. ***Alternaria alternata, Fusarium culmorum, Trichoderma viride, Cladosporium herbarum, Phoma eupyrena and Penicillium*** (Figure 35, Figure 36, Figure 37)**.**

All species found are naturally occurring molds that normally would not have a significant impact on the durability of the concrete structures in question.

Figure 34: Observation of mold samples by microscope
Source: Author

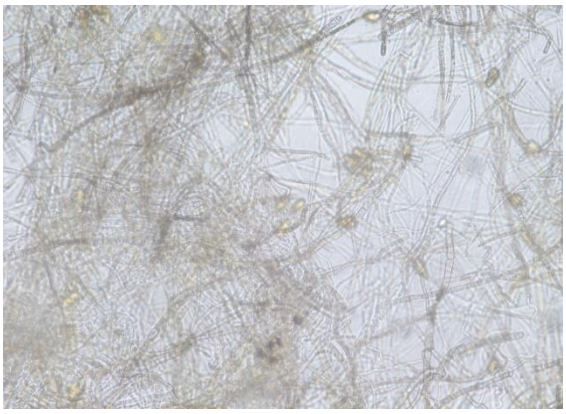

Figure 35: Alternaria alternate
Source: Author

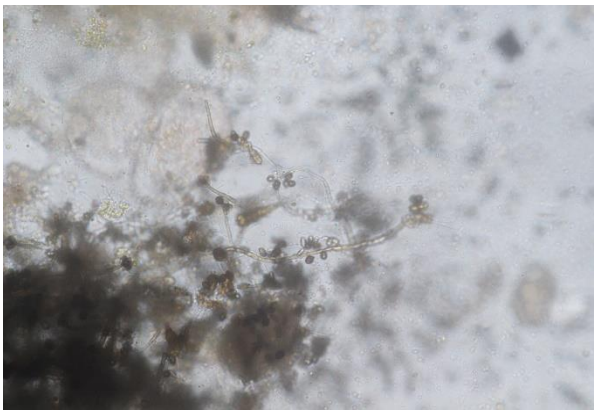

Figure 36: Cladosporium herbarum
Source: Author

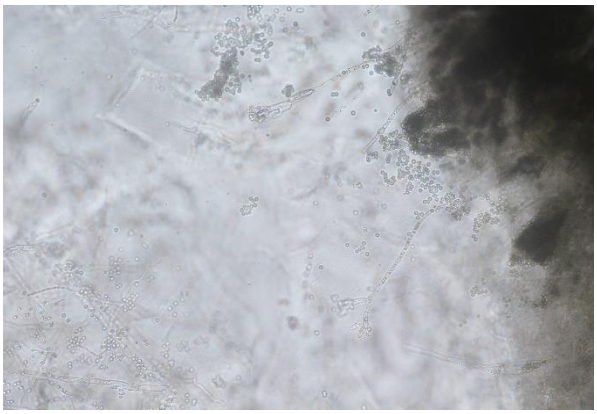

Figure 37: Penicillium
Source: Author

4.2. Results and discussion

Table 3. from the Czech technical standard ČSN P 73 0610 [3]

Degree of salvation of masonry	Salt content in mg/g and percentage by weight					
	Chloride content		Nitrate content		Sulphate content	
	mg/g	% by weight	mg/g	% by weight	mg/g	% by weight
Low values	< 0.75	< 0.075	< 1.0	< 0.1	< 5.0	< 0,5
Increased values	0.75 – 2.0	0.075 – 0.20	1.0 – 2.5	0,1 – 0.25	5.0 - 20	0.5 – 2.0
High values	2.0 – 5.0	0.20 – 0.50	2.5 – 5.0	0.25 – 0.50	20 - 50	2.0 – 5.0
Very high values	> 5.0	> 0.50	> 5.0	> 0.50	> 50	> 5.0

A Spectrogant Pharo 300 UV-VIS photometer gives the result in mg/l, so it is necessary to make a conversion to mg/g. The following table (Table 4) reads the converted values to mg/g.

Table 4. Salinity measurement

Sample identification	Weight	pH	Chloride content	Ammonia content	Nitrate content	Sulphate content
	[g]	-	[mg/g]	[mg/g]	[mg/g]	[mg/g]
1	2.1	8.5	<0.53	0	0.48	7.1
2	2.0	10	0	0	0.42	30*
3	1.9	8.5	<0.48	0	1.178	6.7
4	2.0	8.5	0	0	0.44	7
5	2.0	10	<0.42	0	0.8	35.4*

* Experimental pH measurements for samples 2 and 5 found to be pH higher than 10. For this reason, these samples were diluted 1:10 with distilled water.

Table 5. Samples classification - degree of salinity

Sample identification	Chlorides	Ammonia	Nitrates	Sulphates
1	Low values	-	Low values	Increased
2	Low values	-	Low values	High values
3	Low values	-	Increased values	Increased values
4	Low values	-	Low values	Increased values
5	Low values	-	Low values	Very high values

The pH value ranges from 8.5 to 10, which is common with this old concrete. It can be determined that the water penetrating from the subsoil and the rainwater are not strongly acidic. Salinity sample survey shows very low levels of saturation with chlorides and nitrates. The presence of chemicals was most evident in sample number 2 (interior of the basement of heavy fortification model No. 20) and sample number 5 (the lower part of the wall in the exterior of heavy fortification model No. 20). ***Sulphates at this point are most likely to enter the concrete because of the lack of waterproofing is missing on the walls and floor.***

Knowledge of chemical content in concrete is very important for the future design of remediation measure (such as using crystalline materials [11,12]). Knowing the amount of sulphates is important because of the aggressiveness assessment of lime and cement mortars and plasters. It also influences the possible use of grouts of the same composition.

Another part of the experiment was to determine the presence of mold. A total of 6 common types of mold that have been found should not affect any remediation.

4.3. Conclusion

The concrete used for two analyzed Czech WW2 fortifications successfully resisted the long-lasting effects of chemical corrosion as well as bio-corrosion. The chemical corrosion causes only aesthetic defects. This conclusion applies only to mechanically preserved objects that

have not been damaged by military tests (cannons shooting) or the looting of raw materials from their construction.

The salinity and biological damage values found proved the suitability of this concrete for further experiments with waterproofing screeds.

The results of this part of the Experimental program were published in International Conference "SPECIAL CONCRETE AND COMPOSITES 2018" - NÝVLT, M. a J. PAZDERKA. Analysis of Corrosion Products from WW2 Concrete Bunkers in Czechia. In: SPECIAL CONCRETE AND COMPOSITES 2018. Hotel Skalský Dvůr, Lisek, 2018-10-11/2018-10-12. Praha: České vysoké učení technické v Praze, 2019. s. 77-82. ACTA POLYTECHNICA CTU PROCEEDINGS. sv. 22. ISSN 2336-5382. ISBN 978-80-01-06594-5. DOI 10.14311/APP.2019.22.0077.

5. EXPERIMENTAL PROGRAM – MAIN STUDY - COMPARATIVE STUDY OF DIFFERENT TYPES OF WATERPROOFING SCREEDS WITH A FOCUS ON COHESION WITH SELECTED BUILDING MATERIALS AFTER THE FREEZE-THAW EXPOSURE

The aim of the research was to determine the functionality of waterproofing screeds from the perspective of their use in building structures. Hence, the testing was focused on the mechanical and durability properties.

5.1. Materials and Methods

5.1.1. Basic study – Water pressure test

In the first step, before performing the tear-off tests, it was necessary to verify the water tightness of individual waterproofing screeds (described above) on a common substrate (calcium silicate bricks).

The waterproofing screeds that were used for the research were chosen randomly. These are common representatives of these materials on the market in the Czech Republic. In the section 11, their technical sheets supplied by the manufacturer are attached.

- Bituminous screeds => product name “HYDRO BLOK B 400”
- Polymer screeds => product name “Jednosložková izolace EXTERIÉR”
- Silicate (mineral) screeds with added polymer => product name “SINER TS 2K”

The water pressure test was conducted at the device which allowed loading with low water pressure (0.01 MPa) on a circular surface of 50 mm in diameter. The measurement was performed on calcium silicate bricks (290x140x65mm) with applied screeds. In total, 15 specimens were prepared for the test (Figure 38) – three for each studied screed, i.e. bitumen, polymer, silicate (mineral), and three more for the reference set without any screed.

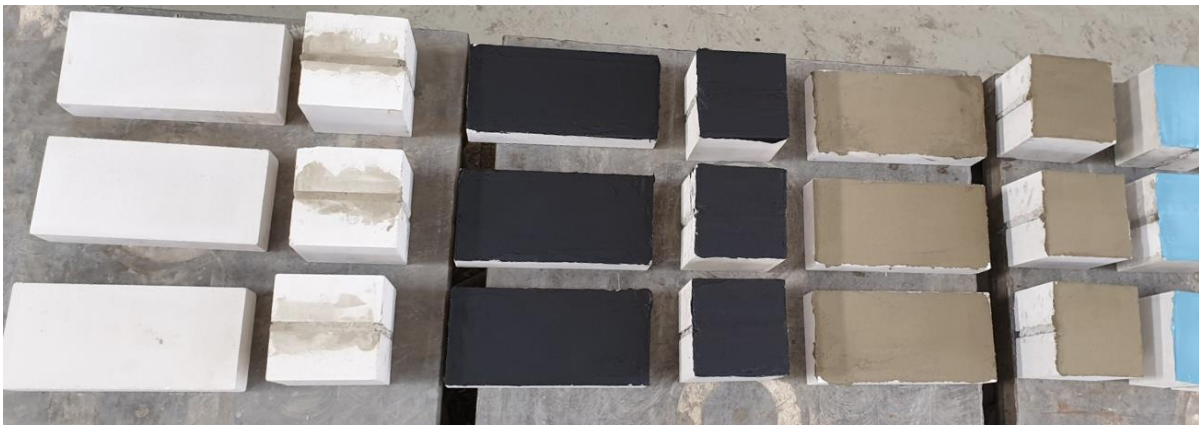

Figure 38: Test specimens
Source: Author

The test was performed 20 days after the screed application. The screeds were ap-plied to one surface of the brick according to the manufacturer's technological guide com-piled for structures (for which the screed is intended).
The specimens were loaded with a water pressure of 0.06 MPa for 5 hours (Figure 39). The pressure of 0.06 MPa was chosen with regard to the use of waterproofing screeds in building structures (basement walls). It corresponds to 6 meters of a water column, i.e. approximately 2 underground floors. Five hours was chosen because it is the time at which the reference specimen was fully saturated with water and water began seeped through the material.

The water pressure was increased to 0.12 MPa for 24 hours after 5 hours except the reference specimens. Subsequently, there was a last increase to 0.24 MPa, which also worked for the next 24 hours.

(**a**) (**b**)

Figure 39. (**a**) Weighing the test specimens; (**b**) Water pressure test
Source: Author

All water pressure tests were performed with water permeability apparatus model No. C0246/6 (Controls, Italy).

5.1.2. Additional “masonry test” - influence of joints

The water test on “whole masonry” specimens was a logical next step after successful results of the previous testing on separate bricks (Section 5.1.1.). It is necessary to analyse the impact of the joints in masonry on the resulting waterproofing effect of selected screeds

For these purposes, special test specimens - sets consisting of two bricks connected by mortar - were created. The lime-cement (mixture of cement clinker, cement dust, inorganic fillers and refining additives) mortar was used for joining the bricks. Each specimen was made up of two halves of the brick – 145x140x65mm (the original size of the brick had been modified with respect to the dimensions of the test equipment). The overall dimensions of the test specimens were thus 145x140x145 mm. For further testing, it was important to create a

perfectly flat surface on which the waterproofing screeds would be further applied. That is why wooden formwork was created (Figure 40a).

(**a**) (**b**)

Figure 40: (**a**) Test specimen – lime-sand bricks and lime-cement mortal in wooden formwork; (**b**) Test specimens with applied waterproof screeds.
Source: Author

A total of 12 test sets were created – 3 with the applied bitumen screed, 3 with the applied polymer screed, 3 with the applied silicate (mineral) screeds, and 3 without any treatment (reference specimen). Each of the waterproofing materials was applied to 3 test specimens to verify the functionality of the experiment. Another 3 specimens were left without a screed or screeds as reference specimens (Figure 40b).

The method of waterproofing testing (Figure 41) was almost identical with the previous case studying individual bricks described in Subsection 5.1.1., however the maximum water pressure applied was reduced. In this case the loading regime consisted of 5 hours of water pressure of 0.06 MPa and following 7 hours – water pressure of 0.12 MPa.

The tested sets of specimens were not designed for water tightness testing at a water pressure higher than 0.12 MPa. The reason was the method of applying stress (shear load) in the proposed test. The limitation was in the ultimate shear strength of the mortar in the joint. The common shear strength values of masonry (lime-sand bricks) with common cement mortar reach the value of approximately 0.15 MPa.

Figure 41: Water pressure test on the sets of specimens.
Source: Author

There is no need for the resistance to higher water pressures on real in-situ masonry. In the case of a higher demand for resistance to pressurized water (deeper substructure), there is an obvious use of a reinforced concrete structure (the White Tank principle-in English-speaking countries and Die Weiße Wanne in German-speaking countries).

5.1.3. Main study – Cohesion to structures

After performing the series of experiments listed in Section 5.1.1. and 5.1.2, the potentiality of further testing to verify the adhesion of waterproofing screeds to various substrates of building materials was verified. The subject of the study was the influence of freeze-thaw cycles on the monitored mechanical properties.
The experiment included more than a hundred specimens (Table 6). All the specimens were created according to the initial model (Figure 42).

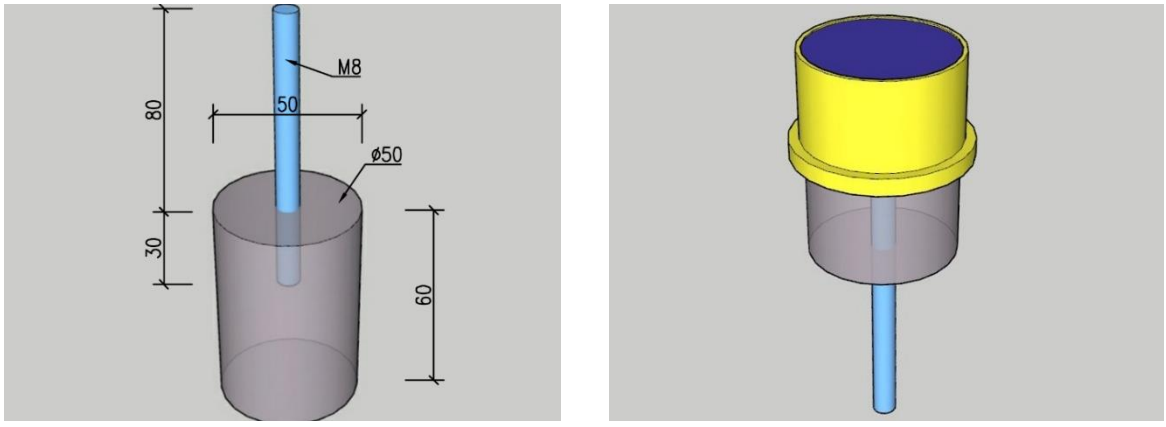

(**a**) (**b**)

Figure 42: (**a**) Model of the specimen; (**b**) Model of the prepared specimen with a delimiting ring and the applied waterproofing screed.
Source: Author

Four sets of specimens were prepared with different materials - ceramics, concrete, lime-sand and marl stone. Sandstone samples were additionally taken in the second stage of the research. All the test specimens were created according to the model as 135 cylinders with a diameter of 50 mm with a core bore. The bore was 8 mm in diameter and 30 mm deep.

Table 6. Total set of specimens.

	Boundary conditions	Bitumen screed			Polymer screed			Silicate (mineral) screed		
Ceramics	Reference	spec. 1	spec. 2	spec. 3	spec. 4	spec. 5	spec. 6	spec. 7	spec. 8	spec. 9
	15 freezing cycles	spec.10	spec.11	spec.12	spec.13	spec.14	spec.15	spec.16	spec.17	spec.18
	30 freezing cycles	spec.19	spec.20	spec.21	spec.22	spec.23	spec.24	spec.25	spec.26	spec.27
Concrete	Reference	spec.28	spec.29	spec.30	spec.31	spec.32	spec.33	spec.34	spec.35	spec.36
	15 freezing cycles	spec.37	spec.38	spec.39	spec.40	spec.41	spec.42	spec.43	spec.44	spec.45
	30 freezing cycles	spec.46	spec.47	spec.48	spec.49	spec.50	spec.51	spec.52	spec.53	spec.54
Lime sand	Reference	spec.55	spec.56	spec.57	spec.58	spec.59	spec.60	spec.61	spec.62	spec.63
	15 freezing cycles	spec. 64	spec. 65	spec. 66	spec. 67	spec. 68	spec. 69	spec. 70	spec. 71	spec. 72
	30 freezing cycles	spec. 73	spec. 74	spec. 75	spec. 76	spec. 77	spec. 78	spec. 79	spec. 80	spec. 81
Marl	Reference	spec. 82	spec. 83	spec. 84	spec. 85	spec. 86	spec. 87	spec. 88	spec. 89	spec. 90
	15 freezing cycles	spec. 91	spec. 92	spec. 93	spec. 94	spec. 95	spec. 96	spec. 97	spec. 98	spec. 99
	30 freezing cycles	spec. 100	spec. 101	spec. 102	spec. 103	spec. 104	spec. 105	spec. 106	spec. 107	spec. 108
Sandstone	Reference	spec. 109	spec.110	spec. 111	spec. 112	spec. 113	spec. 114	spec. 115	spec. 116	spec. 117
	15 freezing cycles	spec. 118	spec. 119	spec. 120	spec. 121	spec. 122	spec. 123	spec. 124	spec. 125	spec. 126
	30 freezing cycles	spec. 127	spec. 128	spec. 129	spec. 130	spec. 131	spec. 132	spec. 133	spec. 134	spec. 135

The borehole was subsequently cleaned with compressed air. A degreased M8 threaded rod, 100 mm long, was glued into the bore. The threaded rod had to be degreased well (Figure 43, Figure 44).

Figure 43: Assembly of all test specimens with glued threaded rods (ceramics, concrete, Lime sand, marl).
Source: Author

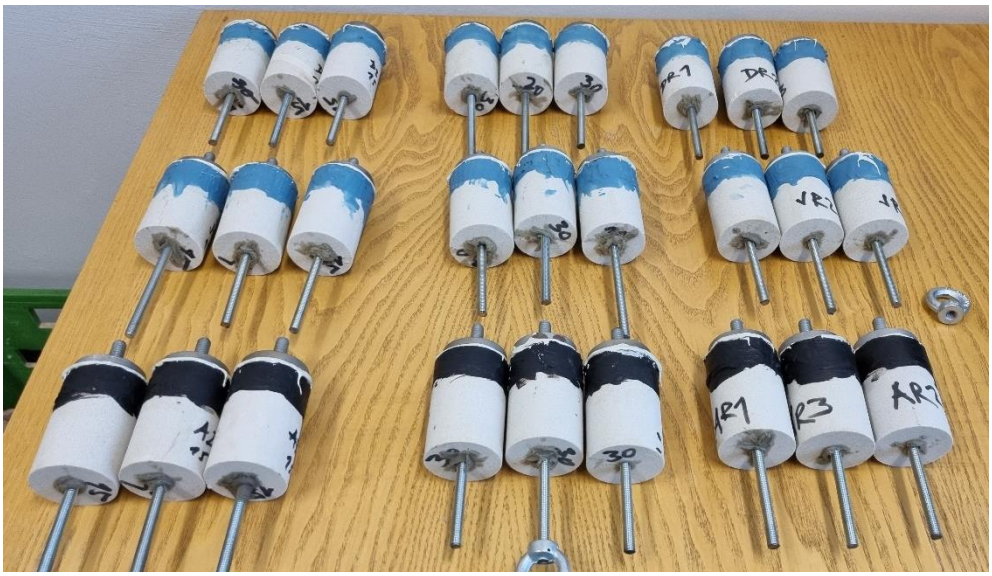

Figure 44: Assembly of all test specimens with glued threaded rods (sandstone).
Source: Author

In the next step, the chipped edges of the cylinders on the side where the waterproofing screed would be applied had to be solved. The flat surface and the accurate thickness of the screed was achieved by help of PVC ring, which was fixed to cylinder during the application of the screed. Thus, the ring created a formwork for the subsequent application of the screed (Figure 45, Figure 46).

Figure 45: Prepared test specimen with glued threaded rod, PVC ring
Source: Author

Figure 46: Prepared front of the test specimen for the application of a waterproofing screed
Source: Author

Three types of waterproofing screeds (bitumen, polymer and silicate) were applied to the test specimens of each type of tested structures (Figure 47, Figure 48).

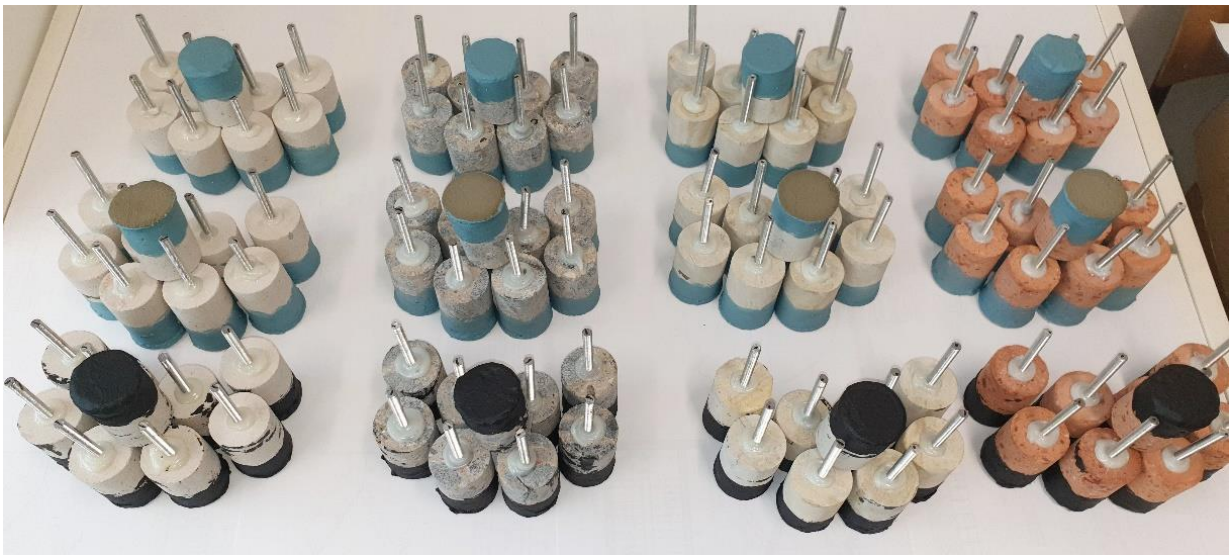

Figure 47: Finished set of specimens with the applied waterproofing screed (ceramics, concrete, lime sand, marl).
Source: Author

Figure 48: Finished set of specimens with the applied waterproofing screed (sandstone).
Source: Author

Three sets of specimens were created, each set with different boundary conditions. Everything will be done three times to verify the accuracy of the measurement. The first set of specimens that will serve as a reference set will be placed indoors at a constant temperature and humidity. The second set was subjected to freezing and thawing.

The test specimens were immersed surface with a surface treatment in water at (+ 20 ± 3 °C) for 6 hours, so that between the screed and the substrate is 10 mm below the water surface. The specimens were then removed and stored vertically in a freezing chamber at a temperature of (-20 ± 2) °C for 18 hours. Thus, one freeze-thaw cycle consisting of water

immersion and following freezing takes 24 hours. The surface of the screeds was visually inspected after each cycle.
After the required number of cycles, the specimens are left to dry at an air temperature of (+20 ± 3) °C and a relative humidity of (55 ± 10) % for at least 14 days. The method of freezing described above is inspired by the Czech national standard ČSN 73 2579 from 1981 [61].

A tear-off test disc with a diameter of 50 mm is glued to the hardened waterproofing screed with a two-component epoxy adhesive. The test disc is made of sheet metal 8 mm in thickness (Figure 49). A threaded rod DN 10 is welded to the sheet metal. The weld is ground on the target from below. Thus, the grinding created a flat contact surface (Figure 50).

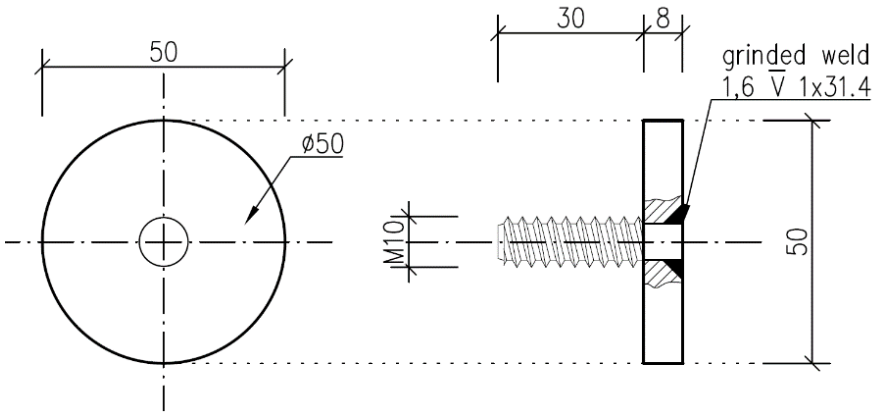

Figure 49: Tear-off test disc target scheme
Source: Author

Figure 50: Gluing tear-off targets
Source: Author

During the tear-off tests, it was necessary to ensure the axial loading. The tension was exerted by a steel ring which is screwed onto the threaded rod. A similar fastening system was used on the opposite side (Figure 51, Figure 52).

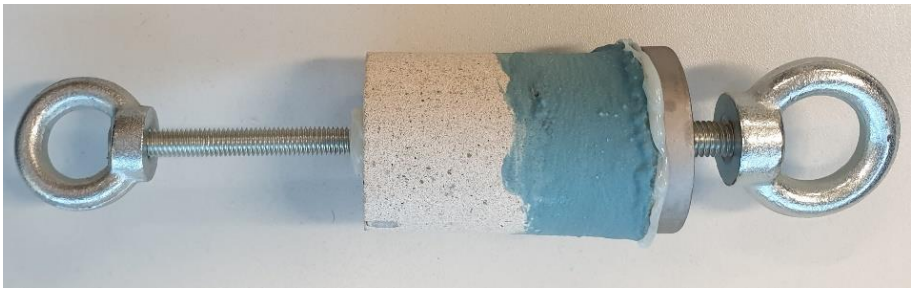

Figure 51: Detail of a test specimen with a glued target.
Source: Author

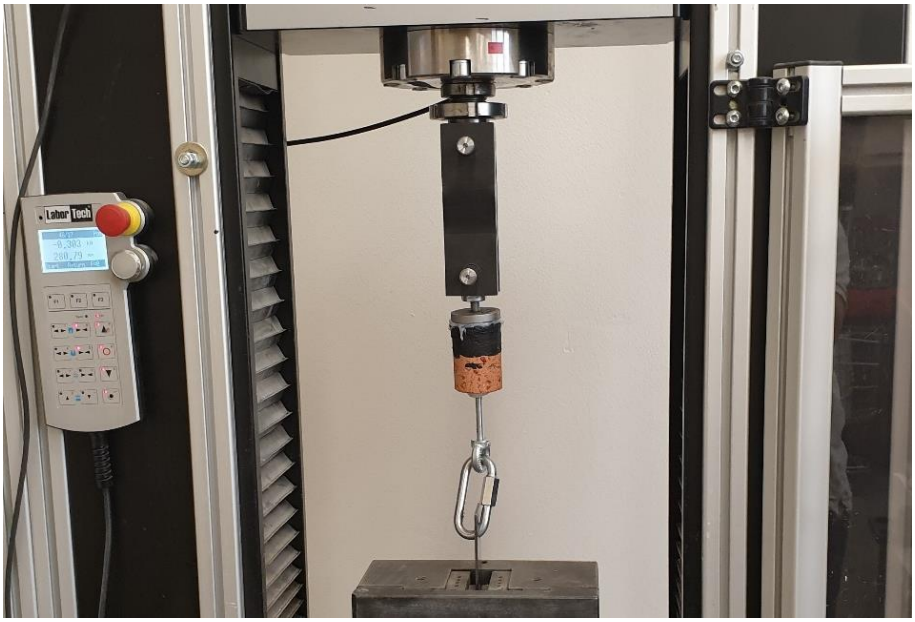

Figure 52: Test specimen prepared for the tear-off test.
Source: Author

Tear-off tests were performed with the electromechanical testing machine LabTest 4.100 ST1 (LaborTech s.r.o., Czech Republic). This testing machines made it possible to monitor and record the course of tensile stress in real time. The accuracy class is according to EN ISO 7500-1, ASTM E4.

5.2. Results and discussion

5.2.1. Basic study – Water pressure test

Each measurement was performed on three specimens so that the measured values could be averaged. The average weight gain values are presented in Table 7.

Table 7. The average weight gain values

Water pressure	0.06 MPa	0.12 MPa		0.24 MPa	
Time [h]	after 5 hours (the reference specimen fully saturated)	after 12 hours	after 24 hours	after 36 hours	after 58 hours
	Average weight gain [%]				
Reference	4.02	-	-	-	-
Bituminous screeds	0.03	0.03	0.03	0.06	0.11
Polymer screeds	0.05	0.06	0.10	0.13	0.15
Silicate (mineral) screeds	0.07	0.24	0.49	0.69	1.03

The waterproofing ability of all types of tested screeds applied on all tested building structures was shown during the test. The maximum level of water pressure (reached in the last phase of loading) corresponded to 0.24 MPa (24m of hydrostatic pressure). The results verified the values in the technical data sheets of the manufacturers but there were some differences in their properties among each other. In the case of the reference specimen, there was a percentage weight gain of 4.02% in 5 hours. After 5 hours of loading by water, the results manifested almost no effect on any of the tested screeds.

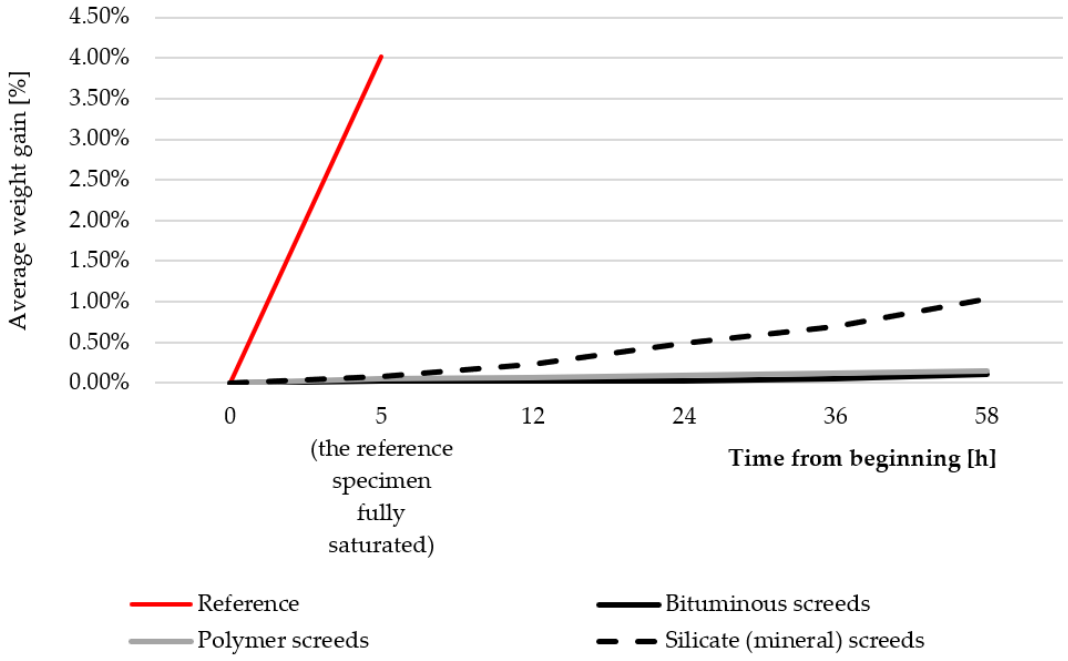

Figure 53: Change in weight during the time (in percentage).
Source: Author

After 5 hours and after increasing the water pressure to 0.12 MPa, the silicate (miner-al) screeds gain weight and continue to increase until 58 hours. The weight gain was al-most linear throughout the test (Figure 53). The weight gains also slowed down over time.
The bitumen and polymer screeds had almost the same measured values throughout all the pressures tested. The weight gain was very small throughout the test. The bitumen and polymer screeds have a higher waterproofing effect compared to the silicate (mineral) screeds. The measured values of leakage were very small, and the waterproofing screeds can be considered (on common building structures at normal pressures) to be watertight.

5.2.2. Additional "masonry test" - influence of joints

The results of the water pressure test showed again (as in the case of separate bricks) that there was a big difference between the specimens with applied screeds and the specimens without any treatment. In the case of the reference specimens (without a screed), water began to penetrate through the mortar joints as well as the brick's sides just several minutes after the test was started (Figure 54). For the specimens with all types of applied screed, there was no leakage of water during the testing time - water had not penetrated through the bricks, nor through the joints. The results clearly confirmed that the water-proofing effect of the screed was not significantly influenced by the joints in masonry.

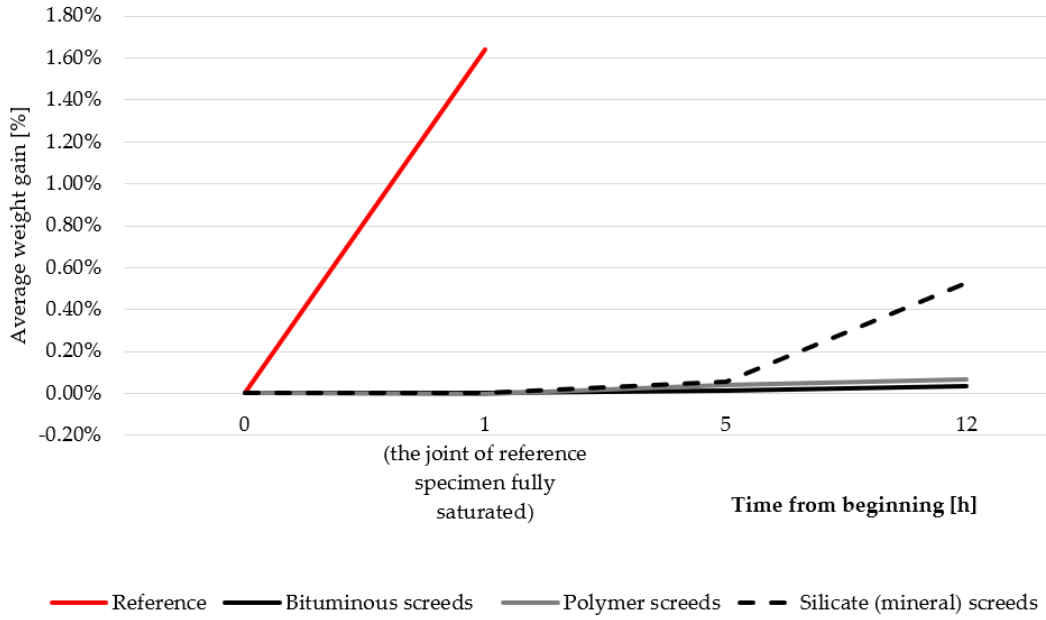

Figure 54: Change in weight during the time (in percentage).
Source: Author

5.2.3. Main study – Cohesion of structures

After the tear-off test, the type of failure was observed. The failure manifested itself at the screed-substrate interface. It can be called "an adhesive failure" (Figure 55b). In some cases, the screed itself was broken, which can be called "a cohesive failure" (Figure 56a).

In some cases, especially after several freezing cycles, the base material itself was broken. The substrate had not withstood the freezing cycles. In this case, the adhesion and the tensile strength of the screed are higher than the strength of the substrate (Figure 56b).

Figure 55a shows a typical record of the test. Specifically, it is Specimen No. 3 - the silicate (mineral) screed on the marl stone after 15 freezing cycles.

(**a**) (**b**)

Figure 55: (**a**) Typical course of tensile force on a test specimen; (**b**) Adhesive failure.
Source: Author

(**a**) (**b**)

Figure 56: (**a**) Cohesive failure; (**b**) Substrate failure.
Source: Author

From the total number of 135 specimens, 80 adhesive failures (60%), 21 cohesive failures (16%) and 33 cases of substrate damage (24%) could be observed after the finish of the experiment.

5.2.3.1. Results with the substrate influence

The detailed results of the tear-off test are presented in (Figure 57), which represent the arithmetical mean of three measurements.

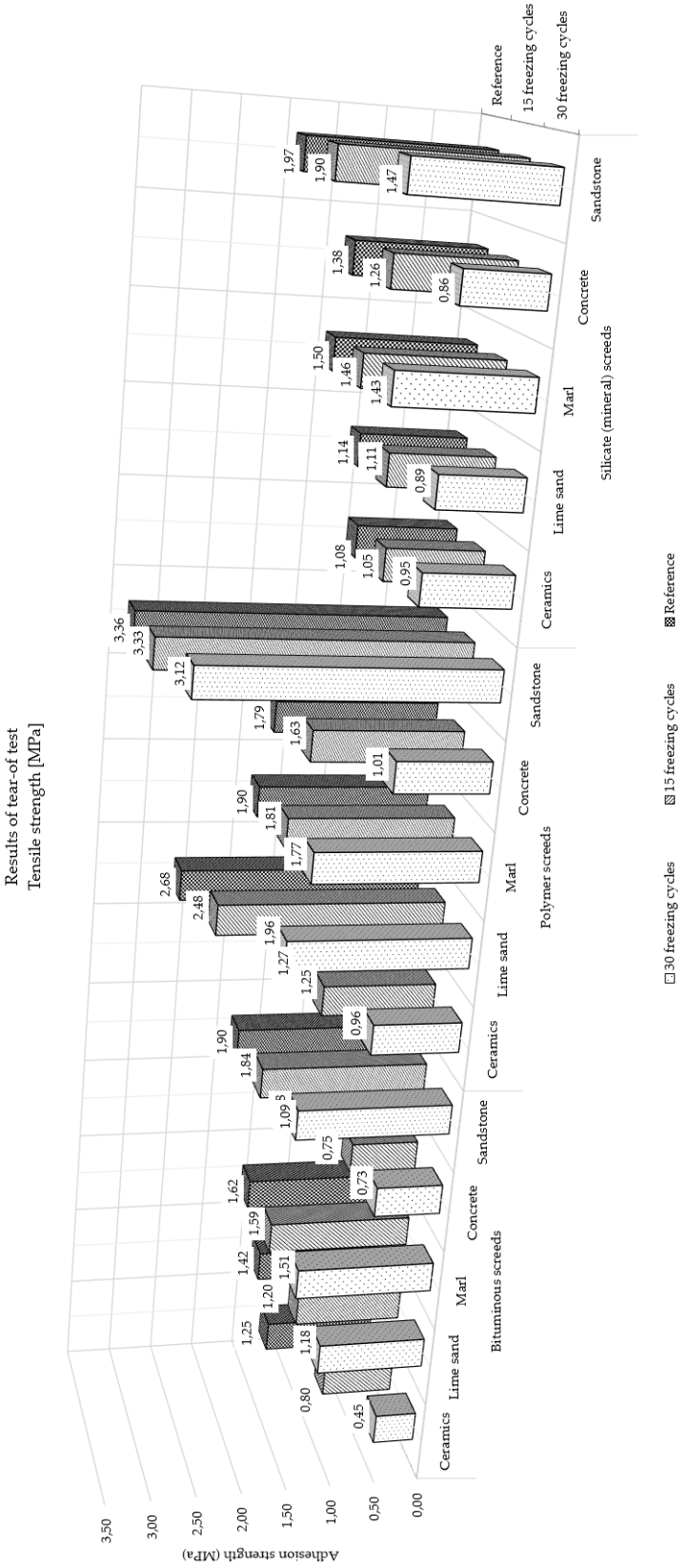

Figure 57. Results of the tear-off test, Tensile strength.

For comparison, it is interesting to express the values in percentages (Table 8).

Table 8. Residual strength in percentage.

Type of the screeds	Type of substrate	After 15 freezing cycles	After 30 freezing cycles
Bituminous screeds	Ceramics	64.0 %	36.3 %
	Lime sand	84.1 %	83.1 %
	Marl	97.8 %	93.0 %
	Concrete	68.8 %	67.1 %
	Sandstone	97.0 %	88.4 %
Polymer screeds	Ceramics	98.1 %	75.4 %
	Lime sand	92.4 %	73.3 %
	Marl	95.1 %	93.1 %
	Concrete	90.9 %	56.5 %
	Sandstone	98.9 %	92.8 %
Silicate (mineral) screeds	Ceramics	96.7 %	87.7 %
	Lime sand	96.9 %	77.9 %
	Marl	97.7 %	95.2 %
	Concrete	91.0 %	62.4 %
	Sandstone	96.3 %	74.5 %

The failure of the substrate manifested especially in the case of ceramic material. The ceramic shard probably lost the most of its strength during the freezing cycles, what indicate low freeze-thaw resistance of used ceramic bricks accompanying by cracks propagation. The decay of strength of the ceramic shard was evinced especially in case of the bituminous screed. Thus, the adhesive strength of the waterproofing screed was higher than the tensile strength of the substrate material after freeze-thaw cycles. The measured values were retained mainly because the boundary conditions were the same for all examined waterproofing screeds.

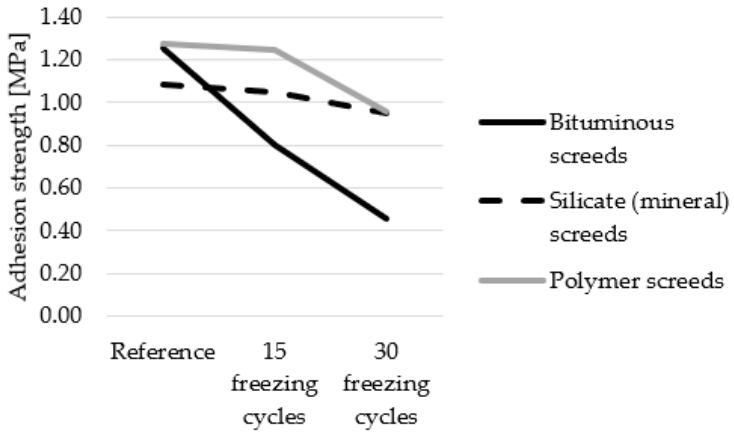

Figure 58. Loss of strength – ceramics

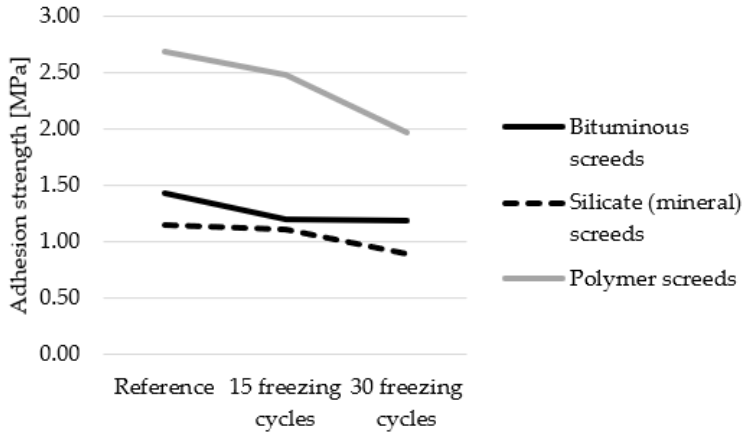

Figure 59. Loss of strength - lime sand

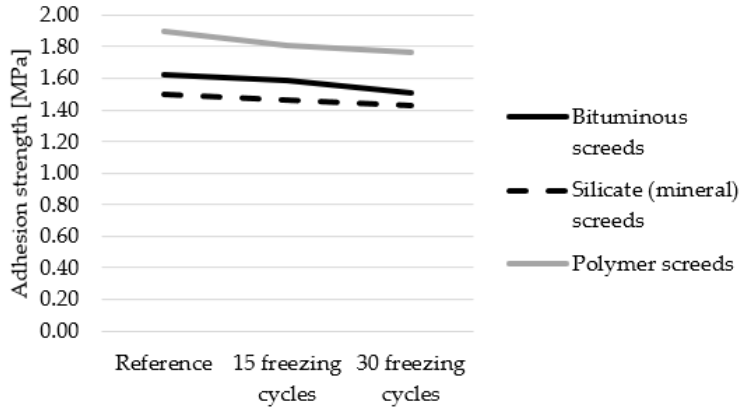

Figure 60. Loss of strength - marl

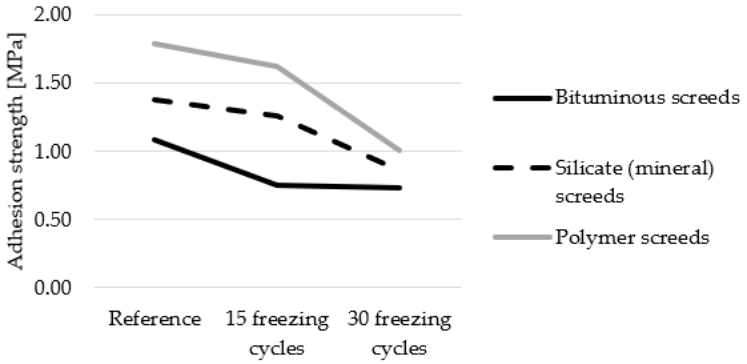

Figure 61. Loss of strength - concrete

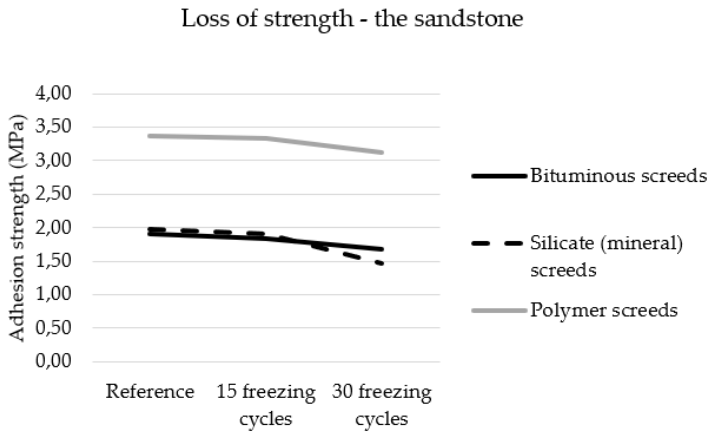

Figure 62. Loss of strength - Sandstone

Results - Bituminous screeds

As mentioned above, in the case of bituminous screeds, the greatest damage in the ceramic specimens was caused due to the failure of the substrate. Therefore, the values measured on the ceramic shard cannot be considered as the adhesion of the screed. Thus, it can be assumed that the bitumen screed cohesion exceeds the tensile strength of the used ceramic. In the case of lime-sand bricks, marl stone, sandstone and concrete, the values are already suitable for making a comparison of the adhesion, which was the goal of this experiment.

The best cohesion and interaction can be observed on the sandstone substrate in the range of 1.9-1.68 [MPa]. In the experiment, the measured values were by about and by 15% higher than those for marl - 1.62-1.51 [MPa], and by 43% higher than those for lime sand - 1.42-1.18 [MPa], and by 112% higher than those for concrete - 1.09-0.73 [MPa].

At the same time, the influence of the freezing cycles on the durability and adhesion of the bitumen screed is visible from (Figure 58 - Figure 62). Comparing the reference specimen and the tested specimen after 15 freezing cycles, there was a decay of adhesion to 87%, and, after additional 15 cycles, the original strength had dropped to 83%. Thus, the total loss between 15 and 30 cycles is marginal. The test results have shown that further freezing cycles already have a minimal effect on the overall adhesion.

Results - Polymer screeds

In opposition to the bituminous screeds described above, polymers screeds have achieved higher adhesion to the substrate (Figure 58 - Figure 62). The highest adhesion and interaction can be observed on the sandstone substrate in the range of 3.36-3.12 [MPa]. In the experiment, the measured values were by about 37% higher than those for lime sand - 2.68-1.96 [MPa], by 80 % higher than those for marl - 1.90-1.77 [MPa], by 120 % higher than those for concrete - 1.79-1.01 [MPa], and by 181% higher than those for ceramic material - 1.27-0.96 [MPa].

The effect of the freezing cycles on the screed's adhesion is the most significant between 15 and 30 cycles. Here, the difference between bitumen and silicate (mineral) screeds can be observed. Comparing the reference specimen and the tested specimen after 15 freezing cycles, there was a loss of adhesion to 95%, and, after another 15 cycles, the original strength had dropped to 78%. Thus, the total loss between 15 and 30 cycles was 17%. The results

showed a significant effect of the number of freezing cycles on the adhesion to the substrate. On the other hand, the measured adhesion values after the cycles performed are higher than the values of the other screeds for the reference specimens. Hence, it can be noted that the adhesion is sufficient for use in construction, often higher than the strength of the base material. The polymer screed has the lowest durability against freeze-thaw cycles (in comparison to the other tested screeds).

Results - Silicate (mineral) screeds

In 43% of the specimens, the screed structure was damaged during the test. This can be assessed as its biggest weakness compared to the other tested screeds. The test results have shown that the adhesion to the substrate is higher than the tensile strength of the screed (Figure 58 - Figure 62). Hence, damaged specimens in such a way were excluded from the experiment evaluation.

In terms of adhesion, the tested mineral screed can be classified very close to the bituminous screeds.

The best adhesion and interaction can be observed on the sandstone substrate in the range of 1.97-1.47 [MPa]. In the study, the measured values were by about 21% higher than those for marl - 1.38-0.86 [MPa], and 52% higher than those for concrete - 1.38-0.86 [MPa], and by 69 % higher than those for lime sand - 1.14-0.89 [MPa]. The values of the ceramic substrate are very similar to lime sand. The maximal measured strength is by 72% higher than that of the ceramic material - 1.08-0.95 [MPa]. The influence of the substrate is the lowest of all tested screeds.

Regardless of the substrate, the effect of freezing cycles on mineral screeds is the most linear of all tested screeds. The decay of the adhesion of mineral screed is proportional to the number of freeze-thaw cycles. Comparing the reference specimen and the tested specimen after 15 freezing cycles, there was a loss of adhesion to 96%, and, after another 15 cycles, the original strength had dropped to 80%. Thus, the total loss between 15 and 30 cycles accounts for 20%. The experiment showed the effect of the freezing cycles similar to that of the bitumen screeds, with the difference that between 15 and 30 cycles, there is a further loss of strength. Thus, it can be noted that the next time the freezing is repeated, the strength will continue to decay over time.

5.2.3.2. Results without the substrate influence

For practical use in construction, it is interesting to place the measured values of individual screeds against each other without the influence of the substrate material. The above values were, therefore, averaged, and the result is an unbiased comparison of individual types of screeds (Table 9).

Table 9. Total adhesion strength and total residual strength after 30 freezing cycles.

Average adhesion strength without the influence of the substrate [MPa]				Average residual strength after 30 freezing cycles without the influence of the substrate [%]
Type of screed	Reference	15 freezing cycles	30 freezing cycles	
Bituminous screeds	1.51	1.34	1.28	82.9 %
Polymer screeds	2.20	2.10	1.76	78.2 %
Silicate (mineral) screeds	1.42	1.36	1.12	79.5 %

When comparing the overall tested screeds, it can be seen from Table 9 that the greatest total adhesion is achieved by polymer screeds, which, at the same time, have the lowest durability during the freezing cycles. Bitumen screeds and silicate (mineral) screeds are very similar in the total values. However, they differ in their ability to withstand freezing cycles over time. In the case of bitumen screeds, the first 15 freezing cycles have the greatest effect, and there is no significant loss of strength. In contrast to this, silicate (mineral) screeds have a linear decrease in tensile strength due to freezing (Figure 63).

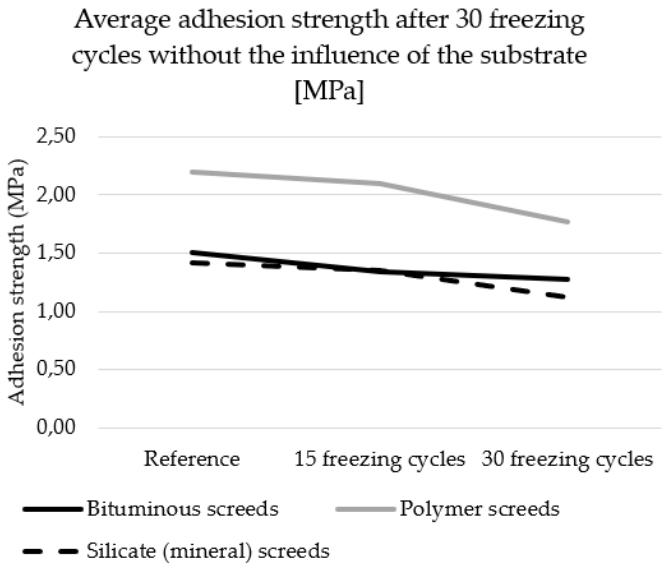

Figure 63. (**a**) Average adhesion strength without the influence of the substrate;

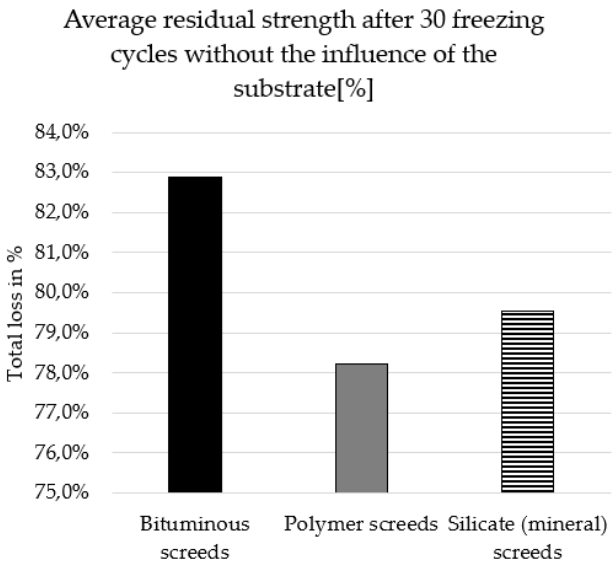

Figure 63. (**b**) Average residual strength after 30 freezing cycles without the influence of the substrate [%]

According to the manufacturer´s technical data sheets for the used screeds, the manufacturers declare a minimum strength of 0.5 MPa for all types. All the tested screeds have manifested a greater adhesion strength even after 30 freezing cycles.

In 2021, the results of the research were published in an impacted journal in the WOS database: "Comparative study of different types of waterproofing screeds with a focus on cohesion with selected building materials after the freeze-thaw exposure" Applied Sciences. 2021, 11(23), ISSN 2076-3417, DOI: 10.3390/app112311256. This is an impacted Swiss journal in the WOS database (with IF=2.67).


applied sciences

an Open Access Journal by MDPI

CITESCORE 3.0 SCOPUS

IMPACT FACTOR 2.679

CERTIFICATE OF ACCEPTANCE

Certificate of acceptance for the manuscript (**applsci-1463194**) titled:

Comparative study of different types of waterproofing screeds with a focus on cohesion with selected building materials after the freeze-thaw exposure

Authored by:

Michal Nývlt; Jiří Pazderka; Pavel Reiterman

has been accepted in *Appl. Sci.* (ISSN 2076-3417) on 24 November 2021

MDPI Academic Open Access Publishing since 1996

Basel, November 2021

Figure 64. Certificate of acceptance

6. EXPERIMENTAL PROGRAM – COMPARATIVE STUDY OF DIFFERENT TYPES OF WATERPROOFING SCREEDS WITH A FOCUS ON RADON PERMEABILITY AFTER THE FREEZE-THAW EXPOSURE

6.1. Materials and Methods

This experimental part is about verify and independently compare the functionality of the waterproofing screeds against the effect of radon with the effect of freezing cycles.
In the previous parts of the dissertation research, the effectiveness of the screeds against water has been addressed. Since waterproofing materials are designed not only as waterproofing but also as insulation against radon penetration into the interior of a building, the logical next step is to verify their functionality and reliability. In the research, the ability of the screed to insulate against radon and the ability to withstand freezing cycles are analysed and tested.

A total of 24 supporting base plates were created. Cement-bonded lightweight material with product name "Fermacel Powerpanel H_2O" was chosen as a permeable but at the same time strong base material. It is a cement-bonded lightweight concrete panel with a sandwich structure and double-sided reinforcement under cover layers with alkali-resistant fiberglass fabric (5 mm x 5 mm). The plate is produced in a thickness of 12.5 mm. The test plates were 325 mm x 135 mm.

Waterproofing screeds, which were used in all previous experiments (polymeric, silicate and bituminous), were applied to the created support plates (Figure 65). To perform the calculation, reference specimen was also created without applied waterproofing screed.

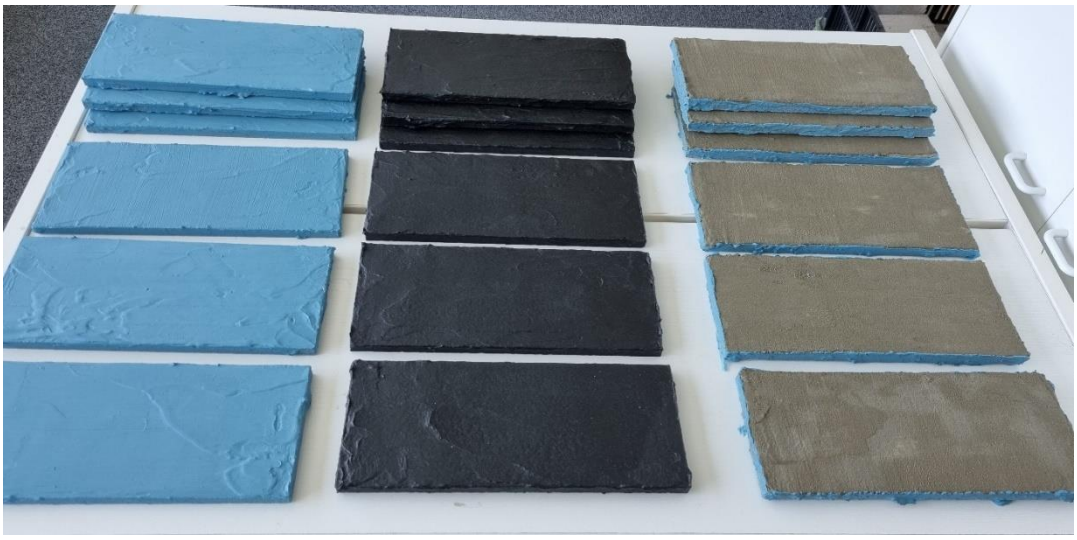

Figure 65. Specimen set with applied waterproofing screeds
Source: Author

The prepared specimens were then placed in a freezing chamber. The method of stressing by freezing cycles is identical to that described in chapter 5.1.3 of the thesis (the test specimens were immersed surface with a surface treatment in water at (+ 20 ± 3 °C) for 6 hours. The specimens were then removed and stored in a freezing chamber at a temperature of (-20 ± 2) °C for 18 hours). A total of 30 freeze cycles were performed in this way. After 30 cycles, the specimens are left to dry at an air temperature of (+20 ± 3) °C and a relative humidity of (55 ± 10) % for at least 14 days.

During the cycling time in the freezing chamber, a device was prepared to measure the radon diffusion coefficient D [m^2/s]. The device used was designed and maintained by the Department of Architectural Engineering of the Faculty of Civil Engineering ČVUT.

It is a measuring device (Figure 66, Figure 67) consisting of three receiving chambers (above the specimen) and one radon source chamber (below the specimen). In the lower chamber (below the specimen) the radon source is common to all 3 specimens. The specimen placed between the two chambers shall be sealed perfectly. A permanently flexible acrylic sealant shall be used for sealing.

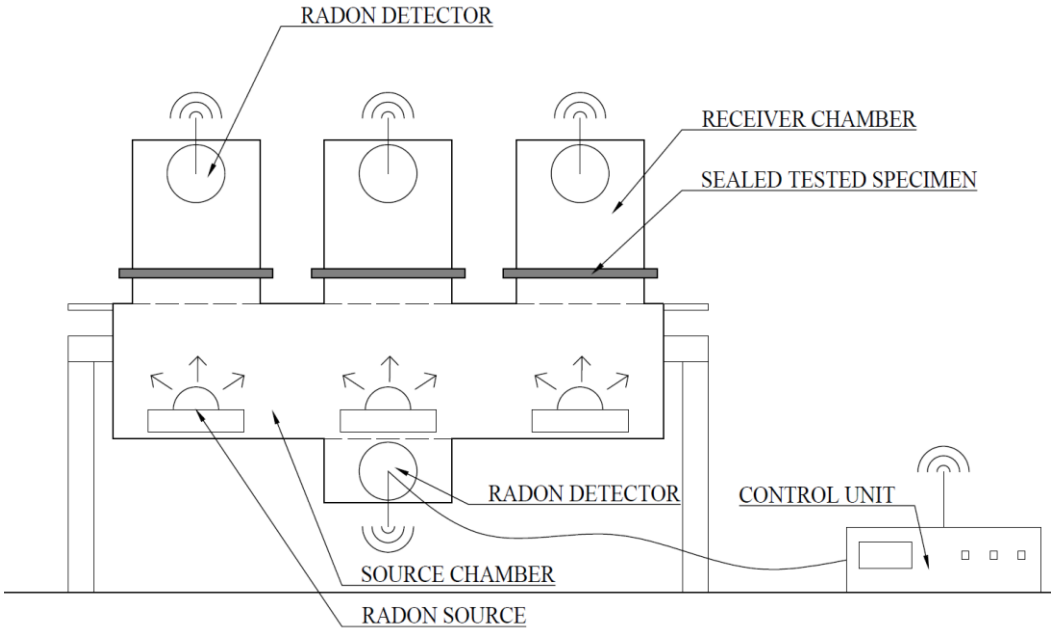

Figure 66. Measuring device with one source chamber and three receiving chambers
Source: Author

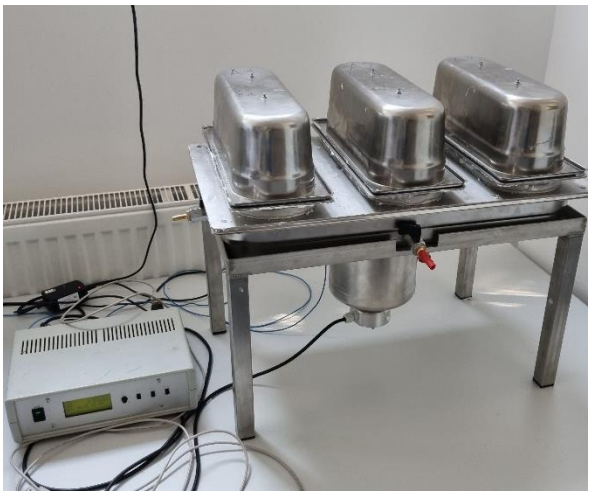

(a)

Figure 67. (a) Used measuring device
Source: Author

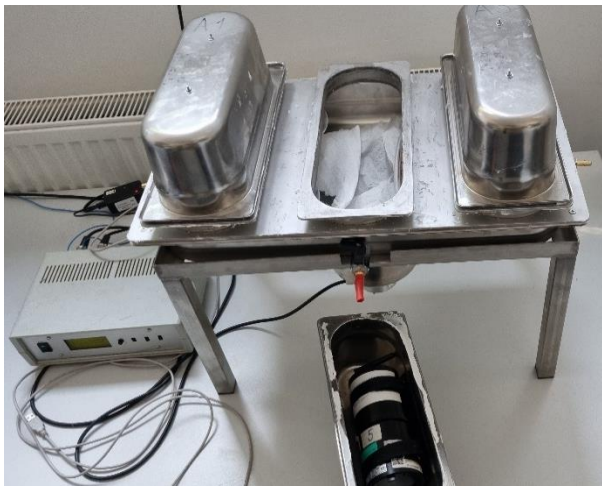

(b)

Figure 67. (b) Used measuring device
Source: Author

The radon concentration in the upper and lower chambers is continuously measured by TESLA radon detectors. These detectors are located inside each upper chamber (the principle is based on detecting Po using a PIN photodiode). In total, there are 3 upper chambers in the measuring device and one detector in each chamber. To measure the concentration below the specimen, one detector common to all three specimens is placed in the lower chamber. The data from the detectors are transmitted wirelessly to a control unit located outside the measuring device. The area of a single specimen was 2.93×10^{-2} m^2. The volume of the source chamber was 13.9×10^{-3} m^3, and the volume of the receiver container was 2.7×10^{-3} m^3.

The specimens were sequentially loaded into the device and sealed [Figure 68, Figure 69]. After specimen sealing, the increase in radon concentration in the upper and lower chambers is monitored until steady state.
For the selected waterproofing screeds, a time interval of 14 days was found to be appropriate. During which time the increase in concentration in the upper chamber was stabilized.

Crushed concrete made of slag with a high content of radium (1000 – 4000 Bq/kg) and sand that had been used as a filter in a water treatment plant were used as a natural radon source. The radon diffusion coefficient D [m^2/s] was determined according to method A of ISO/TS 11665–13 from the known time-dependent curves of the radon concentrations measured on both sides of the tested specimen.

Figure 68. Measuring device with inserted and sealed specimens.
Source: Author

Figure 69. The sealed specimens
Source: Author

A total of 7 sets with three specimens in the measuring device were carried out.

- Set 1 = 3x reference specimen without waterproofing screed
- Set 2 = 3x specimen with polymer waterproofing screed
- Set 3 = 3x specimen with bitumen waterproofing screed
- Set 4 = 3x specimen with silicate waterproofing screed
- Set 5 = 3x specimen with polymer waterproofing screed after 30 freeze thaw cycles
- Set 6 = 3x specimen with bitumen waterproofing screed after 30 freeze thaw cycles
- Set 7 = 3x specimen with silicate waterproofing screed after 30 freeze thaw cycles

The measurements were taken between the autumn of 2022 and the spring of 2023. After the measurements were taken, the specimens were removed (Figure 70) from the measuring device and the thickness of the applied waterproofing screed was measured for each specimen separately (Figure 71).

Figure 70. Specimens removed from the measuring device, sealant visible around the perimeter
Source: Author

Figure 71. (a) Measuring the thickness of the applied waterproofing screed
Source: Author

Figure 71. (b) Measuring the thickness of the applied waterproofing screed
Source: Author

Figure 71. (c) Measuring the thickness of the applied waterproofing screed
Source: Author

6.2. Results and discussion

Since the measurements were made under non-stationary conditions, the calculation is based on the numerical solution for the non-stationary differential equation of radon diffusion. A very detailed description [62] has been published, where the mathematical procedure and method of calculation is described.

In the numerical evaluation of the radon diffusion coefficient using the IterRn software [63], the process relies on time-dependent radon concentration values measured in both the source and receiver containers. The calculation involves iteratively solving equations, starting with an initial estimation of the radon diffusion coefficient range (lower and upper limits) and a defined iteration step (typically 1/10 to 1/20 of the range).

Simplified description of the procedure:
Initialization

- The estimated range of the radon diffusion coefficient and the iteration step were set.
- The transient diffusion of radon through the radon barrier is calculated with the initial radon diffusion coefficient set to the lower limit.

Comparison

- The calculated time-dependent radon concentration results in the receiver container are compared with the measured data.
- Differences between the calculated and measured data sets are recorded.

Iterative Process

- The procedure was repeated with a progressively increasing radon diffusion coefficient in each step.
- The iteration continued until the upper limit of the radon diffusion coefficient range was reached.

Optimization

- The final radon diffusion coefficient was determined by minimizing variations between calculated and measured data, considering metrics such as average difference or sum of deviations.

Efficiency

- The entire iteration process is designed to be computationally efficient and typically took no more than 30 minutes on a standard contemporary computer.

IterRn software (sw.) was developed at CTU for the Microsoft Windows environment. IterRn shares similarities with TransRn software [63]. Contains standard MS Windows procedures and dialogs for creating, saving, reading and editing data files. The input values derived from the measurements were imported from a text record that was stored in a plain text file with the values separated by periods (Figures 72).

Table 10 shows the measured values for each specimen.

Table 10.

Type of the waterproofing screed	**Layer thickness [mm]**			**Average layer thickness [mm]**
	Number of radon detector			
	S1	S2	S3	
Silicate (mineral) screed (reference)	2,73	2,87	3,38	**2,99**
Silicate (mineral) screed (30 freezing cycles)	3,18	2,85	2,96	**3,00**
Polymer screeds (reference)	1,77	1,84	1,28	**1,63**
Polymer screeds (30 freezing cycles)	1,69	1,81	1,73	**1,74**
Bituminous screeds (reference)	1,73	1,87	1,64	**1,73**
Bituminous screeds (30 freezing cycles)	1,71	1,91	1,99	**1,87**

The resulting radon diffusion coefficient D [m^2/s] values were determined as the arithmetic radon diffusion coefficient.

In following figures (Figure 73 - Figure 84) the measured values are observable. On the x-axis is time in hours, on the y-axis are the measured concentrations in the upper chamber.

In some measurements, the measuring detector was damaged. This is the reason for the missing measured values (detector labelled S3). Unfortunately, this was only discovered during the evaluation of the measured data.

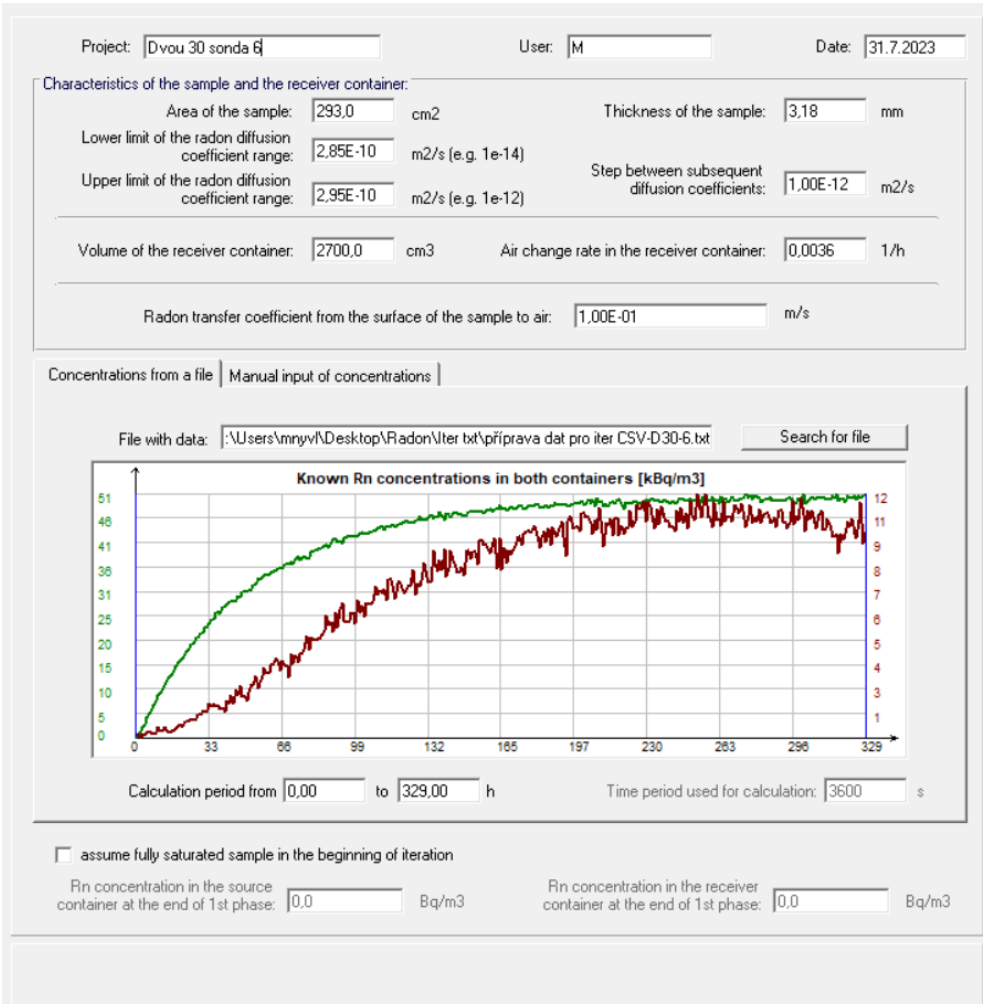

Figure 72. Software IterRn interface [63]

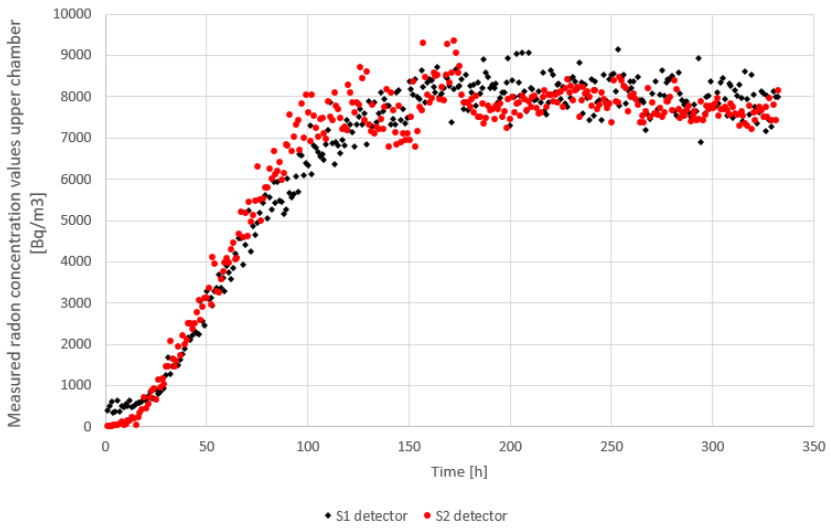

Figure 73. Measured radon concentration (Silicate (mineral) screed - reference) – detector S1, S2

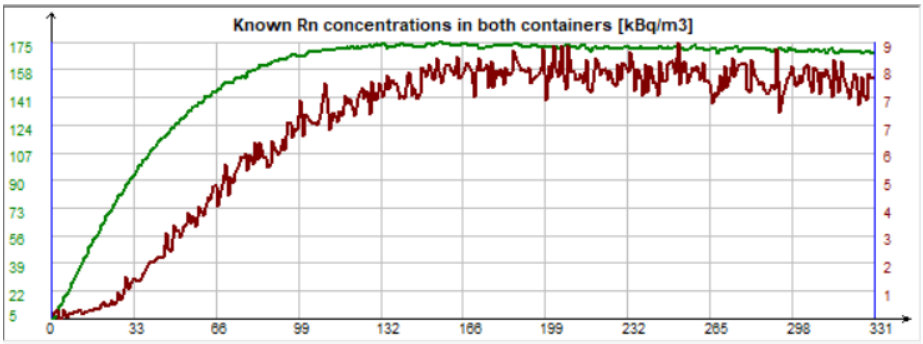

Figure 74. (a) Calculated data in the sw. IterRn (Silicate (mineral) screed - reference) – detector S1

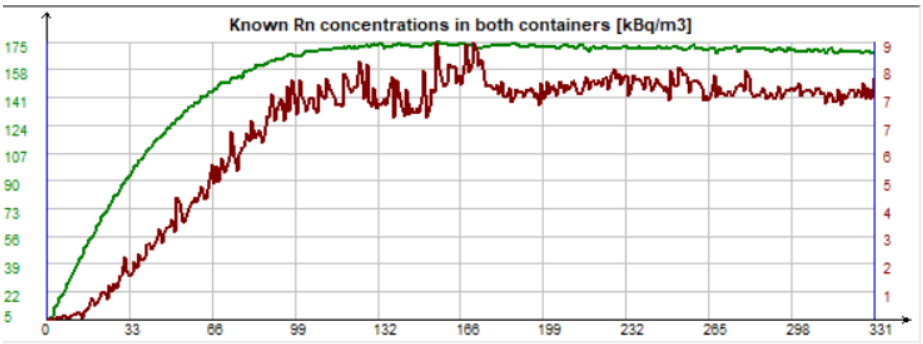

Figure 74. (b) Calculated data in the sw. IterRn (Silicate (mineral) screed - reference) – detector S2

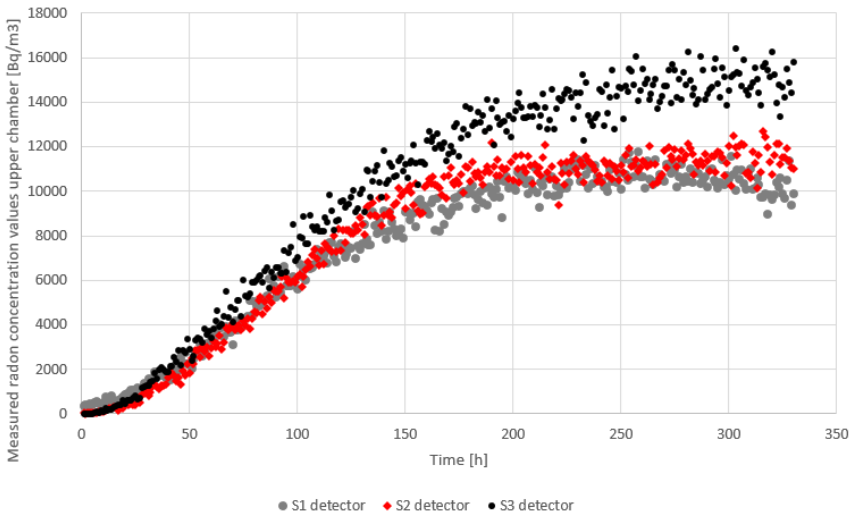

Figure 75. Measured radon (Silicate (mineral) screed – 30 freezing cycle) – detector S1, S2, S3

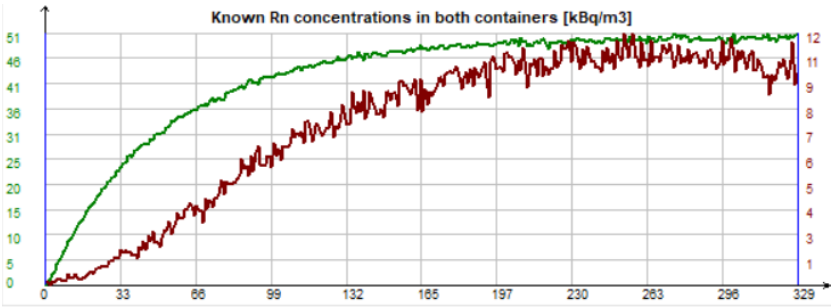

Figure 76. (a) Calculated data in the sw. IterRn (Silicate (mineral) screed - 30 freezing cycle) – detector S1

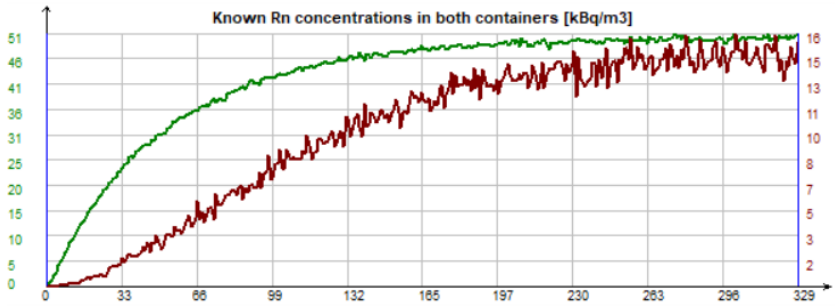

Figure 76. (b) Calculated data in the sw. IterRn (Silicate (mineral) screed - 30 freezing cycle) – detector S2

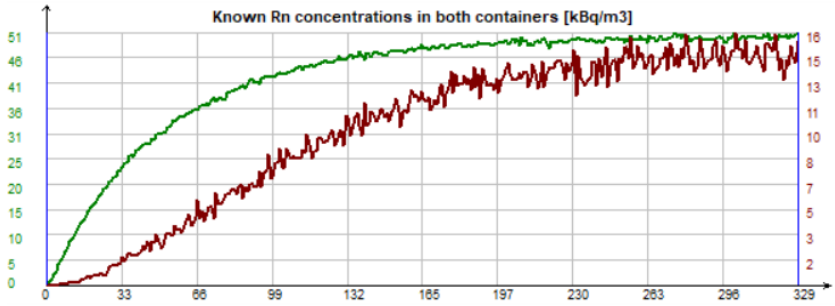

Figure 76. (c) Calculated data in the sw. IterRn (Silicate (mineral) screed - 30 freezing cycle) – detector S3

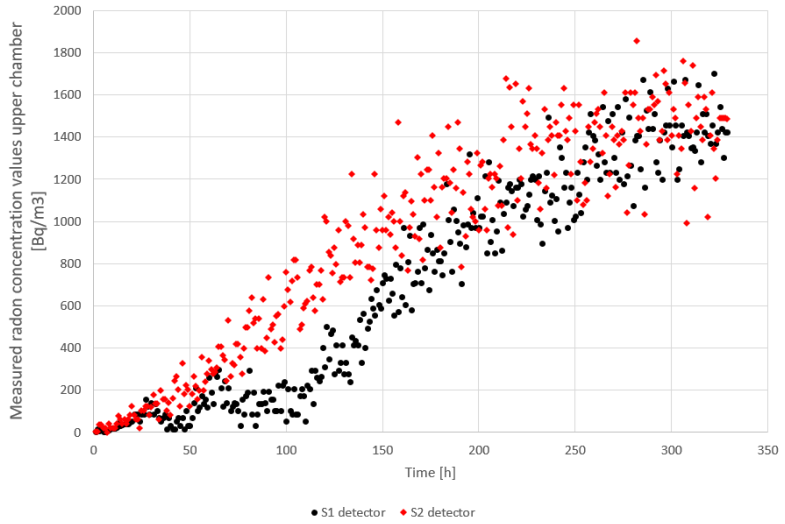

Figure 77. Measured radon concentration (Polymer screed – reference) – detector S1, S2

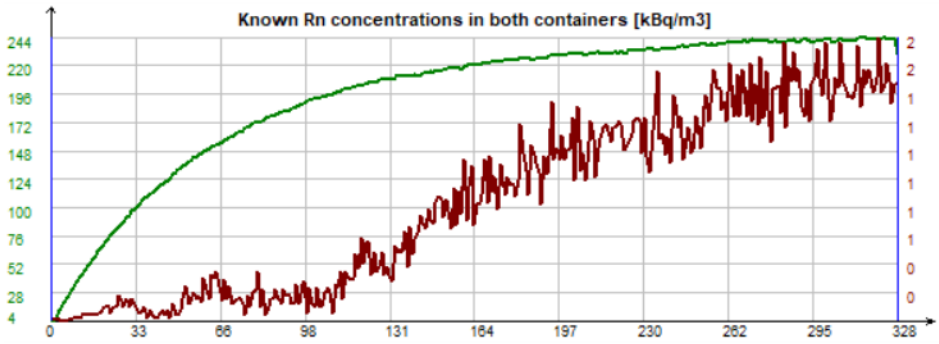

Figure 78. (a) Calculated data in the sw. IterRn (Polymer screed – reference) – detector S1

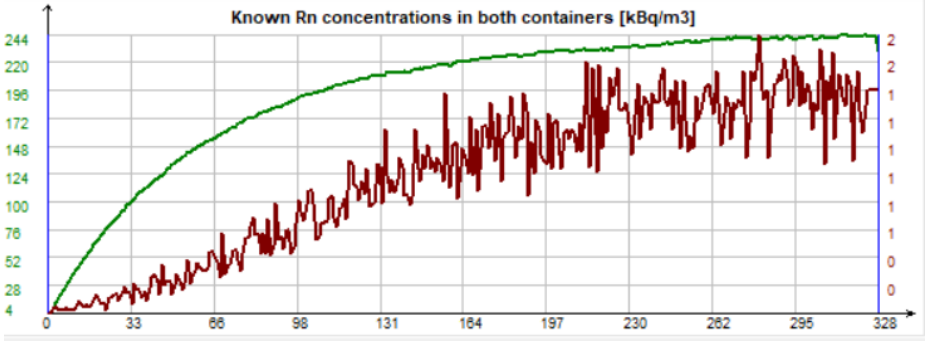

Figure 78. (b) Calculated data in the sw. IterRn (Polymer screed – reference) – detector S2

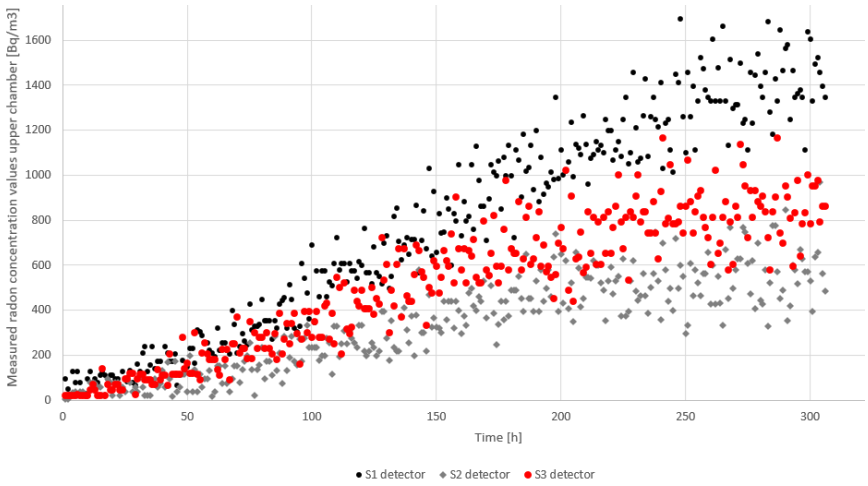

Figure 79. Radon concentration (Polymer screed – 30 freezing cycle) – detector S1, S2, S3

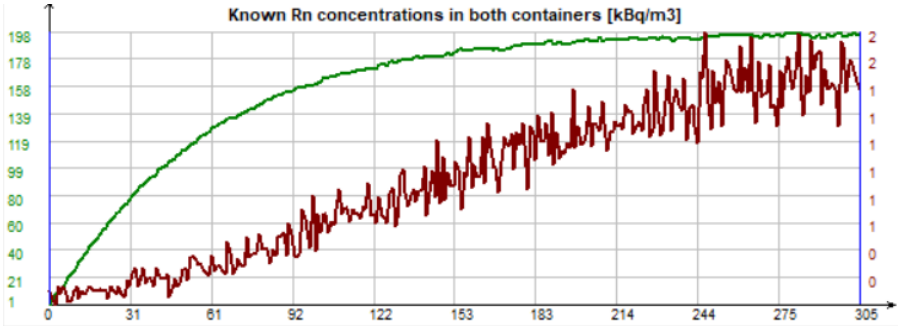

Figure 80. (a) Calculated data in the sw. IterRn (Polymer screed – 30 freezing cycle) – detector S1

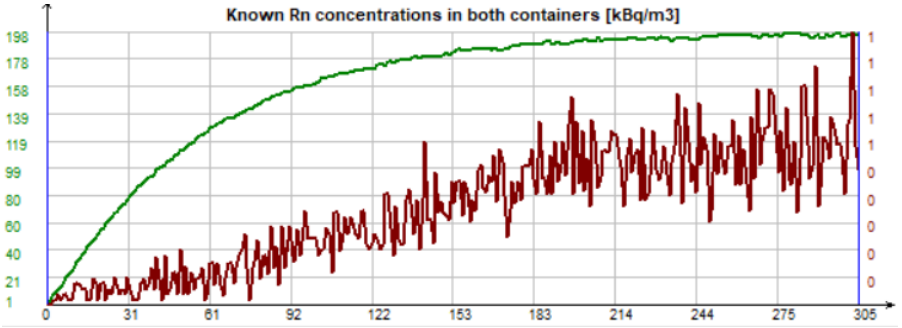

Figure 80. (b) Calculated data in the sw. IterRn (Polymer screed – 30 freezing cycle) – detector S2

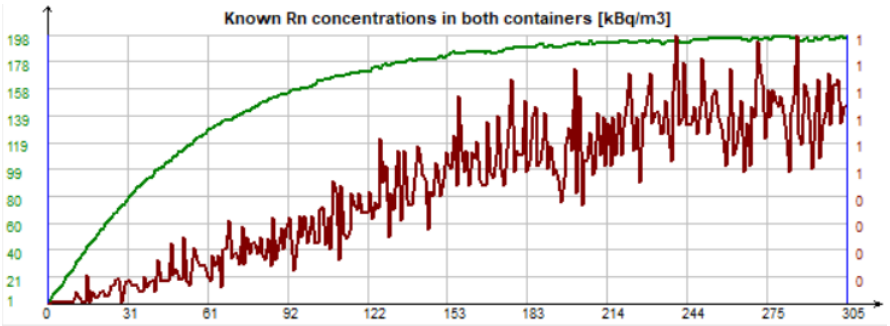

Figure 80. (c) Calculated data in the sw. IterRn (Polymer screed – 30 freezing cycle) – detector S3

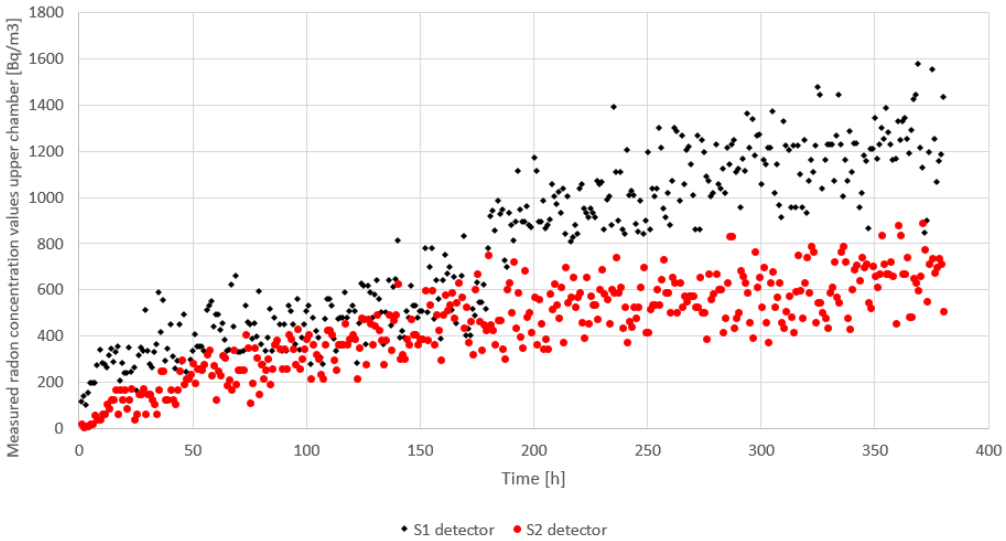

Figure 81. Radon concentration (Bituminous screed - reference) – detector S1, S2

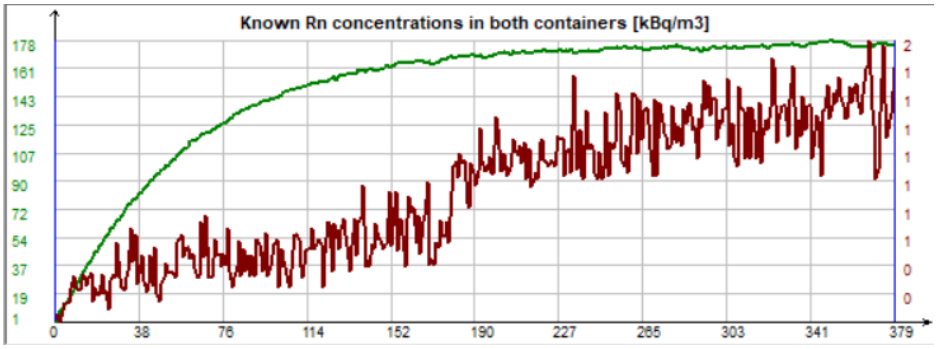

Figure 82. (a) Calculated data in the sw. IterRn (Bituminous screed - reference) – detector S1

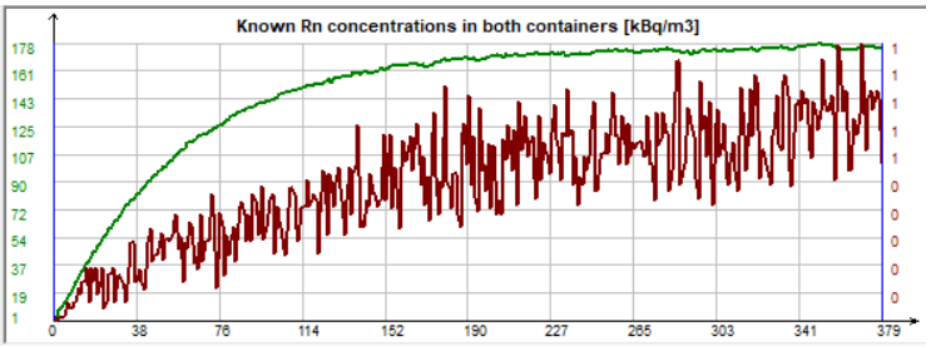

Figure 82. (b) Calculated data in the sw. IterRn (Bituminous screed - reference) – detector S2

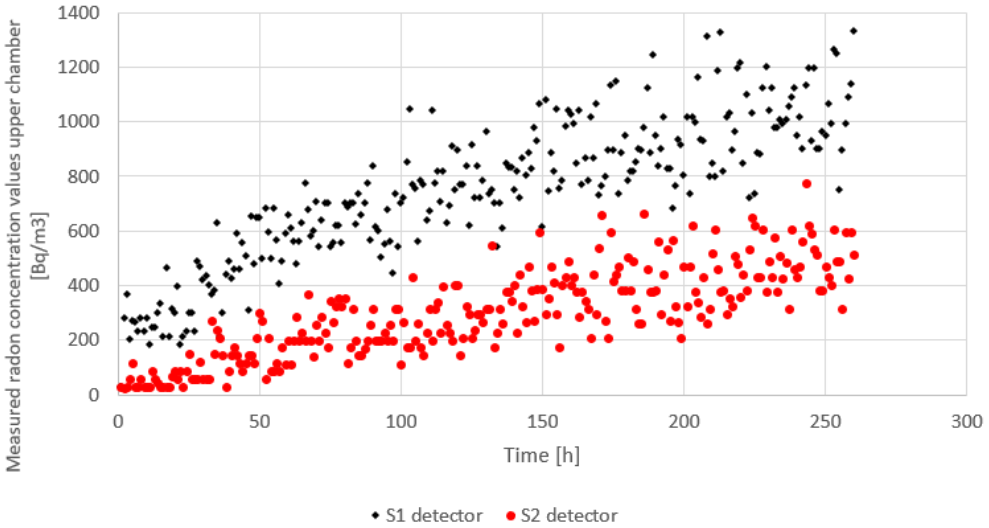

Figure 83. Radon concentration (Bituminous screed – 30 freezing cycle) – detector S1, S2

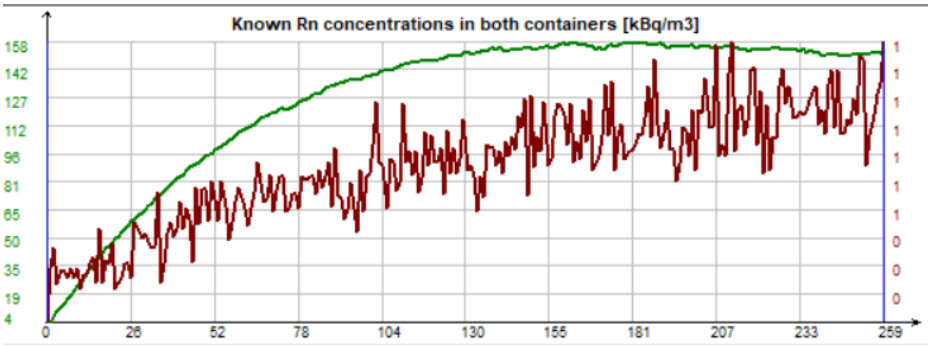

Figure 84. (a) Calculated data in the program IterRn (Bituminous screed – 30 freezing cycle) – detector S1

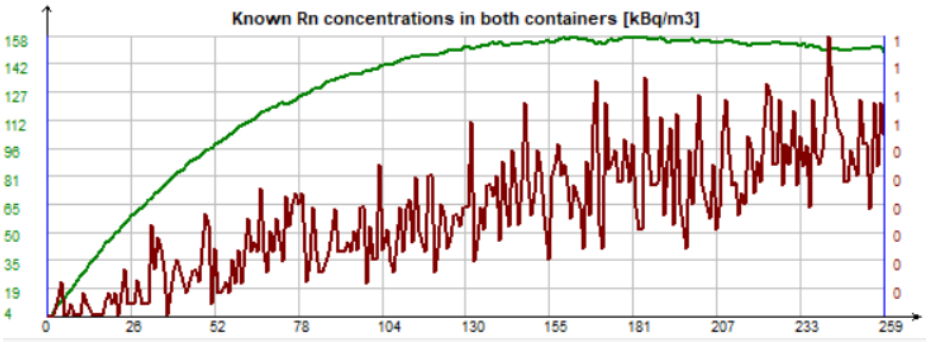

Figure 84. (b) Calculated data in the program IterRn (Bituminous screed – 30 freezing cycle) – detector S2

The measured data shown in the graphs above were subsequently evaluated in IterRn (Figure 72). On the x-axis is time in hours, on the y-axis are the measured concentrations in the both chamber after calculation.

6.2.1. Comparison of all tested waterproofing screeds

The mean values of the radon diffusion coefficient D [m^2/s] are shown in Table 11. These values were calculated from three or two specimens.

Table 11.

Type of the screeds	**Radon diffusion coefficient [m^2/h]**		**Standard deviation [m^2/h]**	
	0 freezing cycle	30 freezing cycle	0 freezing cycle	30 freezing cycle
Polymer screeds	**$4{,}65*10^{-12}$**	**$3{,}73*10^{-12}$**	$3{,}7*10^{-13}$	$8{,}2*10^{-13}$
Bituminous screeds	**$4{,}9*10^{-12}$**	**$3{,}2*10^{-11}$**	$4{,}0*10^{-13}$	$5{,}6*10^{-12}$
Silicate (mineral) screed	**$4{,}15*10^{-12}$**	**$4{,}05*10^{-12}$**	$9{,}1*10^{-14}$	$9{,}2*10^{-14}$

In general, it can be said that the effect of 30 freezing cycles on the resulting values is very low, but visible on the values.

The change in the diffusion coefficient was the lowest in the case of silicate (mineral) waterproofing screeds, at the same time with the highest measurement accuracy, see standard deviation. The measured mean value is 4.15×10^{-12} m^2/h in the case of the reference specimen and 4.05×10^{-12} m^2/h after 30 freezing cycles. It is evident from the measurements that the effect of 30 freezing cycles on the radon sealing ability of the silicate screed is negligible.

A polymer screeds also achieved very similar results. Here we can observe a small change in the radon diffusion coefficient. From the reference value of $4.65x10^{-12}$ m^2/h, the value increased to 3.73×10^{-12} m^2/h. In general, the lower the value of the Radon diffusion coefficient, the tighter the material.

In the case of bitumen screeds, the greatest increase in radon diffusion coefficient D [m^2/h] can be observed. The value measured for the reference sample is 4.9×10^{-12} m^2/h and after 30 cycles 3.2×10^{-11} m^2/h. There was a change of decimal order.

The measured values correspond to commonly used insulation materials, and it can therefore be said that the measurement and evaluation were carried out correctly. Waterproofing screeds are thus a suitable material for use in substructures. Unlike waterproofing made from strips such as bitumen membrane or PVC membrane, they do not contain joints and can thus be a more reliable solution. The measured values show minimal differences between the tested waterproofing screeds.

The results presented here should be considered as preliminary results, more extensive research with a larger number of freezing cycles is necessary to clarify the effect of freezing cycles on the insulating abilities of the tested waterproofing screeds. Such research is very time-consuming not only during the preparation of the specimens themselves in the freezing chamber, but also during the actual measurement of the radon diffusion coefficient D [m^2/s] and the subsequent evaluation of the measured data.

These results will be sent to the proceedings of the "Modern concrete and composites 2024" International Conference, which is indexed in the Scopus database.

7. CONCLUSION

In the introductory part of the dissertation, the suitability of the use of historic reinforced concrete construction as a substrate for the application of waterproofing screeds was assessed.

The concrete used for two analysed Czech WW2 fortifications successfully resisted the long-lasting effects of chemical corrosion as well as bio-corrosion. The chemical corrosion causes only aesthetic defects. This conclusion applies only to mechanically preserved objects that have not been damaged by military tests (cannons shooting) or the looting of raw materials from their construction. In addition, the findings open the way for experimental analysis of waterproofing screeds.

The three most commonly used types of screeds (bitumen, polymer and silicate) on the five types of the most commonly used building structures (ceramics, concrete, lime sand, sandstone and marl) were chosen for the study. The waterproofing ability of used screeds was evaluated in the experimental program in terms modified water permeability test. The cohesion was studied after the freeze-thaw exposure to take into consideration the durability aspects.

The main conclusions could be summarized as follows:

- The suitable waterproofing ability of all types of the tested screeds applied on building materials was confirmed.
- All studied screeds resisted the water pressure of 0.12 MPa, however the mineral screed exhibited a seepage into the substrate material,
- The permeability testing performed on the “whole masonry” blocks declared no negative influence of the joints on the tightness of the studied screeds,
- The best cohesion exhibited the polymer screed, however concurrently achieved the highest decay of the cohesion during freeze-thaw cycling,
- The cohesion of the bitumen and mineral screed were very similar. While, the decay of mechanical properties of mineral screed was proportional to passed freeze-thaw cycles, the bitumen screed exhibited significant drop of the mechanical performance after 15 cycles, however following freeze-thaw exposure caused negligible deterioration.

Furthermore, the effect of freezing cycles on the sealing ability against radon was investigated on the aforementioned screeds.

- The measured values correspond to commonly used insulation materials, and it can therefore be said that the measurement and evaluation were carried out correctly.
- Waterproofing screeds are thus a suitable material for use in substructures. Unlike waterproofing made from strips such as bitumen membrane or PVC membrane, they do not contain joints and can thus be a more reliable solution.

- The measured values show minimal differences between the tested waterproofing screeds. Especially in the case of silicate (mineral) screed and polymer screed, the effect is negligible. The greatest effect of antifreezes on the ability to seal against radon was observed for bitumen screeds.

The performed tests were carried out on masonry from new materials. The next question arises, whether the same results would be achieved in the case of mature masonry from a real structure. In the case of mature masonry, different degrees of chemical salinity due to the penetration of water over time can be observed. The action of chemically impure water (leakage through the masonry) can degrease the mechanical and physical properties of the screed. This should be the subject of a further study conducted in the future.

The knowledge and information gained during the preparation of the dissertation was used in the NAKI II project - DG18P02OVV063.

8. LITERATURE

[1] ROVNANÍKOVÁ, Pavla. S*tavební chemie: Modul 3 - Degradace stavebních materiálů a chemie kovů*. 1. vyd. Brno: CERM, **2005**. 48 s. ISBN 80-7204-410-9.

[2] BALÍK, M. *Odvlhčování staveb*. 2. vyd. Praha: Grada, **2008**, 312 s. ISBN 978-80-247-2693-4

[3] ČSN 73 0610. Hydroizolace staveb – Sanace vlhkého zdiva – základní ustanovení. Český normalizační institut, Praha, **2000**

[4] ŠUHAJDA, Karel. Sanace vlhkého zdiva staveb - Využití tyčové antény při mikrovlnném vysoušení zdiva. PhD thesis, VUT Brno, **2006.**

[5] MRLÍK, František. Vlhkostné problémy stavebných materiálov a konštrukcií. Bratislava: Alfa, 1985. Edícia stavebníckej literatúry (Alfa).

[6] BENEŠ, Petr. Sanace a adaptace budov. Brno: Vysoké učení technické v Brně, Fakulta stavební, **2007**.

[7] BALÍK, Michael. Vysušování zdiva. Vyd. 1. Praha: Grada. **1997**, 113 s., 12 s. barevných obrazových příloh. Profi. ISBN 80-716-9440-1.

[8] WTA – vědeckotechnická společnost pro sanace staveb a péči o památky. Směrnice. Praha : ÚIV – divize nakladatelství TAURIS. **2005**. ISBN 80-02-01741-2.

[9] KÜNZEL, Hartwig M. Simultaneous heat and moisture transport in building components: one- and two-dimensional calculation using simple parameters. Stuttgart: IRB Verlag. **1995,** 102 p. ISBN 38-167-4103-7.

[10] VLČEK, Milan. Poruchy a rekonstrukce staveb. 3. vyd. Brno: ERA, **2006,** 222 s. Technická knihovna (ERA). ISBN 80-736-6073-3.

[11] Článek v časopise Beton, Vlivy prostředí na korozi betonu z pohledu chemických reakcí, Enviromental effect on concrete corrosion in terms of chemical reaction, **02/2017**, http://www.betontks.cz/sites/default/files/2017-2-03_0.pdf

[12] Henning, Otto; *Chemie ve stavebnictví,* Praha: Státní nakladatelství technické literatury (SNTL), **1983**.

[13] WHO handbook on indoor radon: a public health perspective. Geneva, Switzerland: World Health Organization, **2009**. ISBN 9789241547673.

[14] C. Cosma, A. Cucoş-Dinu, B. Papp, R. Begy, C. Sainz, Soil and building material as main sources of indoor radon in Bâiţa-ştei radon prone area (Romania), J. Environ. Radioact. 116 (**2013**) 174–179. https://doi.org/10.1016/j.jenvrad.2012.09.006.

[15] B. Collignan, E. Le Ponner, C. Mandin, Relationships between indoor radon concentrations,thermal retrofit and dwelling characteristics, J. Environ. Radioact. 165 (**2016**) 124–130. https://doi.org/10.1016/j.jenvrad.2016.09.013.

[16] L. Felicioni, A. Lupíšek, M. Jiránek, Embodied Energy and Global Warming Potential of Radon Preventive Measures Applied in New Family Houses, in: Smart Innov. Syst. Technol.,Springer, Singapore, **2022**: pp. 57–68. https://doi.org/10.1007/978-981-16-6269-0_5.

[17] Keller G, Hoffmann B, Feigenspan T. Radon permeability and radon exhalation of building materials. Sci Total Environ. **2001** May 14;272(1-3):85-9. doi: 10.1016/s0048-9697(01)00669-6. PMID: 11379942.

[18] Martin Jiránek, Veronika Kačmaříková. Radon diffusion coefficients and radon resistances of waterproofing materials available on the building market, Journal of Environmental Radioactivity, Volumes 208–209, **2019**, ISSN 0265-931X, https://doi.org/10.1016/j.jenvrad.2019.106019.

[19] Decree No. 307/2002 Coll., on radiation protection, as amended by Decree No. 499/2005 Coll. and Decree No. 389/2012 Coll., establishes so-called guideline values for radon content in existing and new buildings.

[20] Suro.cz, **2013**. Základní informace o radonu [online]. Dostupné z: https://www.suro.cz/cz/faq/radon-v-dome#faq1

[21] ČSN 73 0601. Ochrana staveb proti radonu z podloží. Český normalizační institut, Praha, **2019**

[22] Kateřina Navrátilová Rovenská, Martin Jiránek, Veronika Kačmaříková. The influence of long-term degradation of waterproof membranes on mechanical properties and on the radon diffusion coefficient – preliminary results. Journal of Cleaner Production, Volume 88, **2015**, Pages 369-375, ISSN 0959-6526, https://doi.org/10.1016/j.jclepro.2014.06.012.

[23] M. Kubal, Construction Waterproofing Handbook, (Second Ed.), McGraw-Hill Publishing (**2008**).

[24] M. Chew, N. De Silva, Benchmarks to minimize water leakages in basements, Structural Survey, 21 (4) (**2003**), pp. 131-145.

[25] M. Larisch, Modern concrete technology and placement methods and their influence on waterproofing performance of Diaphragm walls, The New Zealand Concrete Industry Conference 2016 Auckland New Zealand (**2016**).

[26] J. Pazderka, Concrete with Crystalline Admixture for Ventilated Tunnel against Moisture, Key Engineering Materials. 677 (**2016**) pp. 108-113.

[27] V. T. N. Dao, P. F. Dux, P. H. Morris, A. H. Carse, Performance of permeability-reducing admixtures in marine concrete structures, ACI Materials Journal. 107/ 3 (**2010**) pp. 291–296.

[28] Furuya T., et al.: An effective and eternal maintenance method for concrete tunnel structures, Tunnel Structures. Labse Reports: Volume 78, p. 439-447, Stockholm **1998**.

[29] Maher Al-Jabari, Integral Waterproofing of Concrete Structures, Chapter 12 - Waterproofing coatings and membranes, **2022**, 393-435. https://doi.org/10.1016/C2020-0-01212-0

[30] ACI. (**1986**). Committee 515, ACI 515.1R-79 A guide to the use of waterproofing, dampproofing. Protective, and decorative barrier systems for concrete. Farmington Hills, MI, USA: American Concrete Institute.

[31] ACI. (**2013**). Committee 515, ACI 515.2R-13 Guide to selecting protective treatments for concrete. Farmington Hills, MI, USA: American Concrete Institute.

[32] BS. (**1998**). BS 1504-2, Products and systems for the protection and repair of concrete structures—Definitions, requirements, quality control and evaluation of conformity. British Standards Institution.

[33] WTA Merkblatt 4-6-05 Wissenschaftlich-Technische Arbeitsgemeinschaft für Bauwerkserhaltung und Denkmalpflege e.V. -WTA-, ISBN: 978-3-8167-6996-5, Stuttgart (Deutschland): Fraunhofer IRB Verlag, **2005**, 24 S., Abb., Tab.

[34] DIN 18195-1:2000-08 - Water-proofing of buildings - Part 1: Principles, definitions, attribution of waterproofing types, pp. **2000-08**.

[35] Zhu, K., He, X., Quan, Y., Zhong, W., & Zhang, K. (**2019**). Application of non-curing rubber asphalt screed in waterproofing of shield tunnel segment joints in water-rich stratum. Modern Tunnelling Technology, **2019**, 56(5), 201-205. doi:10.13807/j.cnki.mtt.2019.05.027.

[36] C. Kho, S.C. Tan, Y.C. Kog, A Strategy for Waterproofing of Underground Structures, Under. Singapore 2014, Singapore (**2014**).

[37] MARTIN, K., 1970. Flexible plastics sheets for waterproofing. Building Forum, 2(1052), p. 109.

[38] Lim, S., & Kawashima, S. (**2019**). Mechanisms underlying crystalline waterproofing through microstructural and phase characterization. Journal of Materials in Civil Engineering, 31(9) doi:10.1061/(ASCE)MT.1943-5533.0002752.

[39] Z. Song, X. Xue, Y. Li, J. Yang, Z. He, S. Shen, L. Jiang, W. Zhang, L. Xu, H. Zhang, Experimental exploration of the waterproofing mechanism of inorganic sodium silicate-based concrete sealers, Constr. Build. Mater., 104 (**2016**), pp. 276-283.

[40] I.H. Wong, Experience with waterproofness of basements constructed of concrete diaphragm walls in Singapore, Tunn. Undergr. Space Technol., 12 (4) (**1997**), pp. 491-495.

[41] KAYA, D., TOPAL, A., GUPTA, J. and MCNALLY, T. Aging effects on the composition and thermal properties of styrene-butadiene-styrene (SBS) modified bitumen. Construction and Building Materials, p. 235. **2020**.

[42] Yanheng He, Zhilong Cao, Zhaoyang Liu, Jiangting Li, Jianying Yu, Yangyang Ge, Influence of heat and ultraviolet aging on the structure and properties of high dosage SBS modified bitumen for waterproof, Construction and Building Materials, Volume 287, **2021**, 122986, ISSN 0950-0618.

[43] Chuanfeng Zheng, Junpeng Xu, Ting Zhang, Guojin Tan, Study on the microscopic damage of porous asphalt mixture under the combined action of hydrodynamic pressure and ice crystal frost heave, Construction and Building Materials, Volume 303, **2021**, ISSN 0950-0618.

[44] Bader, T., Waldner, B. J., Unterberger, S. H., & Lackner, R. (**2019**). On the performance of film formers versus penetrants as water-repellent treatment of high-performance concrete (HPC) surfaces. Construction and Building Materials, 203, pp. 481-490. doi:10.1016/j.conbuildmat.2019.01.089.

[45] Jihoon Kim, Ryoma Kitagaki, Chemical properties and mass transfer resistance of mortar surface modified with silicate-based surface impregnant, Construction and Building Materials, **2020**, ISSN 0950-0618.

[46] Jun Chang, Wenzheng Li, Dan Wang, Yangyang Zhang, Effect of silicate modulus on tensile properties and microstructure of waterproof coating based on polymer and

sodium silicate-activated GGBS, Construction and Building Materials, Volume 252, **2020**, ISSN 0950-0618.

[47] S.-H. Chang, T.-H. Kang, S.-W. Choi, C. Lee, G.-S. Hwang, M.-S. Choi, An Experimental study on fundamental properties of a sprayable waterproofing membrane, Tunnel Undergr. Space, 26 (3) (**2016**), pp. 220-234.

[48] Rahman, M. and Chamberlain, D. : Performance of crystalline hydrophobic in wet concrete protection, Journal of Materials in Civil Engineering, Volume 29, Issue 6, 1 June **2017**, Article number 04017008.

[49] Almusallam, A., Khan, F., Dulaijan, S. & Al-Amoudi, O. **2003**, Effectiveness of surface screeds in improving concrete durability, Cement and Concrete Composites, vol. 25, no. 4, pp. 473-481.

[50] Scancella, T., Robert, J.: Use of Xypex admixture to concrete as an inhibitor to reinforcement steel corrosion. Proceedings of the Materials Engineering Conference, 2, **1996**, pp. 1276-1280.

[51] Russell, H. G, U.S.. Transportation Research Board National Research Council, National Cooperative Highway Research Program, American Association Of State Highway And Transportation Officials, and United States Federal Highway Administration. Waterproofing Membranes for Concrete Bridge Decks. Washington, D.C.: Transportation Research Board, **2012**. https://lccn.loc.gov/2011943710.

[52] Jappie, L. Literature review of the use of common protective coatings for concrete structures with experiences in the South African context. Engineering and the Built Environment, University of Cape Town. Rondebosch, Cape Town, South Africa. **2019**

[53] Rasiah Sriravindrarajah, Elizebeth Tran. Waterproofing practices in Australia for building construction. MATEC Web Conf. 195 01002 (**2018**). doi: 10.1051/matecconf/201819501002

[54] Xiaoying Pan, Zhenguo Shi, Caijun Shi, Tung-Chai Ling, Ning Li, A review on concrete surface treatment Part I: Types and mechanisms, Construction and Building Materials, Volume 132, **2017**, Pages 578-590, ISSN 0950-0618, https://doi.org/10.1016/j.conbuildmat.2016.12.025.

[55] Jerzy Bochen, Weathering effects on physical–chemical properties of external plaster mortars exposed to different environments, Construction and Building Materials, Volume 79, **2015**, pp. 192-206.

[56] Chatterji S. Aspects of the freezing process in a porous material–water system: part 1. Freezing and the properties of water and ice. Cement Concrete Res. **1999**;29(4):627–30. https://doi.org/10.1016/S0008-8846(99)00035-6.

[57] Klovas, A., Dauksys, M., & Ciuprovaite, G. (**2015**). Frost resistance of concrete surfaces coated with waterproofing materials. Paper presented at the AIP Conference Proceedings, 1653 doi:10.1063/1.4914252.

[58] Xiaoying Pan, Zhenguo Shi, Caijun Shi, Tung-Chai Ling, Ning Li, A review on surface treatment for concrete – Part 2: Performance, Construction and Building Materials, Volume 133, **2017**, pp. 81-90.

[59] SOLAŘ, Jaroslav. Odstraňování vlhkosti: sanace vlhkého zdiva. Praha: Grada, **2013**. Profi & hobby. ISBN 978-80-247-4708-8.

[60] Merck KGaA [online]. Darmstadt, Germany: Merck, ©2018 [cit. **2018-07-16**]. Dostupné z: http://www.merckmillipore.com/CZ/cs

[61] ČSN 73 2579:**1981**- Test for frost resistance of surface finish of building structures, pp. 1981-04.

[62] Jiránek, M. and Svoboda, Z. Transient radon diffusion. through radon-proof membranes: a new technique for more precise determination of the radon diffusion coefficient. Build. Environ. 44, 1318–1327 (**2009**). doi: 10.1016/j.buildenv.2008.09.017.

[63] Svoboda Z. Software packages TransRn & IterRn, version 2008. Prague: Czech Technical University; 2008.

9. PUBLICATION ACTIVITY OF THE AUTHOR

[1] **NÝVLT, M.,** J. PAZDERKA a P. REITERMAN. **Comparative study of different types of waterproofing screeds with a focus on cohesion with selected building materials after the freeze-thaw exposure.** Applied Sciences. **2021**, 11(23), ISSN 2076-3417. DOI 10.3390/app112311256

[2] PAZDERKA, J.; HÁJEK, P.; **NÝVLT, M**.; ŽÁKOVÁ, H. Parapet Structure from Special Shaped TRC Blocks. In: In: Fibre Concrete 2019. Bristol: IOP Publishing Ltd, **2019**. p. 1-6. IOP Conference Series: Materials Science and Engineering. vol. 596. ISSN 1757-899X.

[3] **NÝVLT, M.** a J. PAZDERKA. Analysis of Corrosion Products from WW2 Concrete Bunkers in Czechia. In: SPECIAL CONCRETE AND COMPOSITES 2018. Hotel Skalský Dvůr, Lisek, 2018-10-11/2018-10-12. Praha: České vysoké učení technické v Praze, **2019**. s. 77-82. ACTA POLYTECHNICA CTU PROCEEDINGS. sv. 22. ISSN 2336-5382. ISBN 978-80-01-06594-5. DOI 10.14311/APP.2019.22.0077

[4] PAZDERKA, J., **M. NÝVLT** a H. ŽÁKOVÁ. Underground ventilated wall based on TRC blocks. In: BÍLÝ, P. et al., eds. Fibre Concrete **2019**. Praha, 2019-09-17/2019-09-20. Bristol: IOP Publishing Ltd, 2019. s. 1-6. IOP Conference Series: Materials Science and Engineering. sv. 596. ISSN 1757-899X. DOI 10.1088/1757-899X/596/1/012037

[5] PAZDERKA, J.; HÁJEK, P.; ŽÁKOVÁ, H.; **NÝVLT, M.** Internal Ventilated Plinth as One of the Possible Solution for Moist Buildings. In: SOJKOVÁ, K. et al., eds. Central Europe towards Sustainable Building (CESB19). Central Europe towards Sustainable Building **2019,** Praha, 2019-07-02/2019-07-04. Bristol: IOP Publishing Ltd, 2019. IOP Conference Series:Earth and Environmental Science. sv. 290. ISSN 1755-1307. DOI 10.1088/1755-1315/290/1/012135

[6] PAZDERKA, J.; REITERMAN, P.; ŽENÍŠEK, **M.; NÝVLT**, M.; LUKÁŠ, P.; MOTTL, M.; HOLČAPEK, O.; ZATLOUKALOVÁ, J. et al. Stavebně technické průzkumy pevností z 30. let 20. století a technická řešení jejich obnovy Praha: CTU. Faculty of Civil Engineering, **2022**. ISBN 978-80-01-07070-3.

[7] LUKÁŠ, P.; **NÝVLT, M.;** HOLČAPEK, O.; ZATLOUKALOVÁ, J.Rehabilitation of water leakage in the fortress T-St-S 73 at the Stachelberg artillery complex In: SPECIAL CONCRETE AND COMPOSITES 2021: 18th International Conference. Melville, NY: AIP Publishing, **2023**. AIP Conference Proceedings. vol. 2780. ISSN 0094-243X. ISBN 978-0-7354-4514-7.

10. USED FIGURES

No. figure	Title	Source	
Figure 1	Water vapour diffusion	[F1]	https://www.wbdg.org/resources/moisture-management-concepts
Figure 2	Illustration of Wettability	[F2]	Roles of chemistry modification for laser textured metal alloys to achieve extreme surface wetting behaviors - Scientific Figure on ResearchGate. Available from: https://www.researchgate.net/figure/Classification-of-wetting-based-on-th-w-a-hydrophilic-b-superhydrophilic-c_fig1_341040640 [accessed 14 Jan, 2024]
Figure 3	Interstitial condensation calculations	[F3]	Birchmore, R.; Pivac, A.; Tait, R. Impacts of an Innovative Residential Construction Method on Internal Conditions. Buildings 2015, 5, 179-195. https://doi.org/10.3390/buildings5010179
Figure 4	Adsorption isotherm with a hysteresis loop	[F4]	Role of Excipients in Moisture Sorption and Physical Stability of Solid Pharmaceutical Formulations - Scientific Figure on ResearchGate. Available from: https://www.researchgate.net/figure/A-schematic-representation-of-a-sorption-isotherm-with-a-hysteresis-between-the_fig2_47930642 [accessed 14 Jan, 2024]
Figure 5	Diagram of concrete damage by liquid aggressive environment	[F5]	Schéma poškození betonu kapalným agresivním prostředím [online]. In: . [cit. 2018-05-30]. Dostupné z: http://www.betontks.cz/sites/default/files/2017-2-03_0.pdf
Figure 6	Corrosion I – leachates		Author
Figure 7	Corrosion I – leachates		Author
Figure 8	Type II corrosion (acid corrosion)	[F6]	Koroze II [online]. In: . [cit. 2018-06-01]. Dostupné z: http://www.stavebnictvi3000.cz/obr/xlarge/2011/9_betosan_4.jpg
Figure 9	Type II corrosion (acid corrosion)	[F7]	Koroze II [online]. In: . [cit. 2018-06-01]. Dostupné z: http://www.stavebnictvi3000.cz/obr/xlarge/2011/9_betosan_5.jpg
Figure 10	Corrosion III - sulphate corrosion	[F8]	Corrosion on Bridge Beam [online]. In: . [cit. 2018-06-01]. Dostupné z: https://precast.org/wp-content/uploads/2013/11/ASR-on-Bridge-Beam.jpg
Figure 11	Corrosion III - sulphate corrosion		Author
Figure 12	Surface damage		Author
Figure 13	Bridge ledge deterioration		Author
Figure 14	Biological deterioration		Author
Figure 15	Biological deterioration		Author
Figure 16	Summary of risks of lung cancer from indoor radon based on international pooling studies	[13]	WHO handbook on indoor radon: a public health perspective. Geneva, Switzerland: World Health Organization, 2009. ISBN 9789241547673.

	that have combined individual data from a number of case-control studies		
Figure 17	Relative risks and 95% confidence intervals are shown for categorical analyses and also best fitting straight line. Risks are relative to that at 0 Bq/m3.	[13]	WHO handbook on indoor radon: a public health perspective. Geneva, Switzerland: World Health Organization, 2009. ISBN 9789241547673.
Figure 18	Application of bitumen waterproofing screeds with a reinforcing belt		Author
Figure 19	Application of the bitumen waterproofing screed on a detail with a complex shape		Author
Figure 20	Application of silicate (mineral) waterproofing screeds		Author
Figure 21	Application of the silicate (mineral) waterproofing screed on the drain area		Author
Figure 22	Application of the polymer waterproofing screeds		Author
Figure 23	Application of the polymer waterproofing screed on the detail under the door		Author
Figure 24	Object 1 – T-S 19		Author
Figure 25	Object 2 – T-S 20		Author
Figure 26	The samples are exposed to ultrasound		Author
Figure 27	Inserting the samples into clean glass caps		Author
Figure 28	Samples with added pH indicator		Author
Figure 29	Colorimetric evaluation of pH by colour and scale		Author
Figure 30	Heating the agar solution on an electric cooker		Author
Figure 31	Using sterilization device		Author
Figure 32	Mold on sample number 1		Author
Figure 33	Mold on sample number 2		Author
Figure 34	Observation of mold samples by microscope		Author
Figure 35	Alternaria alternate		Author
Figure 36	Cladosporium herbarum		Author
Figure 37	Penicillium		Author
Figure 38	Test specimens		Author
Figure 39	(a) Weighing the test specimens; (b) Water pressure test		Author
Figure 40	(a) Test specimen – lime-sand bricks and lime-cement mortal in wooden formwork; (b) Test specimens with applied waterproof screeds.		Author
Figure 41	Water pressure test on the sets of specimens.		Author
Figure 42	(a) Model of the specimen; (b) Model of the prepared specimen with a delimiting ring and the applied waterproofing screed.		Author
Figure 43	Assembly of all test specimens with glued threaded rods (ceramics, concrete, Lime sand, marl).		Author
Figure 44	Assembly of all test specimens with glued threaded rods (sandstone).		Author

Figure 45	Prepared test specimen with glued threaded rod, PVC ring		Author
Figure 46	Prepared front of the test specimen for the application of a waterproofing screed		Author
Figure 47	Finished set of specimens with the applied waterproofing screed (ceramics, concrete, Lime sand, marl).		Author
Figure 48	Finished set of specimens with the applied waterproofing screed (sandstone).		Author
Figure 49	Tear-off test disc target scheme		Author
Figure 50	Gluing tear-off targets		Author
Figure 51	Detail of a test specimen with a glued target.		Author
Figure 52	Test specimen prepared for the tear-off test.		Author
Figure 53	Change in weight during the time (in percentage).		Author
Figure 54	Change in weight during the time (in percentage).		Author
Figure 55	(a) Typical course of tensile force on a test specimen; (b) Adhesive failure.		Author
Figure 56	(a) Cohesive failure; (b) Substrate failure.		Author
Figure 57	Results of the tear-off test, Tensile strength.		Author
Figure 58	Loss of strength – ceramics		Author
Figure 59	Loss of strength - lime sand		Author
Figure 60	Loss of strength - marl		Author
Figure 61	Loss of strength - concrete		Author
Figure 62	Loss of strength - Sandstone		Author
Figure 63	Certificate of acceptance		Author
Figure 64	(a) Average adhesion strength without the influence of the substrate; (b) Average residual strength after 30 freezing cycles without the influence of the substrate [%]		Author
Figure 65	Specimen set with applied waterproofing screeds		Author
Figure 66	Measuring device with one source chamber and three receiving chambers		Author
Figure 67	(a) Used measuring device (b) Used measuring device		Author
Figure 68	Measuring device with inserted and sealed specimens.		Author
Figure 69	The sealed specimens		Author
Figure 70	Specimens removed from the measuring device, sealant visible around the perimeter		Author
Figure 71	(a) Measuring the thickness of the applied waterproofing screed (b) Measuring the thickness of the applied waterproofing screed		Author

	(c) Measuring the thickness of the applied waterproofing screed		
Figure 72	Software IterRn interface [63]		Author
Figure 73	Measured radon concentration (Silicate (mineral) screed - reference) – detector S1, S2		Author
Figure 74	(a) Calculated data in the sw. IterRn (Silicate (mineral) screed - reference) – detector S1 (b) Calculated data in the sw. IterRn (Silicate (mineral) screed - reference) – detector S2		Author
Figure 75	Measured radon (Silicate (mineral) screed – 30 freezing cycle) – detector S1, S2, S3		Author
Figure 76	(a) Software IterRn interface b) Calculated data in the sw. IterRn (Silicate (mineral) screed - 30 freezing cycle) – detector S2 (c) Calculated data in the sw. IterRn (Silicate (mineral) screed - 30 freezing cycle) – detector S3		Author
Figure 77	Measured radon concentration (Polymer screed – reference) – detector S1, S2		Author
Figure 78	(a) Calculated data in the sw. IterRn (Polymer screed – reference) – detector S1 (b) Calculated data in the sw. IterRn (Polymer screed – reference) – detector S2		Author
Figure 79	Radon concentration (Polymer screed – 30 freezing cycle) – detector S1, S2, S3		Author
Figure 80	(a) Calculated data in the sw. IterRn (Polymer screed – 30 freezing cycle) – detector S1 (b) Calculated data in the sw. IterRn (Polymer screed – 30 freezing cycle) – detector S2 (c) Calculated data in the sw. IterRn (Polymer screed – 30 freezing cycle) – detector S3		Author
Figure 81	Radon concentration (Bituminous screed – reference) – detector S1, S2		Author
Figure 82	(a) Calculated data in the sw. IterRn (Bituminous screed – reference) – detector S1 b) Calculated data in the sw. IterRn (Bituminous screed – reference) – detector S2		Author
Figure 83	Radon concentration (Bituminous screed – 30 freezing cycle) – detector S1, S2		Author
Figure 84	(a) Calculated data in the program IterRn (Bituminous screed – 30 freezing cycle) – detector S1 (b) Calculated data in the program IterRn (Bituminous screed – 30 freezing cycle) – detector S2		Author

11. TECHNICAL SHEETS OF USED MATERIAL

Den Braven

Technický list
TL 06.93b Jednosložková hydroizolace EXTERIÉR

Produkt

Je již hotová jednosložková, polotekutá hmota s tixotropními vlastnostmi na bázi polymerové disperze. Po zaschnutí hmoty se vytvoří vysoce elastický, těsný, voděodolný a mrazuvzdorný nátěr s dobrou přilnavostí k podkladu. Neobsahuje organické látky.

Vlastnosti

- Vysoká přilnavost ke stavebním materiálům
- Na vodorovné i svislé plochy
- Po vytvrzení trvale pružná
- Odolná proti povětrnostním vlivům, mrazuvzdorná

Použití

- Hydroizolační nátěry pod keramické obklady a dlažby v interiérech i exteriérech budov balkóny, terasy, lodžie, mokré provozy, koupelny, sprchy, toalety, prádelny, sklepy, kuchyně, umývárny apod.
- Jako izolace konstrukcí vystavené kladnému tlaku působení vody

Technické vlastnosti			
Základ	Emulze kopolymerů		
Hustota	kg/m³	≈ 1700 ± 10 %	ČSN 50 3602
Tloušťka jedné vrstvy	mm	0,3 – 0,6	
Sušina, podíl pevných látek	%	60	
Tepelná odolnost při přepravě	min °C	+5	nesmí zmrznout
Tepelná odolnost	°C	-20 / +70	po vytvrzení
Aplikační teplota	°C	+5 / +35	Pro vzduch i podklad
Doba schnutí vrstvy	hod	3 - 6	První vrstva podle savosti podkladu
	hod	6	Druhá vrstva
Doba zakrytí ochranou vrstvou	dnů	Max. 28 dní	Musí být zakryta cementovým lepidlem nebo nátěrem
Pevnost v tahu	MPa	1,64 (N/mm²)	deklarováno ≥ 1,0 (N/mm²)
Přídržnost k podkladu	MPa	0,68	deklarováno ≥ 0,5 (N/mm²)
Poměrné prodloužení	%	560	deklarováno ≥ 300 %
Nasákavost	%	14,9	deklarováno ≤ 15 %
Vodotěsnost	-	vyhovuje	při tlaku 0,8 MPa za 72 hodin
Chování při působení vnějšího požáru	-	$B_{roof}(t_1)$	EN 13501-1:2007 a PN ENV 1187:2004

Balení

- Kbelík 5 kg
- Kbelík 13 kg

Barva

- Modrá

DEN BRAVEN
Czech and Slovak a.s.
793 91, Úvalno 353
Česká republika
IČO: 26872072
DIČ: CZ26872072
+420 554 648 200
info@denbraven.cz
www.denbraven.cz

Den Braven

Skladovatelnost	měsíce	12	při teplotě od +10 / +25 °C
Přibližná spotřeba na 1 m²	kg	1,0 – 1,5	2 nátěry

Druh podkladu

Betonové mazaniny, cementové, vápeno-cementové omítky, zdivo s plnou spárou, stěny z betonu, silikátových i pálených cihel a pórobetonů, cementovláknité, sádrokartonové desky. Podlahy betonové, cementové, anhydritové (mechanicky přebroušené, odsátý prach a zbytková vlhkost povrchu ≤ 0,5 %). Nejvyšší dovolenou vlhkost potěrů před pokládkou nášlapné vrstvy jsou uvedeny v normě ČSN 74 4505.

Ošetření podkladu

Podklad musí být suchý a čistý, bez mastnot, volných částic a antiadhezivních prostředků, soudržný a pevný. Odstraňte staré křehké a olupující se vrstvy se slabou přilnavostí. Poškozený podklad (trhliny a výtluky) je nutné vyspravit např. Opravná hmota na beton Výplň nebo Final. Rohy musí být zaobleny. Nové omítky a betony musí být spojené a vyzrálé. Pórovité a savé podklady opatřete nátěrem S2802A nebo Hloubkovou penetrací. Dilatační spáry, pracovní mezery, podlahové a stěnové spoje je nutné překrýt těsnicími páskami vloženými do první izolační vrstvy. Odtokové šachty a průchody trubek v podlaze opatřete těsnicími manžetami vloženými do izolačního nátěru.

Zpracování

Hmotu před použitím řádně promíchejte pomocí míchadla. Aby byla izolace účinná, je třeba ji nanést minimálně ve dvou vrstvách. První vrstvu nanášejte vydatně pomocí štětky nebo malířského válečku vtíráním hmoty do pokladu. Před nanášením další vrstvy, asi po 3 hod. zkontrolujte stupeň proschnutí (zkouška prstem). Na podlahách v místech vystavených zvýšenému zatížení (např. pěším provozem) je nutno před nanesením další vrstvy počkat asi 6 hodin. Druhou vrstvu je možno nanášet stejným způsobem nebo kovovým hladítkem, křížem k první vrstvě. Každá vrstva musí být na celém povrchu zaschlá. Tloušťka získaného nátěru musí být cca 1 mm. Na zcela suchou izolaci je možné přímo lepit keramický obklad nebo dlažbu. K lepení keramických obkladů používejte flexibilní či elastická lepidla. Použité nářadí omyjte po práci neprodleně vodou.

Upozornění

Do hmoty nepřidávejte žádné látky. Nanesenou hmotu chraňte před nadměrným přesušením a navlhnutím. Hydroizolace není finální povrch, proto musí být chráněna další vrstvou materiálu pro ochranu před UV. Vlivem UV materiál degraduje a ztrácí své vlastnosti. Načaté balení okamžitě uzavřete. Nepoužívat pro izolace konstrukcí se záporným tlakem vody. Zvýšená vlhkost prostředí či podkladu a teplota kolem +5 °C značně zpomaluje vyzrávání. Při použití v exteriéru chraňte během zrání před přímým deštěm.

Čištění

Materiál: ihned vodou
Ruce: mýdlo a voda, reparační krém na ruce

Aktualizace

Aktualizováno dne 22.8.2021
Vyhotoveno dne 20.7.2009

Uvedené informace a poskytnuté údaje spočívají na naší vlastní zkušenosti, výzkumu a objektivním testování a předpokládáme, že jsou spolehlivá a přesná. Přesto však firma nemůže znát nejrůznější použití, kdy bude výrobek aplikován, ani použité metody aplikace, proto neposkytuje za žádných okolností záruku nad rámec uvedených informací, co se týče vhodnosti výrobků pro určitá použití ani na postupy použití. Každý uživatel je povinen se přesvědčit o vhodnosti použití vlastními zkouškami. Pro další informace prosím kontaktujte naše technické oddělení.

Den Braven

Technický list
TL 81.40 Asfaltová izolační stěrka HYDRO BLOK B400

Produkt

Stěrková asfalto-bentonitová, vodou ředitelná hydroizolační hmota s obsahem syntetických armovacích vláken k okamžitému použití z kbelíku. Syntetická vlákna vytvářejí ve směsi flexibilní výztužnou a zpevňující nosnou vložku. Nanesením této hmoty na podklad a po jejím vyschnutí se vytvoří pevný a pružný hydroizolační kompozitní povlak, který nahrazuje běžně používané asfaltové hydroizolační pásy.

Vlastnosti

- Na vodorovné i svislé konstrukce
- Flexibilní – vyztužena vlákny
- Dokonalé spojení s asfaltovými pásy
- Dobrý pevnost v tahu
- Odolná proti povětrnostním vlivům
- Bez obsahu rozpouštědel, bez zápachu
- Vhodná pro novostavby a rekonstrukce
- Izolace přím pod lepidlo na obklady a dlažbu
- Snižuje skladebnou výšku podlahy
- Vysoká pružnost a vodotěsnost
- Odolnost proti stárnutí vlivem vody a tepla
- Tvoří jednolitou hmotu bez nedokonalých spojů

Použití

- K hydroizolaci minerálních materiálů v interiérech i exteriérech budov
- Balkóny, terasy, koupelny, prádelny, umývárny, sklepy, základy atd.

Technické vlastnosti			
Základ	Afalto-bentonitová hmota s obsahem syntetických armovacích vláken		
Konzistence	Tixotropní pasta		
Změna tloušťky při vyschnutí	%	max. 40	
Tepelná odolnost	°C	-20 / +80	
Aplikační teploty	°C	+5 / +30	
Plošná hmotnost	kg/m²	2,5 ± 0,3	
Doba schnutí 3 mm vrstvy	hod	24	při 20 °C/ 60 % relativní vlhkosti, výsledná tl.1,8 mm
Přídržnost	MPa	≥ 1,0	beton
	MPa	≥ 1,0	pozink, plech
	MPa	≥ 0,6	asfaltový pás
Pevnost v tahu	MPa	≥ 1,0	
Poměrné prodloužení	%	≥ 10	

Balení

- Kbelík 5 kg
- Kbelík 10 kg

Barva

- Sytě hnědá až černá

DEN BRAVEN
Czech and Slovak a.s.
793 91, Úvalno 353
Česká republika
IČO: 26872072
DIČ: CZ26872072
+420 554 648 200
info@denbraven.cz
www.denbraven.cz

Den Braven

Nasákavost	%	≤ 7	
Vodotěsnost V_{30} (vrstva 1,8 mm)	l/m²/30 min	0,0	
Faktor difúzního odporu	-	1810	
Propustnost pro vodní páru	g/m²/den	5	při 10 °C a 76 % rel. vlhkosti.
Skladovatelnost	měsíce	24	(+5 / +30 °C, nesmí zmrznout)
Přibližná spotřeba na 1 m²	kg	1,8	vrstva 2 mm

Upozornění

Do izolace nepřidávejte žádné látky. K rozdělání hmoty je nutno použít pitnou vodu. Dodatečné přidávání písku, pojiv a jiných látek se nepovoluje! Nanesenou hmotu chraňte před nadměrným přesušením. Nespotřebovanou hmotu v kbelíku okamžitě uzavřete.

Příprava podkladu

Podklad musí být únosný, pevný, čistý, zbavený prachu, barev, povrchových úprav, solných výkvětů, nečistot a nesoudržných částí, bez biologického napadení. Případná poškození v betonovém podkladu lze opravit např. Opravnou hmotou na beton Výplň. Na povrchu nesmí být zbytky separačních prostředků a musí být zbaven cementového mléka. K penetraci podkladu je vhodné použít penetrační nátěry typu S2802A, Hloubkovou penetraci apod. Hrubší nebo zvětralé povrchy (a povrchy s méně přídržnou vrchní vrstvou) doporučujeme nejprve mechanicky očistit (tryskáním, ocelovými kartáči, rapem, hrubým koštětem aj.) a penetrovat dvakrát. Samotnou aplikaci HYDRO BLOKEM B400 provedeme po zaschnutí penetračního nátěru (dle teplotních podmínek po 0,5 - 4 hod.).

Pozn.: Hlavním účelem penetračního nátěru je zpevnění vrchních vrstev podkladu a snížení jeho savosti. Toto následně zajišťuje velmi dobrou přídržnost k podkladu.

Pracovní postup

IZOLACE VODOROVNÝCH A SVISLÝCH KONSTRUKCÍ (náhrada těžkých lepenek)

Podklad pro provedení vodorovné a svislé izolace musí být pevný, na povrchu bezprašný. Provedeme celoplošnou penetraci a po zaschnutí stěrkujeme vrstvu min. 2 mm. Spotřeba cca 1,8 kg/m². Po zaschnutí vizuálně zkontrolujeme kvalitu povrchu. Jestliže se objeví nedokonale izolovaná místa, opravíme je přestěrkováním (nové vrstvy se homogenně spojí s předchozími). Po vyschnutí izolační vrstvy se může provést betonáž vodorovné plochy nebo zahrnutí materiálu ke kolmé stěně stavby.

IZOLACE BALKÓNŮ, TERAS A KOUPELEN

Při izolaci balkónů a teras postupujeme stejně jako v bodě A. Zde je však nutné stěrku v rohu vytáhnout min. 20 cm na kolmou stěnu. Při velkém dilatačním pnutí, doporučujeme ve vnitřních koutech použít mezi první a druhou vrstvu pás S-T8. HYDRO BLOK B400 umožňuje opravu balkónů a teras bez bourání původního podkladu. Při opravě se plocha očistí (případně se odstraní vydrolený beton), opláchne vodou a penetruje (viz. odstavec příprava podkladu). Po zaschnutí stěrkujeme min. 2 mm vrstvu, a to i na kolmé stěny do výšky min. 20 cm. Na zaschlou vrstvu HYDRO BLOKU B400 můžeme přímo cementovým lepidlem třídy C2 lepit dlažbu a obklady. Obdobně postupujeme při izolaci koupelen a sprchových koutů, ale musíme dbát na výšku izolace svislé stěny a brát v úvahu, výšku dosahu vody při používání.

IZOLACE PODZEMNÍCH KONSTRUKCÍ

Provede se podobně jako u izolace vodorovných a svislých konstrukcí. Základovou desku izolujeme celoplošně. Po dokončení vyzdívky stěny omítneme. Provedeme vizuální kontrolu kvality povrchu.

Pozn.: Na HYDRO BLOK B400 je možno nanášet běžné disperzní barvy (např. Balakryl, Eternal apod.) a většinu syntetických nátěrových hmot (např. Bisil, Krastenol - emaily odolné vůči vodě a UV záření). Nátěrové hmoty zde neuvedené doporučujeme předem vyzkoušet.

Čištění

Materiál: ihned vodou
Ruce: voda a mýdlo, reparační krém na ruce

imesta®
BARVY IMPREGNACE SANACE
www.imesta.com
+420 487 870 419
info@imesta.com

SINER® TS 2K

polymercementová izolační stěrka

Charakteristika
SINER® TS 2K je dvousložková minerální izolace na bázi polymercementu. Složka T je tekutá a složka S sypká. Po vytvrzení vytváří pružnou izolaci odolávající tlakové vodě i negativnímu tlaku vody. Působí jako protiradonová bariera.

Použití
Hydroizolační protiradonová vrstva pro aplikaci v interiéru i exteriéru budov. Zejména pro izolaci spodní stavby jak při rekonstrukcích, tak pro novostavby.

Zpracování
Tekutou složku SINER T smíchat s práškovou složkou SINER S, aby vznikla hmota bez hrudek. Při aplikaci stříkání je možno pro úpravu konzistence přidat vodu (podrobnosti viz. technický list). Nanáší se kovovou stěrkou nebo štětkou. Nanáší se min. ve dvou vrstvách. Max. tloušťka jedné vrstvy je cca 1-2 mm. Doba vytvrzení jedné vrstvy je 24 hodin. SINER TS je nutno zpracovat do cca 45 minut po zamíchání (dle teploty okolí a podkladu). Pro bezproblémovou bezpečnou funkčnost izolace je nutné SINER TS 2K nanést na nosný soudržný podklad bez olejů a mastnot. V místech předpokládaného vyššího namáhání tahem (např. dilatace) vložte do první vrstvy armovací tkaninu. V rozích je nutné vytvořit zaoblení s poloměrem cca 4 - 5 cm nanesením polymercementové malty (připravené z disperze BEFIX viz. technický list zpracování č. 2). Nenanášejte více než 1,5 kg/m² materiálu v jednom kroku, důsledkem vysokého procenta disperze hrozí vznik trhlin. Do doby úplného vytvrzení zamezte přístupu vody na nanesenou izolaci. Voda prosáklá do materiálu z neizolované strany může při mrazu zapříčinit odtržení izolační vrstvy od podkladu.

Spotřeba:
Izolace pro obklady a dlažby v interiéru:
Spotřeba cca 1,9 kg/m²
Minimální tloušťka vrstvy po vyschnutí 1 mm.
Izolace proti zemní vlhkosti a beztlakové povrchové vodě: Spotřeba cca 3 - 8 kg/m²
Minimální tloušťka vrstvy po vyschnutí min. 2 mm.
Izolace v nádržích a bazénech do hloubky 5 m:
Spotřeba cca 5,5 - 5,7 kg/m²
Minimální tloušťka vrstvy po vyschnutí min. 3 mm.

Balení
PE obaly 40 kg (T 10 kg a S 30 kg)
PE obaly 4 kg (T 1 kg a S 3 kg)

Technické parametry
SINER® T

Báze:	polymerní disperze
Barva:	bílá

SINER® S

Báze:	cement, plniva, přísady
Barva:	bílá nebo šedá
Poměr míchání T:S:	1:3,3 (přídavek vody do 10%)
Doba míchání:	3 min. (300 ot./min.) rozmíchat a pak 2 min. zrát za občasného mírného promíchání
Zpracovatelnost:	45 min. při teplotě 20°C
Teplota zpracování:	+5° až 30°C
Vytvrzení:	24 hodin (1 vrstva)
Čištění nářadí:	v čerstvém stavu vodou
Součinitel difuze radonu	1,9 +/-0,2. 10^{-11} m^2/s
Vodotěsnost dle ČSN 731319 V12	

Skladování
Skladujte v suchém prostoru a spotřebujte do 12 měsíců od data výroby. Kapalná složka nesmí zmrznout. Datum výroby a šarže jsou vyznačeny na identifikačním štítku na boční straně obalu.

Ekologie a bezpečnost práce
Nebezpečí
Dráždí kůži. Může vyvolat alergickou kožní reakci. Způsobuje vážné poškození očí. Může způsobit podráždění dýchacích cest. Uchovávejte mimo dosah dětí. Zamezte vdechování prachu. Používejte chranné rukavice/ochranný oděv/ochranné brýle/obličejový štít. PŘI ZASAŽENÍ OČÍ: Několik minut opatrně vyplachujte vodou. Vyjměte kontaktní čočky, jsou-li nasazeny a pokud je lze vyjmout snadno. Pokračujte ve vyplachování. PŘI STYKU S KŮŽÍ: Omyjte velkým množstvím vody a mýdla. PŘI VDECHNUTÍ: Přeneste osobu na čerstvý vzduch a ponechte ji v poloze usnadňující dýchání. Odstraňte obsah/obal jako nebezpečný odpad v souladu s místními předpisy. Směs může vyvolat senzibilizaci při styku s kůží, viz bod 11.1.d) bezpečnostního listu. Obsah látek PBT a vPvB: směs nepodléhá kritériím pro látky PBT nebo vPvB v souladu s přílohou XIII Nařízení EU č. 1907/2006, žádná ze složek v množství ≥ 0,1 % není uvedena v Kandidátském seznamu látek vyvolávajících velké obavy (SVHC).
Obsahuje nebezpečné látky: portlantský cement CAS 65997-15-1

K výrobku bylo vydáno prohlášení o shodě.

IMESTA, spol. s r.o.
Dubá, Dřevčice 9, 472 01 pošta Doksy
IČO: 42714851 DIČ: CZ42714851 Společnost je zapsaná u Krajského soudu v Ústí nad Labem, oddíl C, vložka 9468.

Technický list **fermacell**

Popis materiálu

fermacell Powerpanel H_2O je cementem pojená lehká betonová deska se sendvičovou strukturou. Pod krycími vrstvami je oboustranná výztužná mřížka z alkalicky rezistentní sklovláknité tkaniny. Deska nabízí řadu výhod u stěnových a stropních konstrukcí s vysokým zatížením vlhkostí.

Oblasti použití

- Interiérové použití (stěny a stropy)
  - domácí vlhké prostory (koupelny, sprchy)
  - veřejné prostory (bazény, sanitární prostory, wellness zařízení)
  - průmyslové prostory (mlékárny, pivovary, závodní kuchyně)
- Exteriérové použití
  - podkladová deska pro omítku v zavěšených provětrávaných fasádách a na soklech
  - podkladová deska pro lepení kamene
  - zavěšené podhledy v exteriéru (s povrchovou úpravou odolnou proti povětrnostním vlivům)

Osvědčení

- Stavebně technické osvědčení: ETA-07/0087
- Třída reakce na oheň (dle ČSN EN 13501-1): nehořlavá, A1

Povrch

Hladká pohledová strana s razítkem, zadní strana lehce zvlněná nebo zbroušená při kalibraci. Barva cementošedivá.

Povrchové úpravy

Výborný povrch pro celoplošné tmelení, nátěrové systémy, dlažbu a kamenné obklady, omítky a další.

Informační materiály **fermacell**: Telefon: +420 296 384 330| fax: +420 296 384 333| e-mail: fermacell-czf@xella.com | www.fermacell.cz

fermacell Powerpanel H_2O

Charakteristika materiálu	
Objemová hmotnost	~ 1000 kg/m³
Plošná hmotnost	~ 12,5 kg/ m²
Ustálení vlhkosti	~ 5 %
Součinitel difúzního Odporu (podle ČSN EN 12572)	μ = 56
Součinitel tepelné vodivost	$\lambda_{10,tr}$ = 0,17 W/mK
Tepelný odpor (podle ČSN EN 12664)	$R_{10,tr}$ = 0,07 m²K/W
Měrná tepelná kapacita	c_p =1000 J/ (kgK)
Pevnost v ohybu	⩾ 6,0 N/mm²
E-modul v ohybu	~ 4200 N/mm²
Hodnota pH	~ 10
Relativní změna délky (podle ČSN EN 318)	0,15 mm/m* 0,10 mm/m**
Nasákavost povrchu	650 g/m²
Celková nasákavost desky (podle EN 520)	8,5 %

* mezi 30 % a 65 % relativní vlhkosti vzduchu
** mezi 65 % a 85 % relativní vlhkosti vzduchu

Rozměrové tolerance při ustálené vlhkosti pro standardní formáty desek	
Tloušťka desky	12,5 mm
Délka, šířka	± 1 mm
Rozdíl diagonál	≤ 2 mm
Tolerance tloušťky	± 0,5 mm
Formáty desek	1000 x 1250 mm 2000 x 1250 mm 2600 x 1250 mm 3010 x 1250 mm*

*termín dodání na vyžádání, přířezy jsou možné

Informační materiály **fermacell**: Telefon: +420 296 384 330| fax: +420 296 384 333| e-mail: fermacell-cz@xella.com | www.fermacell.cz
Technické změny vyhrazeny. Stav 06/2016. Nejnovější vydání této brožury je k dispozici na www.fermacell.cz
fermacell® je registrovaná značka a společnost skupiny XELLA